

AN ABSTRACT OF THE THESIS OF

Axel P. Vischer for the degree of Doctor of Philosophy in Physics presented on February 14, 1992.

Title: Relativistic Field-Theoretical Transport in Condensed Matter

Redacted for Privacy

Abstract approved: \_\_\_\_\_

We discuss a relativistic transport theory of condensed matter based on a microscopic system containing bosonic and fermionic degrees of freedom interacting via 3- and 4-point interactions. We use the Dyson hierarchy as a solution to the underlying field theory and truncate this hierarchy by parametrizing the 2-particle-irreducible kernels of the 4- and 5-point vertex functions. We then perform a complete crossing-symmetric reduction of the 2-particle intermediate states of the theory. We obtain a reduction hierarchy and show how to explore the quality of our truncation scheme using this reduction hierarchy. Finally we discuss the problem of regularization of the theory in the case of hadronic matter by either putting form factors directly in the action or by using dispersion relations to introduce causal form factors into singular diagrams.

Relativistic Field-Theoretical Transport in Condensed Matter

by

Axel P. Vischer

A THESIS

submitted to

Oregon State University

in partial fulfillment of  
the requirement for the  
degree of

Doctor of Philosophy

Completed February 14, 1992

Commencement June 1992

APPROVED:

Redacted for Privacy

\_\_\_\_\_  
Professor of Physics in charge of major

Redacted for Privacy

\_\_\_\_\_  
Head of department of Physics

Redacted for Privacy

\_\_\_\_\_  
Dean of Graduate School

Date thesis is presented February 14, 1992

Typed by Cristin Howell for Axel P. Vischer

## TABLE OF CONTENTS

1. INTRODUCTION	1
1.1 FUNDAMENTAL INTERACTIONS AND CONDENSED MATTER	1
1.2 THE DYSON HIERARCHY	2
2. CONNECTED GREEN'S FUNCTIONS AND THEIR ONE-PARTICLE- IRREDUCIBLE COMPONENTS	7
2.1 GREEN'S FUNCTIONS AND VERTEX FUNCTIONS	7
2.2 THE RELATIONSHIP BETWEEN THE CONNECTED GREEN'S FUNCTIONS AND THE VERTEX FUNCTIONS	13
3. THE DYSON HIERARCHY	27
3.1 THE LAGRANGIAN AND THE EQUATIONS OF MOTION	27
3.2 DERIVATION AND TRUNCATION OF THE DYSON EQUATIONS	35
4. CROSSING-SYMMETRIC REDUCTION	52
4.1 TOPOLOGICAL CLASSIFICATION AND THE REDUCTION HIERARCHY	52
4.2 CROSSING-SYMMETRIC REDUCTION OF THE SCATTERING TYPE OF 2-PARTICLE INTERMEDIATE STATES	60
4.3 THE DECAY TYPE OF 2-PARTICLE INTERMEDIATE STATES	77
5. REGULARIZATION	81
6. CONCLUSION	84
7. REFERENCES	85

## LIST OF FIGURES

<u>FIGURE</u>	<u>PAGE</u>
1. Analogies between methods in classical statistical mechanics and field theories	4
2. Relationship between the connected 3- and 4-point Green's functions and the 3- and 4-point vertex functions	25
3. Relation between the connected 5-point Green's functions and the 5-point vertex functions	26
4. Mean-field equation for the boson field	34
5. Diagrammatic representation of equation (3.13)	41
6. Diagrammatic representation of equation (3.14)	42
7. Dyson equations for the propagators.	43
8. Diagrammatic representation of the equation for the bare 2-boson vertex function (equation 3.18)	44
9. Diagrammatic representation of the Dyson equations for the 3-point vertex functions.	45
10. Dyson equations for a Lagrangian containing only 3-point interactions	47
11. Definition of the $T$ matrix	48
12. Definition of the completely reducible 5-point vertex function $P$	49
13. Diagrammatic representation of the Dyson equations up to $O(3)$ after introduction of the $T$ matrix.	50
14. Diagrammatic representation of the Dyson equations up to $O(4)$ after introduction of the $T$ matrix with only 3-point interactions in the Lagrangian.	51
15. Topological classification of diagrams containing 1-, 2- and 3-particle intermediate states appearing in the Dyson hierarchy up to $O(6)$	57
16. 2-particle reduction of the 1-particle-irreducible 3-point vertex function	58
17. Perturbative expansion of the 2-particle-irreducible kernel of the 3-boson vertex function	59
18. Diagrammatic representation of the crossing-symmetric reduction of the 1-particle intermediate states of the $T$ matrix	69

<u>FIGURE</u>	<u>PAGE</u>
19. Diagrammatic representation of the crossing-symmetric reduction of the 1-particle intermediate states of the pentagon	70
20. Scattering-reducible diagrams of the $T$ matrix in two channels	71
21. Scattering-reducible diagrams of the pentagon in more than one channel	72
22. Generic decay diagram and its different generic pieces in terms of 3-,4-, 5-, 6-, 7-, and 8-point 1-particle-irreducible vertex functions	80

## LIST OF TABLES

<u>TABLE</u>		<u>PAGE</u>
1.	Definition of the connected $n$ -point Green's functions and $n$ -point vertex functions	11
2.	Relation between connected Green's functions and vertex functions	22
3.	Rules for constructing a diagrammatic representation for integral equations	24
4.	Relations between the bare vertices in the equation of motion and the bare vertices in the Lagrangian	33

# RELATIVISTIC FIELD-THEORETICAL TRANSPORT IN CONDENSED MATTER

## 1. INTRODUCTION

The aim of this paper is to develop a relativistic condensed matter theory based upon a microscopic, i.e. field theoretical picture. In particular, we will use the Dyson hierarchy as a solution to the underlying field theory of the condensed state and will discuss regularization procedures suitable specifically for hadronic matter.

### 1.1 FUNDAMENTAL INTERACTIONS AND CONDENSED MATTER

With the advent of the Standard Model of the fundamental particles and their interactions and the intensive search for a possible quantum field theory of the gravitational interaction (Quantum Gravity) it became more and more luring and urgent to base all condensed matter theories on the underlying fundamental forces of nature. This microscopic approach to the condensed state leads directly to a rough classification of solid state physics being the theory of electromagnetically interacting condensed matter and nuclear physics being the theory of strongly interacting condensed matter. On the other hand, we have to exclude the weak and gravitational interactions from a discussion of condensed matter theories based on a microscopic picture.

While we find gravitationally interacting condensed matter on a macroscopic scale all around us (conventionally we call this theory Astrophysics, *e.g.* the earth or the solar system are condensed states of gravity), we cannot go to microscopic scales due to a lack of Quantum Gravity. It is interesting to note that this kind of a microscopic condensed state of gravity has only played an important role in the very early stages of the universe ( $t < 10^{-43}$  s after the big bang).

For the weak interaction, we are able to formulate reasonable microscopic theories for condensed states, but we cannot detect them. This is due to the short range of the weak force. Even if we go to the densest nuclei we know, the gravitationally bound neutron stars [1], the binding energy due to the weak interaction will still be an order of magnitude smaller than the temperature of the system. The binding energy of neutrinos in a neutron weak mean field in the neutron star is, for example, in the Hartree approximation given by  $E_B = -\frac{1}{\sqrt{2}} G_F n_n$ , where  $n_n$  is the neutron density and  $G_F$  is the Fermi constant (the weak charges due to protons and electrons cancel each other for an electrically neutral neutron star nucleus). Assuming that the neutron density is several times the nuclear density, we obtain a binding energy on the order of a few keV, while the temperature of the neutron star



is on the order of a few tens of MeV. So overall the weak interaction in condensed states can be considered noise to the overwhelming electromagnetic and strong foreground.

So at this point only the electromagnetic interaction based on QED and the strong interaction seem to be suitable for investigating their condensed states with field theoretical tools. But, considering problems that especially occur in the regularization of these theories we have to limit ourselves even further. Due to confinement we have to split the strong force into its fundamental interaction based on QCD and its long-range residual interaction based on QHD. Not only is QCD rather complicated due to its large coupling and non-abelian group structure, it is also a gauge theory, so that we have to use the Faddeev-Popov technique to fix the gauge which introduces inconvenient ghost fields, which in contrast to QED, do not decouple from the theory. Therefore, discussing QCD is outside the scope of this paper. This leaves us with QED and QHD.

In most of this paper we stay completely general and our theory can be applied to any of the interactions. Only in the chapter about regularization we do choose QHD and therefore hadronic matter to be our condensed state. The advantage of QHD in comparison to QED is that it is a phenomenological theory with a natural cut-off, the hadron size. In contrast, QED is a fundamental theory where we don't have the freedom of introducing cut-offs, which as we will see, complicates its discussion.

## 1.2 THE DYSON HIERARCHY

Any theory that wants to describe condensed matter has as its final aim the derivation of the equations of state of the matter and its transport coefficients. The equations of state give functional relationships for one of the intensive parameters of the theory in terms of the independent extensive parameters in the steady state. These equations can be calculated from the moments of the  $n$ -particle density matrices of the system (the 1-particle density matrix is the phase-space distribution function). The fluctuations of the time dependence of the  $n$ -particle density matrices determine the transport coefficients of the matter which in turn govern the time-dependent behavior of the theory. Therefore if we are able to calculate the  $n$ -particle density matrices and their fluctuations we have a complete transport theory of the condensed state.

Before continuing our discussion of the field theoretical tools we use to formulate a transport theory microscopically, we wish to remind the reader of the two main methods developed in classical statistical mechanics for gases to achieve this goal: the BBGKY hierarchy and Mayer's Linked Cluster Expansion [2]. To derive the BBGKY hierarchy, we start with defining correlation functions  $f_s$  which give the probability that  $s$  particles

have specified positions and momenta in our system of interest which represents a Gibbs ensemble. The derivation starts with Liouville's Theorem which governs the time evolution of the Hamiltonian of our  $N$  particle system and leads then to the BBGKY hierarchy. This hierarchy is a set of  $N$  coupled integro-differential equations, each one consisting of a streaming term for the correlation functions  $f_s$  and a "collision integral" which relates  $f_s$  to  $f_{s+1}$  and therefore discusses the scattering of the  $s$  particles under consideration with an additional particle.

For an actual physical system  $N$  is very large and the coupled system can therefore not be solved. Instead one truncates the hierarchy, setting the 3-particle correlations to zero and approximating the 2-particle correlations using the "Hypothesis of Molecular Chaos" which states that the range of the two-body potential between two particles  $r_0$  is small in comparison to the average particle separation, or in other words; that the particles are approximately uncorrelated:

$$f_2(\mathbf{r}_1, \mathbf{p}_1; \mathbf{r}_2, \mathbf{p}_2; t) \rightarrow f_1(\mathbf{r}_1, \mathbf{p}_1) f_1(\mathbf{r}_2, \mathbf{p}_2) \quad \text{for } |\mathbf{r}_1 - \mathbf{r}_2| \gg r_0$$

This condition is well fulfilled for gases of atoms and molecules interacting via van der Waals forces. The approximations then lead us directly to the Boltzmann equation which we can solve for  $f_1$ , the usual phase space distribution function. Since Liouville's Theorem is an equal-time relation we can only get fluctuations depending on one time variable out of the BBGKY hierarchy and therefore also the Boltzmann equation does not contain any further fluctuations. One gets the fluctuations of the phase-space distribution function in special regimes, like the hydrodynamic regime where the mean free path is small compared to the scale of the system, by treating the time dependence of the solution to the free gas perturbatively in the Boltzmann equation.

Another approach to obtain the phase space distribution function is the Linked Cluster Expansion of Ursell and Mayer. Here we start from the partition function for the Hamiltonian of a gas interacting only via two-body potentials (which is the reason that in this theory we don't need or obtain higher-order density matrices). These two-body interactions represent a perturbation on the partition function of the non-interacting gas. The exponential of the potential in the phase-space integral of the partition function can then be expanded in terms of two-particle correlation functions (these are correlations defined in terms of the potential but they do directly relate to the probability correlations like the ones in the BBGKY hierarchy). Ursell and Mayer then developed a diagrammatic technique to represent the different contributions of this perturbation expansion and finally summed up the series and obtained the equation of state. Like in the Boltzmann equation we only

obtain fluctuations in one time variable out of the theory since our Hamiltonian is instantaneous in its time dependence.

The important point to notice here is that both approaches, the BBGKY hierarchy as well as the Linked Cluster Expansion, are two independent solutions to the many-body problem of the condensed state. Furthermore, the classical Linked Cluster Expansion is the direct predecessor to all quantum-mechanical cluster expansions and their diagrammatic representations as well as the perturbative expansions in field theories and their diagrammatic representation due to Feynman. Especially the striking similarities between the classical Linked Cluster Expansion and the perturbative solution to a field theory leads then to the question if there is an analog to the BBGKY hierarchy, which yields an additional method to solve a field theory.

The answer to this question is the Dyson hierarchy. The Dyson hierarchy consists of an infinite set of coupled integro-differential equations, each equation relating an  $n$ -point Green's function to the  $(n + 1)$ - or  $(n + 2)$ - point Green's function for the case of 3- and 4-point interactions in the Lagrangian respectively. It is important to realize that the Dyson hierarchy indeed represents an independent way to solve a field theory. It can be shown that the Dyson hierarchy is sufficient to be uniquely solved for the Feynman perturbation series [3].

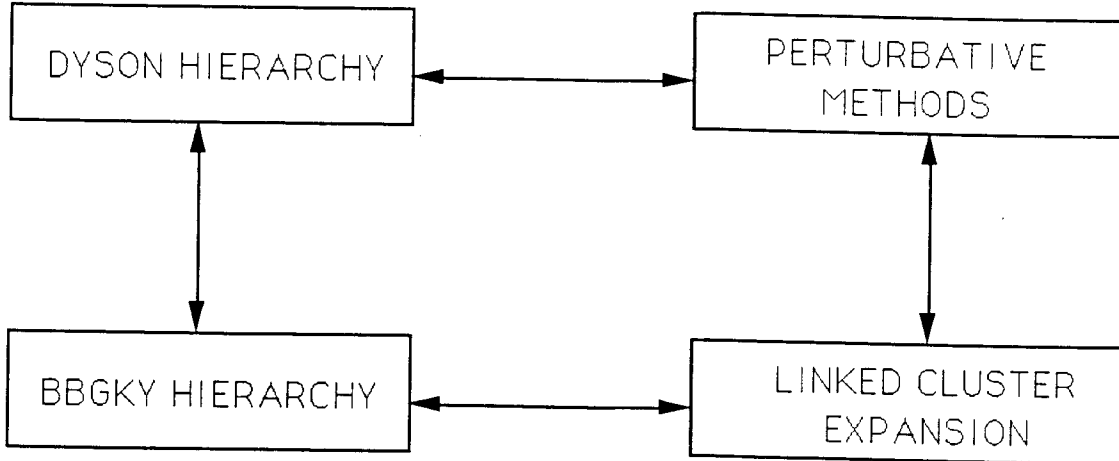


Fig. 1. Analogies between methods in classical statistical mechanics and field theories.

This paper will discuss the use of the Dyson hierarchy as a tool to investigate the microscopic structure of a relativistic condensed state. We start in chapter 2 by defining precisely the Green's functions of the theory and give their properties. Chapter 3 contains the derivation of the Dyson hierarchy from a generic Lagrangian containing fermionic and

bosonic degrees of freedom interacting via 3 - and 4 - point interactions, and a recipe for truncating this hierarchy at the level of the 4 - point Green's function. In chapter 4, we discuss the crossing-symmetric reduction of the Dyson hierarchy, a procedure which explicitly extracts the lowest excitations of the system out of the equations. Finally, in chapter 5, we explore the regularization of the theory for the special case of hadronic matter. In chapter 6 we conclude with a summary and an outlook. This work adds as a new contribution to the field the discussion of the Dyson hierarchy with 4-point interactions in the Lagrangian and a generic procedure to do a crossing-symmetric reduction of a vertex function to any order in the intermediate states. It also discusses problems arising in the regularization of the theory and indicates possible solutions to this problem.

We would like to close this chapter by discussing how the  $n$  -point Green's functions, the quantities we obtain from the Dyson hierarchy, can be used to generate the  $n$  -particle density matrices and their fluctuations and so determine our transport theory. The Green's functions are defined as expectation values of time-ordered products of fields, with the fields being functions of their space-time coordinates. To relate these quantities to the correlation functions of the BBGKY hierarchy we have to consider the Green's functions at equal times (E.T.) and perform a Wigner transformation over the leftover space-time coordinates.

For example, the connected 2-point Green's function of two adjoint fields  $\phi_\alpha(x_1)$ ,  $\phi_\beta(x_2)$  is defined as (see chapter 2 for more details):

$$G_{\alpha\beta}^{(2)}(x_1, x_2) \equiv \langle T \phi_\beta(x_2) \phi_\alpha(x_1) \rangle - \langle \phi_\beta(x_2) \rangle \langle \phi_\alpha(x_1) \rangle$$

If we let the time separation of the fields go to zero ( $(t_2 - t_1) \rightarrow 0^+$ ) we obtain the probability density matrix  $n_{\alpha\beta}(x_1, x_2)$ :

$$n_{\alpha\beta}(x_1, x_2) \equiv \langle \phi_\alpha^+(x_2) \phi_\beta(x_1) \rangle$$

corrected by the disconnected part of the Green's function. From this comparison we see that a Wigner transform of the 2-point Green's function:

$$\hat{G}_{\alpha\beta}^{(2)}(x, p) \equiv \int d^4x' G_{\alpha\beta}^{(2)}[x + \frac{x'}{2}, x - \frac{x'}{2}]_{\text{E.T.}} e^{i p x'}$$

combined with an integration over the energy variable of  $\hat{G}_{\alpha\beta}^{(2)}$  yields directly the phase-

space distribution function we used in the Boltzmann equation.

In an analogous fashion we can obtain the  $n$ -particle density matrices from the corresponding  $n$ -point Green's functions. In addition we can calculate all the fluctuations from the Green's functions because they contain all the time variables explicitly in a symmetric way and can therefore be explicitly used to obtain the transport coefficients which are due to the non-instantaneous aspects of the time dependence of the system. Thus, the Green's functions are preferable to the density matrices as the dynamical quantities because they are not only covariant, but also contain all the information about the fluctuations of the system.

We conclude therefore that, by solving the Dyson hierarchy for the Green's functions, we completely determine our transport theory of the condensed state.

## 2. CONNECTED GREEN'S FUNCTIONS AND THEIR ONE-PARTICLE IRREDUCIBLE COMPONENTS

In this section we define the Green's functions of the theory and discuss their properties. The different kinds of generating functionals are introduced. The generating functional for one-particle irreducible components of the connected Green's functions, the so called vertex functions or proper vertices, are obtained by Legendre transforming the generating functional of the connected Green's functions, and the relationship between the connected Green's functions and the vertex functions is derived.

### 2.1 GREEN'S FUNCTIONS AND VERTEX FUNCTIONS [7]

The dynamical quantities we want to derive from our theory are the  $n$ -point Green's functions which are defined as the vacuum expectation value of the time-ordered product of  $n$  generic fields of the theory. These Green's functions satisfy both the laws of relativity and the postulates of quantum mechanics and, as we saw in the last chapter, carry all the information we need to determine the transport properties of the condensed state uniquely.

To concentrate now all of this information into one expression we introduce the generating functional  $Z[j; \eta, \bar{\eta}]$  for the Green's functions. Here  $j; \eta$  and  $\bar{\eta}$  are the source terms which produce the bosonic fields  $\phi$  and fermionic fields  $\bar{\psi}$  and  $\psi$  respectively.

A generating function can be understood as the most efficient way to incorporate a sequence of numbers  $g_0, g_1, g_2, \dots$  into one function:

$$Z(j) \equiv \sum_{m=0}^{\infty} g_m \frac{j^m}{m!} \quad (2.1)$$

Once we know  $Z(j)$  we can reproduce the  $g$ 's by taking derivatives with respect to  $j$  at  $j=0$ . To reproduce the Green's functions from the generating functional  $Z[j; \eta, \bar{\eta}]$  we use in analogy functional variation with respect to the sources and then let the sources approach zero.

A standard generating function in physics is the partition function  $Z(T)$  of statistical mechanics (here  $T$  is the temperature). It actually turns out that the partition function is a rather theoretical construct and that it is much more convenient to introduce the Helmholtz free energy  $F$  as the generating function:

$$Z(T) \equiv e^{-\frac{F(T)}{NkT}}$$

where  $N$  is the number of particles in the Gibbs ensemble and  $k$  is the Boltzmann constant. From the free energy we can then derive all thermodynamic properties of the system in a straightforward way.

We apply the same procedure for our generating functional  $Z[j; \eta, \bar{\eta}]$ . Here we want to get rid of the disconnected parts which only yield contributions to the normalization of physical quantities. The generating functional for the connected Green's function  $W[j; \eta, \bar{\eta}]$  is therefore defined as:

$$Z[j; \eta, \bar{\eta}] \equiv e^{W[j; \eta, \bar{\eta}]} \quad (2.2)$$

Until now we only found a way to proceed from the generating functional  $W$  to the connected Green's functions of the theory. The next step is to derive an independent way to calculate this generating functional. In statistical mechanics we use the phase space integral of the exponential of the reduced Hamiltonian  $\frac{H}{kT}(T; (\mathbf{r}, \mathbf{p}))$  of the system of interest to obtain the partition function  $Z(T)$ :

$$Z(T) \equiv \int d\Gamma(\mathbf{r}, \mathbf{p}) e^{-A(T; (\mathbf{r}, \mathbf{p}))},$$

where  $d\Gamma(\mathbf{r}, \mathbf{p})$  stands for the phase space integration of the  $n$ -particle system and  $A(\mathbf{r}, \mathbf{p})$  is given by the reduced Hamiltonian  $\frac{H}{kT}$ :

$$A(T; (\mathbf{p}, \mathbf{q})) \equiv \frac{H}{kT}(T; (\mathbf{p}, \mathbf{q})).$$

In analogy we use in the calculation of the generating functional  $Z[j; \eta, \bar{\eta}]$  the functional integration over the fields of the exponential of the action  $A[j; \eta, \bar{\eta}(\phi; \psi, \bar{\psi})]$  of our field theory:

$$Z[j; \eta, \bar{\eta}] \equiv \int \mathcal{D}(\phi; \psi, \bar{\psi}) e^{iA[j; \eta, \bar{\eta}(\phi; \psi, \bar{\psi})]} \quad (2.3)$$

where  $\mathcal{D}(\phi; \psi, \bar{\psi})$  stands for the functional integration over the boson and fermion fields of our theory and the action  $A$  is given by:

$$A[j; \eta, \bar{\eta}(\phi; \psi, \bar{\psi})] \equiv I(\phi; \psi, \bar{\psi}) + \int d^4x [\sum_{\alpha} j_{\alpha}(x)\phi_{\alpha}(x) + \sum_a (\bar{\eta}_a(x)\psi_a(x) + \bar{\psi}_a(x)\eta_a(x))] . \quad (2.4)$$

Here  $I$  stands for the classical action of the theory:

$$I(\phi; \psi, \bar{\psi}) \equiv \int d^4x \mathcal{L}[\phi(x); \psi(x), \bar{\psi}(x)] \quad (2.5)$$

This completes the procedure of how to get the Green's functions, the dynamical quantities of the theory: we start by defining our Lagrangian  $\mathcal{L}$ , then calculate the generating functional for the connected Green's functions  $W$  using (2.2), (2.3), (2.4) and (2.5) and finally find the Green's function by varying  $W$  with respect to the sources and then letting the sources go to zero. The Green's functions we obtain in this way are the connected Green's functions. They are tabulated in Table 1 up to the 4-point Green's function. So, the basic input in our theory is the Lagrangian of the system of interest. This Lagrangian is only a function of the fields, not of the sources. It seems to be reasonable therefore to ask if there is also a generating functional that does not depend on the sources but rather on the fields.

The same question arises in statistical mechanics where we have the Helmholtz free energy depending on the intensive variable temperature  $T$ . By making a Legendre transform to the internal energy  $U$  we obtain a quantity that only depends on extensive variables, *i.e.* we replace the temperature  $T$  by the entropy  $S$ :

$$F(T, V, N) \equiv U(S, V, N) - TS$$

In analogy we Legendre transform the generating functional of the connected Green's functions  $W$ , which is a functional of the source terms, to obtain the generating functional of the vertex functions  $\Gamma$ , which is a functional of the fields only.

$$W[j; \eta, \bar{\eta}] \equiv i \Gamma[\phi; \psi, \bar{\psi}] + i \int dx \{ \sum_{\alpha} j_{\alpha}(x)\phi_{\alpha}(x) + \sum_a (\bar{\eta}_a(x)\psi_a(x) + \bar{\psi}_a(x)\eta_a(x)) \} \quad (2.6)$$



It turns out that the vertex functions we obtain by a functional variation of  $\Gamma$  with respect to the fields (see table 1) are 1-particle irreducible and therefore represent the highly connected pieces of diagrams.

Finally if we expand the generating functional of the vertex functions  $\Gamma$  semiclassically in the number of loops we find that  $\Gamma$  is equal to the classical action  $I$  up to order  $\hbar^2$ .  $\Gamma$  is therefore conventionally called the effective action of the theory since the higher order terms in  $\hbar$  represent the quantum fluctuations of the theory. This is again analogous to the internal energy  $U$  of statistical mechanics, which not only represents the expectation value of the Hamiltonian of the system but also the thermodynamic fluctuations due to the statistical nature of the system.

This concludes the discussion of the Green's and vertex functions. For explicit derivations of the statements we derived from analogy to statistical mechanics we refer the reader to references [3,4,5,6,8].

order	connected Green's function	definition in terms of time ordered products	definition in terms of functional variation	corresponding vertex function and its definition
1	$G_\alpha^{(1)}(x)$	$\langle \phi_\alpha(x) \rangle$	$\left. \frac{\delta W(j; \eta, \bar{\eta})}{i\delta j_\alpha(x)} \right _{j\eta \bar{\eta} \rightarrow 0}$	$j_\alpha(x) \equiv - \frac{\delta \Gamma(\phi; \psi, \bar{\psi})}{\delta \phi_\alpha(x)}$
1				$\eta_b(x) \equiv - \frac{\delta \Gamma(\phi; \psi, \bar{\psi})}{\delta \psi_b(x)}$
1				$\bar{\eta}_a(x) \equiv \frac{\delta \Gamma(\phi; \psi, \bar{\psi})}{\delta \psi_a(x)}$
2	$G_{\alpha\beta}^{(2)}(x_1, x_2)$	$\langle T \phi_\beta(x_2) \phi_\alpha(x_1) \rangle$ $- \langle \phi_\beta(x_2) \rangle \langle \phi_\alpha(x_1) \rangle$	$\left. \frac{\delta^2 W}{i\delta j_\beta(x_2) i\delta j_\alpha(x_1)} \right _{j\eta \bar{\eta} \rightarrow 0}$	$\Gamma_{\alpha\beta}^{(2)}(x_1, x_2) \equiv \left. \frac{\delta^2 \Gamma}{\delta \phi_\beta(x_2) \delta \phi_\alpha(x_1)} \right _{j\eta \bar{\eta} \rightarrow 0}$
2	$G_{\alpha\bar{b}}^{(2)}(x_1, x_2)$	$\langle T \psi_b(x_2) \bar{\psi}_a(x_1) \rangle$	$\left. \frac{\delta^2 W}{i\delta \bar{\eta}_b(x_2) i\delta \eta_a(x_1)} \right _{j\eta \bar{\eta} \rightarrow 0}$	$\Gamma_{\alpha\bar{b}}^{(2)}(x_1, x_2) \equiv \left. \frac{\delta^2 \Gamma}{\delta \bar{\psi}_b(x_2) \delta \psi_a(x_1)} \right _{j\eta \bar{\eta} \rightarrow 0}$
3	$G_{\alpha\beta\gamma}^{(3)}(x_1, x_2, x_3)$	$\langle T \phi_\gamma(x_3) \phi_\beta(x_2) \phi_\alpha(x_1) \rangle$ $- \langle \phi_\gamma(x_3) \rangle \langle \phi_\beta(x_2) \rangle \langle \phi_\alpha(x_1) \rangle$ $- \langle \phi_\gamma(x_3) \rangle G_{\alpha\beta}^{(2)}(x_1, x_2)$ $- \langle \phi_\beta(x_2) \rangle G_{\alpha\gamma}^{(2)}(x_1, x_3)$ $- \langle \phi_\alpha(x_1) \rangle G_{\beta\gamma}^{(2)}(x_2, x_3)$	$\left. \frac{\delta^3 W}{i\delta j_\gamma(x_3) i\delta j_\beta(x_2) i\delta j_\alpha(x_1)} \right _{j\eta \bar{\eta} \rightarrow 0}$	$\Gamma_{\alpha\beta\gamma}^{(3)}(x_1, x_2, x_3) \equiv$ $\left. - \frac{\delta^3 \Gamma}{\delta \phi_\gamma(x_3) \delta \phi_\beta(x_2) \delta \phi_\alpha(x_1)} \right _{j\eta \bar{\eta} \rightarrow 0}$
3	$G_{abc}^{(3)}(x_1, x_2, x_3)$	$\langle T \psi_c(x_3) \bar{\psi}_b(x_2) \phi_a(x_1) \rangle$ $- \langle \phi_a(x_1) \rangle G_{bc}^{(2)}(x_2, x_3)$	$\left. \frac{\delta^3 W}{i\delta \bar{\eta}_c(x_3) i\delta \eta_b(x_2) i\delta j_a(x_1)} \right _{j\eta \bar{\eta} \rightarrow 0}$	$\Gamma_{abc}^{(3)}(x_1, x_2, x_3) \equiv$ $\left. \frac{\delta^3 \Gamma}{\delta \bar{\psi}_b(x_3) \delta \psi_a(x_2) \delta \phi_a(x_1)} \right _{j\eta \bar{\eta} \rightarrow 0}$
4	$G_{abcd}^{(4)}(x_1, x_2, x_3, x_4)$	$\langle T \psi_d(x_4) \bar{\psi}_c(x_3) \bar{\psi}_b(x_2) \psi_a(x_1) \rangle$ $- G_{cd}^{(2)}(x_3, x_4) G_{ab}^{(2)}(x_1, x_2)$ $+ G_{ad}^{(2)}(x_1, x_4) G_{cb}^{(2)}(x_3, x_2)$	$\left. \frac{\delta^4 W}{i\delta \bar{\eta}_d(x_4) i\delta \eta_c(x_3) i\delta \bar{\eta}_b(x_2) i\delta \eta_a(x_1)} \right _{j\eta \bar{\eta} \rightarrow 0}$	$\Gamma_{abcd}^{(4)}(x_1, x_2, x_3, x_4) \equiv$ $\left. \frac{\delta^4 \Gamma}{\delta \bar{\psi}_d(x_4) \delta \psi_c(x_3) \delta \bar{\psi}_b(x_2) \delta \psi_a(x_1)} \right _{j\eta \bar{\eta} \rightarrow 0}$

Table 1. Definition of the connected  $n$ -point Green's functions and  $n$ -point vertex functions. Fermion number conservation requires the 1-point Green's functions of fermions and anti-fermions to be zero. The phases of the vertex functions are chosen in such a way that to lowest order in perturbation theory the vertex functions have the same phase as the bare vertices of the Lagrangian. Greek indices are reserved for boson fields, latin indices for fermion fields.

4	$G_{\alpha\beta\gamma\delta}^{(4)}(x_1, x_2, x_3, x_4)$	$\langle T \phi_\delta(x_4) \phi_\gamma(x_3) \phi_\beta(x_2) \phi_\alpha(x_1) \rangle$ $- G_{\gamma\delta}^{(2)}(x_3, x_4) G_{\alpha\beta}^{(2)}(x_1, x_2)$ $- G_{\beta\delta}^{(2)}(x_2, x_4) G_{\alpha\gamma}^{(2)}(x_1, x_3)$ $- G_{\alpha\delta}^{(2)}(x_1, x_4) G_{\beta\gamma}^{(2)}(x_2, x_3)$ $- G_{\beta\gamma\delta}^{(3)}(x_2, x_3, x_4) \langle \phi_\alpha(x_1) \rangle$ $- G_{\alpha\gamma\delta}^{(3)}(x_1, x_3, x_4) \langle \phi_\beta(x_2) \rangle$ $- G_{\alpha\beta\delta}^{(3)}(x_1, x_2, x_4) \langle \phi_\gamma(x_3) \rangle$ $- G_{\alpha\beta\gamma}^{(3)}(x_1, x_2, x_3) \langle \phi_\delta(x_4) \rangle$ $- G_{\gamma\delta}^{(2)}(x_3, x_4) \langle \phi_\beta(x_2) \rangle \langle \phi_\alpha(x_1) \rangle$ $- G_{\alpha\beta}^{(2)}(x_1, x_2) \langle \phi_\delta(x_4) \rangle \langle \phi_\gamma(x_3) \rangle$ $- G_{\beta\delta}^{(2)}(x_2, x_4) \langle \phi_\gamma(x_3) \rangle \langle \phi_\alpha(x_1) \rangle$ $- G_{\alpha\delta}^{(2)}(x_1, x_4) \langle \phi_\gamma(x_3) \rangle \langle \phi_\beta(x_2) \rangle$ $- G_{\alpha\gamma}^{(2)}(x_1, x_3) \langle \phi_\delta(x_4) \rangle \langle \phi_\beta(x_2) \rangle$ $- G_{\beta\gamma}^{(2)}(x_2, x_3) \langle \phi_\delta(x_4) \rangle \langle \phi_\alpha(x_1) \rangle$ $- \langle \phi_\delta(x_4) \rangle \langle \phi_\gamma(x_3) \rangle$ $\times \langle \phi_\beta(x_2) \rangle \langle \phi_\alpha(x_1) \rangle$	$\frac{\delta^4 W}{i\delta j_\delta(x_4) i\delta j_\gamma(x_3) i\delta j_\beta(x_2) i\delta j_\alpha(x_1)} \Big _{j\eta \bar{\eta} \rightarrow 0}$	$\Gamma_{\alpha\beta\gamma\delta}^{(4)}(x_1, x_2, x_3, x_4) \equiv \frac{\delta^4 \Gamma}{\delta\phi_\delta(x_4) \delta\phi_\gamma(x_3) \delta\phi_\beta(x_2) \delta\phi_\alpha(x_1)} \Big _{j\eta \bar{\eta} \rightarrow 0}$
4	$G_{\alpha\beta c d}^{(4)}(x_1, x_2, x_3, x_4)$	$\langle T \psi_d(x_4) \bar{\psi}_c(x_3) \phi_\beta(x_2) \phi_\alpha(x_1) \rangle$ $- G_{\alpha\beta}^{(2)}(x_1, x_2) G_{cd}^{(2)}(x_3, x_4)$ $+ \langle \phi_\beta(x_2) \rangle \langle \phi_\alpha(x_1) \rangle G_{cd}^{(2)}(x_3, x_4)$	$\frac{\delta^4 W}{i\delta\eta_d(x_4) - i\delta\eta_c(x_3) i\delta j_\beta(x_2) i\delta j_\alpha(x_1)} \Big _{j\eta \bar{\eta} \rightarrow 0}$	$\Gamma_{\alpha\beta c d}^{(4)}(x_1, x_2, x_3, x_4) \equiv \frac{\delta^4 \Gamma}{\delta\bar{\psi}_d(x_4) \delta\psi_c(x_3) \delta\phi_\beta(x_2) \delta\phi_\alpha(x_1)} \Big _{j\eta \bar{\eta} \rightarrow 0}$

Table 1. continued

## 2.2 THE RELATIONSHIP BETWEEN THE CONNECTED GREEN'S FUNCTIONS AND THE VERTEX FUNCTIONS

In the last section we showed how to obtain the Green's functions of the theory starting from its Lagrangian. The procedure relied heavily on functional integration and variation which puts harsh constraints on its feasibility in the real (computer) world. To avoid this procedure we use either perturbative methods or the Dyson hierarchy. In this paper we want to discuss the Dyson hierarchy which yields integro-differential relationships between the Green's functions of the theory (see chapter 3). It is now advantageous to cast the Dyson hierarchy in terms of vertex functions instead of Green's functions. The reason for this is two-fold. First of all the vertex functions are directly related to the bare vertices in the Lagrangian which actually represent the lowest order approximation to the vertex functions (therefore also called dressed vertices) and secondly the vertex functions are one-particle irreducible so that they do not contain singularities due to propagators. They still contain singularities corresponding to 2-particle intermediate states and in general many-particle intermediate states. Based on its one-particle irreducibility we will, in chapter 4, perform a crossing-symmetric reduction of the 2-particle intermediate states in the equations to also remove the cuts due to these 2-particle intermediate states. We finally will be left with highly connected vertex functions, rather well behaved and containing all the complicated information of dressed vertices.

In this section we show now how to obtain the vertex functions directly from the connected Green's functions without going through a Legendre transformation and vice versa. Let's start for example with a relation between the boson propagator and the boson 2-point vertex function. The boson field is given by (see table 1):

$$\phi_{\alpha}(x) = \frac{\delta W[j; \eta, \bar{\eta}]}{i\delta j_{\alpha}(x)}, \quad (2.7)$$

differentiating now with respect to the field  $\phi_{\beta}$  we obtain:

$$\begin{aligned} \frac{\delta}{\delta\phi_{\beta}(x_2)} \left( \frac{\delta W}{i\delta j_{\alpha}(x_1)} \right) &= \delta_{\alpha\beta} \delta^4(x_1-x_2) \\ &= i \int dx_3 \left[ \sum_{\gamma} \frac{\delta^2 W}{\delta j_{\gamma}(x_3) \delta j_{\alpha}(x_1)} \frac{\delta^2 \Gamma}{\delta\phi_{\beta}(x_2) \delta\phi_{\gamma}(x_3)} + \sum_c \frac{\delta^2 W}{\delta\eta_c(x_3) \delta j_{\alpha}(x_1)} \frac{\delta^2 \Gamma}{\delta\phi_{\beta}(x_2) \delta\bar{\psi}_c(x_3)} \right] \end{aligned}$$

$$- \sum_c \frac{\delta^2 W}{\delta \bar{\eta}_c(x_3) \delta j_\alpha(x_1)} \frac{\delta^2 \Gamma}{\delta \phi_\beta(x_2) \delta \psi_c(x_3)} \Big]. \quad (2.8)$$

Taking the sources to zero, we find using the definitions of table 1:

$$i \delta_{\alpha\beta} \delta^4(x_1-x_2) = \sum_\gamma \int dx_3 G_{\alpha\gamma}^{(2)}(x_1, x_3) \Gamma_{\gamma\beta}^{(2)}(x_3, x_2). \quad (2.9)$$

We proceed in a similar fashion to obtain the relationship between the fermion propagator and the fermion 2-point vertex function. The antifermion field is given by:

$$\bar{\psi}_a(x) = \frac{\delta W[j; \eta, \bar{\eta}]}{-i \delta \eta_a(x)}. \quad (2.10)$$

We would like to remark here that taking the sources for the fermion fields to zero, which, as we saw, yields the same result as taking the expectation value of the corresponding time ordered fields, forces the expectation values to be zero since we can produce fermions only in fermion - antifermion pairs. Therefore, also all expectation values over an odd number of fermion fields will vanish. Differentiating now (2.10) with respect to  $\bar{\psi}_b(x)$  we obtain:

$$\begin{aligned} \frac{\delta}{\delta \bar{\psi}_b(x_2)} \left( \frac{\delta W}{-i \delta \eta_a(x_1)} \right) &= \delta_{ab} \delta^4(x_1-x_2) \\ &= i \int dx_3 \left[ - \sum_\gamma \frac{\delta^2 W}{\delta j_\gamma(x_3) \delta \eta_a(x_1)} \frac{\delta^2 \Gamma}{\delta \bar{\psi}_b(x_2) \delta \phi_\gamma(x_3)} - \sum_c \frac{\delta^2 W}{\delta \eta_c(x_3) \delta \eta_a(x_1)} \frac{\delta^2 \Gamma}{\delta \bar{\psi}_b(x_2) \delta \psi_c(x_3)} \right. \\ &\quad \left. + \sum_c \frac{\delta^2 W}{\delta \bar{\eta}_c(x_3) \delta \eta_a(x_1)} \frac{\delta^2 \Gamma}{\delta \bar{\psi}_b(x_2) \delta \psi_c(x_3)} \right]. \quad (2.11) \end{aligned}$$

In this expression explicit care has to be taken about the ordering of sources and fields since the sources obey a Grassmann algebra necessary due to the anticommuting property of fermion fields.

Taking the sources to zero, we find from the definitions of table 1:

$$-i \delta_{ab} \delta^4(x_1-x_2) = \sum_c \int dx_3 G_{ac}^{(2)}(x_1, x_3) \Gamma_{cb}^{(2)}(x_3, x_2). \quad (2.12)$$

From equation (2.9) and (2.12) we see that the vertex functions  $\Gamma^{(2)}$  are the inverses of the Green's functions  $G^{(2)}$ . Differentiating (2.8) and (2.11) with respect to further fields yields the relationships between higher order Green's functions and vertex functions. These relations and the equations they are obtained from (*i.e.* higher order differentials of (2.8) and (2.11)) can be found in table 2 for the Green's functions up to the 4-point Green's function.

We see from table 2 that the relations become more and more complicated the more legs the Green's functions have. It is therefore very useful to use a diagrammatic recipe to depict these integral relations. The symbols used in this diagrammatic representation are listed in table 3.

The suffix (0) indicates here the bare quantities. Furthermore every loop or tadpole supplies a factor of  $(-i)$  if we go from the equations to the graph and finally arrows have to be put on fermion lines to indicate the motion in time of the fermion along the line, *i.e.* the arrow points from the creation of the fermion to its destruction. The different symbols are connected at corners which have a common summation index and a common integration variable which is to be summed and integrated over respectively. Figure 2 represents the relationship between Green's functions and vertex functions for 3 and 4 legs diagrammatically.

We would like to conclude this chapter by reviewing the whole procedure discussed in this chapter for the 5-point Green's function. In chapter 3 we will truncate the Dyson hierarchy at the level of the 4-point Green's function. The 5-point Green's function will still survive this truncation as a relic of the 4-point interactions contained in our Lagrangian which connect the  $n$ -leg Green's function to the  $(n+2)$ -leg Green's functions in the Dyson hierarchy. Therefore we need to discuss the 5-point Green's function explicitly (This extends the discussion of [6]).

The first step is to construct the three connected 5-point Green's functions from the generating functional  $W$ :

$$G_{\alpha\beta\gamma\delta\epsilon}^{(5)}(x_1, x_2, x_3, x_4, x_5) \equiv \frac{\delta^5 W}{i\delta j_\epsilon(x_5) i\delta j_\delta(x_4) i\delta j_\gamma(x_3) i\delta j_\beta(x_2) i\delta j_\alpha(x_1)} \Bigg|_{\bar{j}\eta \rightarrow 0} \quad (2.13)$$

$$G_{\alpha\beta\gamma de}^{(5)}(x_1, x_2, x_3; x_4, x_5) \equiv \frac{\delta^5 W}{i\delta j_\gamma(x_3) i\delta j_\beta(x_2) i\delta j_\alpha(x_1) i\delta \bar{\eta}_e(x_5) - i\delta \eta_d(x_4)} \Big|_{j\eta \bar{\eta} \rightarrow 0} \quad (2.14)$$

$$G_{abcde}^{(5)}(x_1, x_2, x_3, x_4, x_5) \equiv \frac{\delta^5 W}{i\delta \bar{\eta}_e(x_5) - i\delta \eta_d(x_4) i\delta \bar{\eta}_c(x_3) - i\delta \eta_b(x_2) i\delta j_\alpha(x_1)} \Big|_{j\eta \bar{\eta} \rightarrow 0} \quad (2.15)$$

The Lagrangian we will choose in chapter 3 does not contain any 5-point interaction but we have to choose our phase convention consistent with the crossing-symmetric 1-particle reduction of the 5-point vertex functions discussed in chapter 4:

$$\Gamma_{\alpha\beta\gamma\delta e}^{(5)}(x_1, x_2, x_3, x_4, x_5) \equiv - \frac{\delta^5 \Gamma}{\delta\phi_\epsilon(x_5)\delta\phi_\delta(x_4)\delta\phi_\gamma(x_3)\delta\phi_\beta(x_2)\delta\phi_\alpha(x_1)} \Big|_{j\eta \bar{\eta} \rightarrow 0} \quad (2.16)$$

$$\Gamma_{\alpha\beta\gamma de}^{(5)}(x_1, x_2, x_3; x_4, x_5) \equiv \frac{\delta^5 \Gamma}{\delta\phi_\gamma(x_3)\delta\phi_\beta(x_2)\delta\phi_\alpha(x_1)\delta\bar{\psi}_e(x_5)\delta\psi_d(x_4)} \Big|_{j\eta \bar{\eta} \rightarrow 0} \quad (2.17)$$

$$\Gamma_{abcde}^{(5)}(x_1, x_2, x_3; x_4, x_5) \equiv - \frac{\delta^5 \Gamma}{\delta\bar{\psi}_e(x_5)\delta\psi_d(x_4)\delta\bar{\psi}_c(x_3)\delta\psi_b(x_2)\delta\phi_\alpha(x_1)} \Big|_{j\eta \bar{\eta} \rightarrow 0} \quad (2.18)$$

Starting now from

$$\frac{\delta}{\delta\phi_\epsilon(x_5)} \frac{\delta}{\delta\phi_\delta(x_4)} \frac{\delta}{\delta\phi_\gamma(x_3)} \frac{\delta}{\delta\phi_\beta(x_2)} \left( \frac{\delta W}{i\delta j_\alpha(x_1)} \right) \Big|_{j\eta \bar{\eta} \rightarrow 0} = 0 \quad (2.19)$$

$$\frac{\delta}{\delta\phi_\epsilon(x_5)} \frac{\delta}{\delta\phi_\delta(x_4)} \frac{\delta}{\delta\phi_\gamma(x_3)} \frac{\delta}{\delta\bar{\psi}_b(x_2)} \left( \frac{\delta W}{-i\delta \eta_a(x_1)} \right) \Big|_{j\eta \bar{\eta} \rightarrow 0} = 0 \quad (2.20)$$

$$\frac{\delta}{\delta\phi_\varepsilon(x_5)} \frac{\delta}{\delta\bar{\psi}_d(x_4)} \frac{\delta}{\delta\psi_c(x_3)} \frac{\delta}{\delta\bar{\psi}_b(x_2)} \left( \frac{\delta W}{-i\delta\eta_a(x_1)} \right) \Bigg|_{j\eta\bar{\eta} \rightarrow 0} = 0 \quad (2.21)$$

we obtain the relations between the connected Green's functions and the vertex functions:

$$\begin{aligned} G_{\alpha\varepsilon'\kappa'\rho'\xi'}^{(5)}(x_1, x_5', x_6', x_7', x_9') &= -i \sum_{\varepsilon\beta\gamma\delta\phi} \int dx_2 dx_3 dx_4 dx_5 dx_8 \Gamma_{\varepsilon\beta\gamma\delta\phi}^{(5)}(x_5, x_2, x_3, x_4, x_8) \\ &\times G_{\alpha\varepsilon'}^{(2)}(x_1, x_5) G_{\beta\varepsilon'}^{(2)}(x_2, x_5') G_{\gamma\kappa'}^{(2)}(x_3, x_6') G_{\delta\rho'}^{(2)}(x_4, x_7') G_{\phi\xi'}^{(2)}(x_8, x_9') \\ &\quad -i \sum_{\varepsilon\beta\gamma\delta} \int dx_2 dx_3 dx_4 dx_5 \Gamma_{\varepsilon\beta\gamma\delta}^{(4)}(x_5, x_2, x_3, x_4, ) \\ &\quad \times G_{\alpha\varepsilon\xi'}^{(3)}(x_1, x_5, x_9') G_{\beta\varepsilon'}^{(2)}(x_2, x_5') G_{\gamma\kappa'}^{(2)}(x_3, x_6') G_{\delta\rho'}^{(2)}(x_4, x_7') \\ &\quad -i \sum_{\varepsilon\beta\gamma\phi} \int dx_2 dx_3 dx_5 dx_8 \Gamma_{\varepsilon\beta\gamma\phi}^{(4)}(x_5, x_2, x_3, x_8) \\ &\quad \times G_{\alpha\varepsilon\rho'}^{(3)}(x_1, x_5, x_7') G_{\beta\varepsilon'}^{(2)}(x_2, x_5') G_{\gamma\kappa'}^{(2)}(x_3, x_6') G_{\phi\xi'}^{(2)}(x_8, x_9') \\ &\quad -i \sum_{\varepsilon\beta\delta\phi} \int dx_2 dx_4 dx_5 dx_8 \Gamma_{\varepsilon\beta\delta\phi}^{(4)}(x_5, x_2, x_4, x_8) \\ &\quad \times G_{\alpha\varepsilon\kappa'}^{(3)}(x_1, x_5, x_6') G_{\beta\varepsilon'}^{(2)}(x_2, x_5') G_{\delta\rho'}^{(2)}(x_4, x_7') G_{\phi\xi'}^{(2)}(x_8, x_9') \\ &\quad -i \sum_{\gamma\delta\kappa\phi} \int dx_3 dx_4 dx_6 dx_8 \Gamma_{\kappa\gamma\delta\phi}^{(4)}(x_6, x_3, x_4, x_8) \\ &\quad \times G_{\alpha\varepsilon'\kappa'}^{(3)}(x_1, x_5', x_6) G_{\gamma\kappa'}^{(2)}(x_3, x_6') G_{\delta\rho'}^{(2)}(x_4, x_7') G_{\phi\xi'}^{(2)}(x_8, x_9') \\ &\quad + \sum_{\beta\gamma\delta\varepsilon\kappa\phi} \int dx_2 dx_3 dx_4 dx_5 dx_6 dx_8 \Gamma_{\varepsilon\beta\gamma}^{(3)}(x_5, x_2, x_3) \Gamma_{\kappa\delta\phi}^{(3)}(x_6, x_4, x_8) \\ &\quad \times G_{\alpha\varepsilon\kappa'}^{(3)}(x_1, x_5, x_6) G_{\beta\varepsilon'}^{(2)}(x_2, x_5') G_{\gamma\kappa'}^{(2)}(x_3, x_6') G_{\delta\rho'}^{(2)}(x_4, x_7') G_{\phi\xi'}^{(2)}(x_8, x_9') \\ &\quad + \sum_{\beta\gamma\delta\varepsilon\kappa\phi} \int dx_2 dx_3 dx_4 dx_5 dx_6 dx_8 \Gamma_{\varepsilon\beta\delta}^{(3)}(x_5, x_2, x_4) \Gamma_{\kappa\gamma\phi}^{(3)}(x_6, x_3, x_8) \\ &\quad \times G_{\alpha\varepsilon\kappa'}^{(3)}(x_1, x_5, x_6) G_{\beta\varepsilon'}^{(2)}(x_2, x_5') G_{\gamma\kappa'}^{(2)}(x_3, x_6') G_{\delta\rho'}^{(2)}(x_4, x_7') G_{\phi\xi'}^{(2)}(x_8, x_9') \\ &\quad + \sum_{\beta\gamma\delta\varepsilon\kappa\phi} \int dx_2 dx_3 dx_4 dx_5 dx_6 dx_8 \Gamma_{\varepsilon\beta\phi}^{(3)}(x_5, x_2, x_8) \Gamma_{\kappa\gamma\delta}^{(3)}(x_6, x_3, x_4) \\ &\quad \times G_{\alpha\varepsilon\kappa'}^{(3)}(x_1, x_5, x_6) G_{\beta\varepsilon'}^{(2)}(x_2, x_5') G_{\gamma\kappa'}^{(2)}(x_3, x_6') G_{\delta\rho'}^{(2)}(x_4, x_7') G_{\phi\xi'}^{(2)}(x_8, x_9') \\ &\quad -i \sum_{\varepsilon\beta\gamma} \int dx_2 dx_3 dx_5 \Gamma_{\varepsilon\beta\gamma}^{(3)}(x_5, x_2, x_3) \end{aligned}$$



$$\begin{aligned}
& \times G_{\alpha\varepsilon\rho\xi}^{(4)}(x_1, x_5, x_7, x_9) G_{\beta\varepsilon'}^{(2)}(x_2, x_5) G_{\gamma\kappa'}^{(2)}(x_3, x_6) \\
& \quad - i \sum_{\beta\delta\varepsilon} \int dx_2 dx_4 dx_5 \Gamma_{\varepsilon\beta\delta}^{(3)}(x_5, x_2, x_4) \\
& \times G_{\alpha\varepsilon\kappa'\xi}^{(4)}(x_1, x_5, x_6, x_9) G_{\beta\varepsilon'}^{(2)}(x_2, x_5) G_{\delta\rho}^{(2)}(x_4, x_7) \\
& \quad - i \sum_{\gamma\delta\kappa} \int dx_3 dx_4 dx_6 \Gamma_{\kappa\gamma\delta}^{(3)}(x_6, x_3, x_4) \\
& \times G_{\alpha\varepsilon'\kappa\xi}^{(4)}(x_1, x_5, x_6, x_9) G_{\gamma\kappa'}^{(2)}(x_3, x_6) G_{\delta\rho}^{(2)}(x_4, x_7) \\
& \quad - i \sum_{\beta\varepsilon\phi} \int dx_2 dx_5 dx_8 \Gamma_{\varepsilon\beta\phi}^{(3)}(x_5, x_2, x_8) \\
& \times G_{\alpha\varepsilon\kappa'\rho}^{(4)}(x_1, x_5, x_6, x_7) G_{\beta\varepsilon'}^{(2)}(x_2, x_5) G_{\phi\xi}^{(2)}(x_8, x_9) \\
& \quad - i \sum_{\gamma\kappa\phi} \int dx_3 dx_6 dx_8 \Gamma_{\gamma\kappa\phi}^{(3)}(x_3, x_6, x_8) \\
& \times G_{\alpha\varepsilon'\kappa\rho}^{(4)}(x_1, x_5, x_6, x_7) G_{\gamma\kappa'}^{(2)}(x_3, x_6) G_{\phi\xi}^{(2)}(x_8, x_9) \\
& \quad - i \sum_{\delta\phi\rho} \int dx_4 dx_7 dx_8 \Gamma_{\rho\delta\phi}^{(3)}(x_7, x_4, x_8) \\
& \times G_{\alpha\varepsilon'\kappa'\rho}^{(4)}(x_1, x_5, x_6, x_7) G_{\delta\rho}^{(2)}(x_4, x_7) G_{\phi\xi}^{(2)}(x_8, x_9) \tag{2.22}
\end{aligned}$$

$$\begin{aligned}
G_{\kappa'\rho\xi'ae}^{(5)}(x_6, x_7, x_9; x_1, x_5) &= -i \sum_{eb\gamma\delta\phi} \int dx_2 dx_3 dx_4 dx_5 dx_8 \Gamma_{eb\gamma\delta\phi}^{(5)}(x_5, x_2; x_3, x_4, x_8) \\
& \times G_{ae}^{(2)}(x_1, x_5) G_{be}^{(2)}(x_2, x_5) G_{\gamma\kappa'}^{(2)}(x_3, x_6) G_{\delta\rho}^{(2)}(x_4, x_7) G_{\phi\xi}^{(2)}(x_8, x_9) \\
& \quad - i \sum_{eb\gamma\delta} \int dx_2 dx_3 dx_4 dx_5 \Gamma_{eb\gamma\delta}^{(4)}(x_5, x_2; x_3, x_4, ) \\
& \times G_{ae\xi}^{(3)}(x_1, x_5; x_9) G_{be}^{(2)}(x_2, x_5) G_{\gamma\kappa'}^{(2)}(x_3, x_6) G_{\delta\rho}^{(2)}(x_4, x_7) \\
& \quad - i \sum_{eb\gamma\phi} \int dx_2 dx_3 dx_5 dx_8 \Gamma_{eb\gamma\phi}^{(4)}(x_5, x_2; x_3, x_8) \\
& \times G_{aep}^{(3)}(x_1, x_5; x_7) G_{be}^{(2)}(x_2, x_5) G_{\gamma\kappa'}^{(2)}(x_3, x_6) G_{\phi\xi}^{(2)}(x_8, x_9) \\
& \quad - i \sum_{eb\delta\phi} \int dx_2 dx_4 dx_5 dx_8 \Gamma_{eb\delta\phi}^{(4)}(x_5, x_2; x_4, x_8) \\
& \times G_{\alpha\varepsilon\kappa}^{(3)}(x_1, x_5, x_6) G_{\beta\varepsilon'}^{(2)}(x_2, x_5) G_{\delta\rho}^{(2)}(x_4, x_7) G_{\phi\xi}^{(2)}(x_8, x_9) \\
& \quad - i \sum_{\gamma\delta\kappa\phi} \int dx_3 dx_4 dx_6 dx_8 \Gamma_{\kappa\gamma\delta\phi}^{(4)}(x_6, x_3, x_4, x_8) \\
& \times G_{ae'\kappa}^{(3)}(x_1, x_5; x_6) G_{\gamma\kappa'}^{(2)}(x_3, x_6) G_{\delta\rho}^{(2)}(x_4, x_7) G_{\phi\xi}^{(2)}(x_8, x_9)
\end{aligned}$$

$$\begin{aligned}
& + \sum_{eb\gamma\delta\kappa\phi} \int dx_2 dx_3 dx_4 dx_5 dx_6 dx_8 \Gamma_{eb\gamma}^{(3)}(x_5, x_2; x_3) \Gamma_{\kappa\delta\phi}^{(3)}(x_6, x_4, x_8) \\
& \times G_{ae\kappa}^{(3)}(x_1, x_5; x_6) G_{be'}^{(2)}(x_2, x_5') G_{\gamma\kappa'}^{(2)}(x_3, x_6') G_{\delta\rho'}^{(2)}(x_4, x_7') G_{\phi\xi'}^{(2)}(x_8, x_9') \\
& + \sum_{eb\gamma\delta\kappa\phi} \int dx_2 dx_3 dx_4 dx_5 dx_6 dx_8 \Gamma_{eb\phi}^{(3)}(x_5, x_2; x_8) \Gamma_{\kappa\gamma\delta}^{(3)}(x_6, x_3, x_4) \\
& \times G_{ae\kappa}^{(3)}(x_1, x_5; x_6) G_{be'}^{(2)}(x_2, x_5') G_{\gamma\kappa'}^{(2)}(x_3, x_6') G_{\delta\rho'}^{(2)}(x_4, x_7') G_{\phi\xi'}^{(2)}(x_8, x_9') \\
& + \sum_{eb\gamma\delta\kappa\phi} \int dx_2 dx_3 dx_4 dx_5 dx_6 dx_8 \Gamma_{eb\delta}^{(3)}(x_5, x_2, x_4) \Gamma_{\kappa\gamma\phi}^{(3)}(x_6, x_3, x_8) \\
& \times G_{ae\kappa}^{(3)}(x_1, x_5; x_6) G_{be'}^{(2)}(x_2, x_5') G_{\gamma\kappa'}^{(2)}(x_3, x_6') G_{\delta\rho'}^{(2)}(x_4, x_7') G_{\phi\xi'}^{(2)}(x_8, x_9') \\
& - i \sum_{eb\gamma} \int dx_2 dx_3 dx_5 \Gamma_{eb\gamma}^{(3)}(x_5, x_2, x_3) \\
& \times G_{ae\rho'\xi'}^{(4)}(x_1, x_5; x_7, x_9') G_{be'}^{(2)}(x_2, x_5') G_{\gamma\kappa'}^{(2)}(x_3, x_6') \\
& - i \sum_{eb\delta} \int dx_2 dx_4 dx_5 \Gamma_{eb\delta}^{(3)}(x_5, x_2; x_4) \\
& \times G_{ae\kappa'\xi'}^{(4)}(x_1, x_5; x_6, x_9') G_{be'}^{(2)}(x_2, x_5') G_{\delta\rho'}^{(2)}(x_4, x_7') \\
& - i \sum_{\gamma\delta\kappa} \int dx_3 dx_4 dx_6 \Gamma_{\kappa\gamma\delta}^{(3)}(x_6, x_3, x_4) \\
& \times G_{ae'\kappa'\xi'}^{(4)}(x_1, x_5; x_6, x_9') G_{\gamma\kappa'}^{(2)}(x_3, x_6') G_{\delta\rho'}^{(2)}(x_4, x_7') \\
& - i \sum_{be\phi} \int dx_2 dx_5 dx_8 \Gamma_{eb\phi}^{(3)}(x_5, x_2; x_8) \\
& \times G_{ae\kappa'\rho'}^{(4)}(x_1, x_5; x_6, x_7') G_{be'}^{(2)}(x_2, x_5') G_{\phi\xi'}^{(2)}(x_8, x_9') \\
& - i \sum_{\gamma\kappa\phi} \int dx_3 dx_6 dx_8 \Gamma_{\gamma\kappa\phi}^{(3)}(x_3, x_6, x_8) \\
& \times G_{ae'\kappa\rho'}^{(4)}(x_1, x_5; x_6, x_7') G_{\gamma\kappa'}^{(2)}(x_3, x_6') G_{\phi\xi'}^{(2)}(x_8, x_9') \\
& - i \sum_{\delta\phi\rho} \int dx_4 dx_7 dx_8 \Gamma_{\rho\delta\phi}^{(3)}(x_7, x_4, x_8) \\
& \times G_{ae'\kappa\rho'}^{(4)}(x_1, x_5; x_6, x_7') G_{\delta\rho'}^{(2)}(x_4, x_7') G_{\phi\xi'}^{(2)}(x_8, x_9')
\end{aligned} \tag{2.23}$$

$$\begin{aligned}
G_{\xi'ae'\kappa\rho'}^{(5)}(x_9'; x_1, x_5; x_6, x_7') & = -i \sum_{bcde\phi} \int dx_2 dx_3 dx_4 dx_5 dx_8 \Gamma_{ebcd\phi}^{(5)}(x_5, x_2, x_3, x_4; x_8) \\
& \times G_{ae}^{(2)}(x_1, x_5) G_{be'}^{(2)}(x_2, x_5') G_{k'c}^{(2)}(x_6, x_3) G_{df}^{(2)}(x_4, x_7') G_{\phi\xi'}^{(2)}(x_8, x_9') \\
& - i \sum_{bc\epsilon\phi} \int dx_2 dx_3 dx_5 dx_8 \Gamma_{cb\epsilon\phi}^{(4)}(x_2, x_3; x_5, x_8)
\end{aligned}$$

$$\begin{aligned}
& \times G_{af'e}^{(3)}(x_1, x_7'; x_5) G_{be'}^{(2)}(x_2, x_5') G_{k'c}^{(2)}(x_6', x_3) G_{\phi\xi}^{(2)}(x_8, x_9') \\
& \quad + i \sum_{bcde} \int dx_2 dx_3 dx_4 dx_5 \Gamma_{ebcd}^{(4)}(x_5, x_2; x_3, x_4) \\
& \times G_{ae\xi}^{(3)}(x_1, x_5, x_6') G_{be'}^{(2)}(x_2, x_5') G_{k'c}^{(2)}(x_6', x_3) G_{\phi\xi}^{(2)}(x_8, x_9') \\
& \quad + i \sum_{cd\kappa\phi} \int dx_3 dx_4 dx_6 dx_8 \Gamma_{cd\kappa\phi}^{(4)}(x_3, x_4; x_6, x_8) \\
& \times G_{ae'\kappa}^{(3)}(x_1, x_5'; x_6) G_{k'c}^{(2)}(x_6', x_3) G_{df'}^{(2)}(x_4, x_7') G_{df'}^{(2)}(x_8, x_9') \\
& + \sum_{bcde\kappa\phi} \int dx_2 dx_3 dx_4 dx_5 dx_6 dx_8 \Gamma_{eb\phi}^{(3)}(x_5, x_2; x_8) \Gamma_{cd\kappa}^{(3)}(x_3, x_4; x_6) \\
& \times G_{aek}^{(3)}(x_1, x_5; x_6) G_{be'}^{(2)}(x_2, x_5') G_{k'c}^{(2)}(x_6', x_3) G_{df'}^{(2)}(x_4, x_7') G_{\phi\xi}^{(2)}(x_8, x_9') \\
& - \sum_{bcd\kappa e\phi} \int dx_2 dx_3 dx_4 dx_5 dx_6 dx_8 \Gamma_{cb\epsilon}^{(3)}(x_3, x_2; x_5) \Gamma_{kd\phi}^{(3)}(x_6, x_4; x_8) \\
& \times G_{aek}^{(3)}(x_1, x_5; x_6) G_{be'}^{(2)}(x_2, x_5') G_{k'c}^{(2)}(x_6', x_3) G_{df'}^{(2)}(x_4, x_7') G_{\phi\xi}^{(2)}(x_8, x_9') \\
& \quad - i \sum_{bc\epsilon} \int dx_2 dx_3 dx_5 \Gamma_{cb\epsilon}^{(3)}(x_2, x_3; x_5) \\
& \times G_{af'e\xi}^{(4)}(x_1, x_7'; x_5, x_9') G_{be'}^{(2)}(x_2, x_5') G_{k'c}^{(2)}(x_6', x_3) \\
& \quad - i \sum_{cd\kappa} \int dx_3 dx_4 dx_6 \Gamma_{cd\kappa}^{(3)}(x_3, x_4; x_6) \\
& \times G_{ae'\kappa\xi}^{(4)}(x_1, x_5'; x_6, x_9') G_{k'c}^{(2)}(x_6', x_3) G_{df'}^{(2)}(x_4, x_7') \\
& \quad - i \sum_{bef} \int dx_2 dx_5 dx_7 \Gamma_{eb\phi}^{(3)}(x_5, x_2; x_8) \\
& \times G_{aek'f}^{(4)}(x_1, x_5, x_6', x_7') G_{be'}^{(2)}(x_2, x_5') G_{\phi\xi}^{(2)}(x_4, x_7') \\
& \quad - i \sum_{df\phi} \int dx_4 dx_7 dx_8 \Gamma_{fd\phi}^{(3)}(x_7, x_4; x_8) \\
& \times G_{ae'k'f}^{(4)}(x_1, x_5', x_6', x_7') G_{df'}^{(2)}(x_4, x_7') G_{\phi\xi}^{(2)}(x_8, x_9') \\
& \quad - i \sum_{ck\phi} \int dx_3 dx_6 dx_8 \Gamma_{ck\phi}^{(3)}(x_3, x_6; x_8) \\
& \times G_{ae'k'f}^{(4)}(x_1, x_5', x_6', x_7') G_{k'c}^{(2)}(x_6', x_3) G_{\phi\xi}^{(2)}(x_8, x_9')
\end{aligned} \tag{2.24}$$

whose diagrammatic representation is given in Figure 3. The symbols  $S(n,m)$  and  $A(n,m)$  with  $n,m$  integers appearing in Figure 3 are the usual permutation symbols. They stand for keeping  $n$  legs of the diagram fixed and permuting the other  $m$  legs freely. For example in the equation for the 5-point boson vertex the first symmetrization operator  $S(0,5)$  represents the  $\frac{5!}{2!3!}$  possible permutations of the diagram. The denominator here corrects for the indistinguishability of the legs linked to the 3- and 4-point vertices. Another example is the first symmetrization operator in the equation for the 3-boson-2-fermion vertex  $S(2,3)$ . It stands for  $\frac{3!}{2!}$  possible permutations of the diagram. The two legs to be kept fixed are the fermion legs, while we permute the 3 boson legs on the 4-point interaction. It is important here to realize that we have to imagine the 4-point interaction to be the geometric analog of a tetrahedron, so that the arrow of the fermion line does not enable us to distinguish between the boson legs of this diagram. Finally, we also need the antisymmetrization operator  $A$ . The symbol  $A(1,2,2)$  in the equation for the 4-fermion-1-boson vertex function antisymmetrizes each pair of fermion and antifermion lines separately and so generates four possible diagrams out of each diagram it operates upon.

order	basic equation	relation
2	$\frac{\delta}{\delta\phi_\beta(x_2)} \left( \frac{\delta W}{i\delta j_\alpha(x_1)} \right) = \delta_{\alpha\beta} \delta^4(x_1-x_2)$	$i \delta_{\alpha\beta} \delta^4(x_1-x_2) = \sum_Y \int dx_3 G_{\alpha\gamma}^{(2)}(x_1, x_3) \Gamma_{\gamma\beta}^{(2)}(x_3, x_2)$
2	$\frac{\delta}{\delta\bar{\psi}_b(x_2)} \left( \frac{\delta W}{-i\delta\eta_a(x_1)} \right) = \delta_{ab} \delta^4(x_1-x_2)$	$-i \delta_{ab} \delta^4(x_1-x_2) = \sum_C \int dx_3 G_{\alpha c}^{(2)}(x_1, x_3) \Gamma_{cb}^{(2)}(x_3, x_2)$
3	$\frac{\delta}{\delta\phi_\gamma(x_3)} \frac{\delta}{\delta\phi_\beta(x_2)} \left( \frac{\delta W}{i\delta j_\alpha(x_1)} \right) = 0$	$G_{\alpha\delta\epsilon}^{(3)}(x_1, x_4, x_5) =$ $-i \sum_{\beta\gamma\zeta} \int dx_2 dx_3 dx_6 G_{\alpha\zeta}^{(2)}(x_1, x_6) \Gamma_{\zeta\beta\gamma}^{(3)}(x_6, x_2, x_3) G_{\beta\delta}^{(2)}(x_2, x_4) G_{\gamma\epsilon}^{(2)}(x_3, x_5)$
3	$\frac{\delta}{\delta\phi_\gamma(x_3)} \frac{\delta}{\delta\bar{\psi}_b(x_2)} \left( \frac{\delta W}{-i\delta\eta_a(x_1)} \right) = 0$	$G_{\beta ac}^{(3)}(x_5, x_1, x_4) =$ $-i \sum_{abd} \int dx_2 dx_3 dx_6 G_{ad}^{(2)}(x_1, x_6) \Gamma_{\alpha db}^{(3)}(x_3, x_6, x_2) G_{\alpha\beta}^{(2)}(x_3, x_5) G_{bc}^{(2)}(x_2, x_4)$
4	$\frac{\delta}{\delta\phi_\delta(x_4)} \frac{\delta}{\delta\phi_\gamma(x_3)} \frac{\delta}{\delta\phi_\beta(x_2)} \left( \frac{\delta W}{i\delta j_\alpha(x_1)} \right) = 0$	$G_{\alpha\epsilon\kappa\rho}^{(4)}(x_1, x_5, x_6, x_7) =$ $-i \sum_{\beta\gamma\delta\epsilon} \int dx_2 dx_3 dx_4 dx_5 G_{\alpha\epsilon}^{(2)}(x_1, x_5) \Gamma_{\epsilon\beta\gamma\delta}^{(4)}(x_5, x_2, x_3, x_4) G_{\beta\epsilon'}^{(2)}(x_2, x_5) G_{\gamma\kappa'}^{(2)}(x_3, x_6) G_{\delta\rho'}^{(2)}(x_4, x_7)$ $-\sum_{\beta\gamma\epsilon} \sum_{\omega\tau\theta} \int dx_2 dx_3 dx_4 dx_5 dx_8 dx_9 dx_{10} \Gamma_{\epsilon\beta\gamma}^{(3)}(x_5, x_2, x_3) G_{\beta\epsilon'}^{(2)}(x_2, x_5) G_{\gamma\kappa'}^{(2)}(x_3, x_6) G_{\alpha\omega}^{(2)}(x_1, x_8)$ $\quad \times \Gamma_{\omega\tau\theta}^{(3)}(x_8, x_9, x_{10}) G_{\tau\epsilon}^{(2)}(x_9, x_3) G_{\tau\rho}^{(2)}(x_{10}, x_7)$ $-\sum_{\beta\delta\epsilon} \sum_{\omega\tau\theta} \int dx_2 dx_4 dx_5 dx_8 dx_9 dx_{10} \Gamma_{\epsilon\beta\delta}^{(3)}(x_5, x_2, x_4) G_{\beta\epsilon'}^{(2)}(x_2, x_5) G_{\delta\rho'}^{(2)}(x_4, x_7) G_{\alpha\omega}^{(2)}(x_1, x_8)$ $\quad \times \Gamma_{\omega\tau\theta}^{(3)}(x_8, x_9, x_{10}) G_{\tau\epsilon}^{(2)}(x_9, x_3) G_{\tau\kappa'}^{(2)}(x_{10}, x_6)$ $-\sum_{\gamma\delta\kappa} \sum_{\omega\tau\theta} \int dx_3 dx_4 dx_5 dx_8 dx_9 dx_{10} \Gamma_{\kappa\gamma\delta}^{(3)}(x_6, x_3, x_4) G_{\gamma\kappa'}^{(2)}(x_3, x_6) G_{\delta\rho'}^{(2)}(x_4, x_7) G_{\alpha\omega}^{(2)}(x_1, x_8)$ $\quad \times \Gamma_{\omega\tau\theta}^{(3)}(x_8, x_9, x_{10}) G_{\tau\epsilon}^{(2)}(x_9, x_5) G_{\tau\kappa}^{(2)}(x_{10}, x_6)$

Table 2. Relation between connected Green's functions and vertex functions.

4	$\frac{\delta}{\delta\phi_\delta(x_4)} \frac{\delta}{\delta\phi_\gamma(x_3)} \frac{\delta}{\delta\psi_b(x_2)} \left( \frac{\delta IV}{-i\delta\eta_a(x_1)} \right) = 0$	$G_{\kappa\rho'ae'}^{(4)}(x_6, x_7; x_1, x_5) =$ $+ i \sum_{\delta\gamma be} \int dx_2 dx_3 dx_4 dx_5 G_{\alpha}^{(2)}(x_1, x_5) \Gamma_{\gamma\delta eb}^{(4)}(x_3, x_4; x_5, x_2) G_{\gamma\kappa'}^{(2)}(x_5, x_6) G_{be'}^{(2)}(x_2, x_5) G_{\delta\rho'}^{(2)}(x_4, x_7)$ $- \sum_{\gamma be \omega i u} \int dx_2 dx_3 dx_5 dx_8 dx_9 dx_{10} \Gamma_{\gamma eb}^{(3)}(x_3; x_5, x_2) G_{\gamma\kappa'}^{(2)}(x_3, x_6) G_{be'}^{(2)}(x_2, x_5) G_{\alpha}^{(2)}(x_1, x_9)$ $\times \Gamma_{\omega i u}^{(3)}(x_8; x_9, x_{10}) G_{\omega\rho'}^{(2)}(x_8, x_7) G_{ue}^{(2)}(x_{10}, x_5)$ $- \sum_{\delta be \omega i u} \int dx_2 dx_4 dx_6 dx_8 dx_9 dx_{10} \Gamma_{\delta eb}^{(3)}(x_4; x_5, x_2) G_{\delta\rho'}^{(2)}(x_4, x_7) G_{be'}^{(2)}(x_2, x_5) G_{\alpha}^{(2)}(x_1, x_9)$ $\times \Gamma_{\omega i u}^{(3)}(x_8; x_9, x_{10}) G_{\omega\kappa'}^{(2)}(x_8, x_6) G_{ue}^{(2)}(x_{10}, x_5)$ $- \sum_{\gamma\delta\kappa\omega i u} \int dx_3 dx_4 dx_6 dx_8 dx_9 dx_{10} \Gamma_{\kappa\gamma\delta}^{(3)}(x_6, x_3, x_4) G_{\gamma\kappa'}^{(2)}(x_3, x_6) G_{\delta\rho'}^{(2)}(x_4, x_7) G_{\alpha}^{(2)}(x_1, x_9)$ $\times \Gamma_{\omega i u}^{(3)}(x_8; x_9, x_{10}) G_{\omega\kappa'}^{(2)}(x_8, x_6) G_{ue}^{(2)}(x_{10}, x_5)$
4	$\frac{\delta}{\delta\psi_d(x_4)} \frac{\delta}{\delta\psi_c(x_3)} \frac{\delta}{\delta\psi_b(x_2)} \left( \frac{\delta IV}{-i\delta\eta_a(x_1)} \right) = 0$	$G_{ae'kf'}^{(4)}(x_1, x_5, x_6, x_7) =$ $- i \sum_{bcde} \int dx_2 dx_3 dx_4 dx_5 G_{\alpha}^{(2)}(x_1, x_5) \Gamma_{ebcd}^{(4)}(x_5, x_2, x_3, x_4) G_{k'c}^{(2)}(x_6, x_3) G_{be'}^{(2)}(x_2, x_5) G_{df'}^{(2)}(x_4, x_7)$ $+ \sum_{\epsilon bc \alpha\rho q} \int dx_2 dx_3 dx_5 dx_9 dx_{10} dx_{11} \Gamma_{\epsilon cb}^{(3)}(x_5; x_3, x_2) G_{k'c}^{(2)}(x_6, x_3) G_{be'}^{(2)}(x_2, x_5) G_{\alpha\rho}^{(2)}(x_1, x_{10})$ $\times \Gamma_{\alpha\rho q}^{(3)}(x_9; x_{10}, x_{11}) G_{\alpha\epsilon}^{(2)}(x_9, x_4) G_{qf'}^{(2)}(x_{11}, x_7)$ $- \sum_{\kappa cd \alpha\rho q} \int dx_3 dx_4 dx_6 dx_9 dx_{10} dx_{11} \Gamma_{\kappa cd}^{(3)}(x_6; x_3, x_4) G_{k'c}^{(2)}(x_6, x_3) G_{df'}^{(2)}(x_4, x_7) G_{\alpha\rho}^{(2)}(x_1, x_{10})$ $\times \Gamma_{\alpha\rho q}^{(3)}(x_9; x_{10}, x_{11}) G_{\alpha\kappa}^{(2)}(x_9, x_6) G_{qe}^{(2)}(x_4, x_5)$

Table 2. continued























quantity in equation	corresponding symbol
$iG_{(0)}^{(2)}$	 or 
$iG^{(2)}$	 or 
$G^{(3)}$	 or 
$\Gamma_{(0)}^{(3)}$	
$\Gamma^{(3)}$	 or 
$G^{(4)}$	 or  or 
$\Gamma_{(0)}^{(4)}$	
$\Gamma^{(4)}$	 or  or 
$G^{(5)}$	 or  or 
$\Gamma^{(5)}$	 or  or 

Table 3. Rules for constructing a diagrammatic representation for integral equations. Dashed lines with arrows and continuous lines represent fermion lines, dashed lines without arrows and wiggly lines represent boson lines.

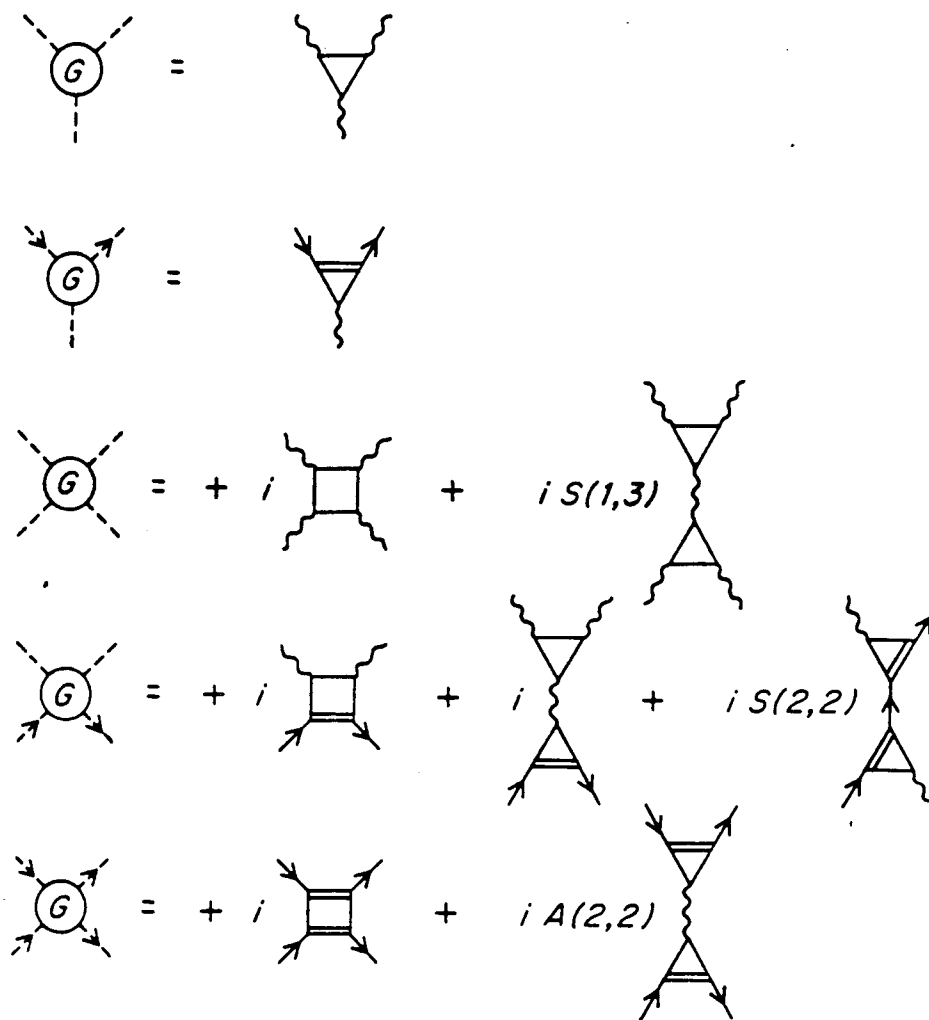


Fig. 2. Relationship between the connected 3- and 4-point Green's functions and the 3- and 4-point vertex functions.



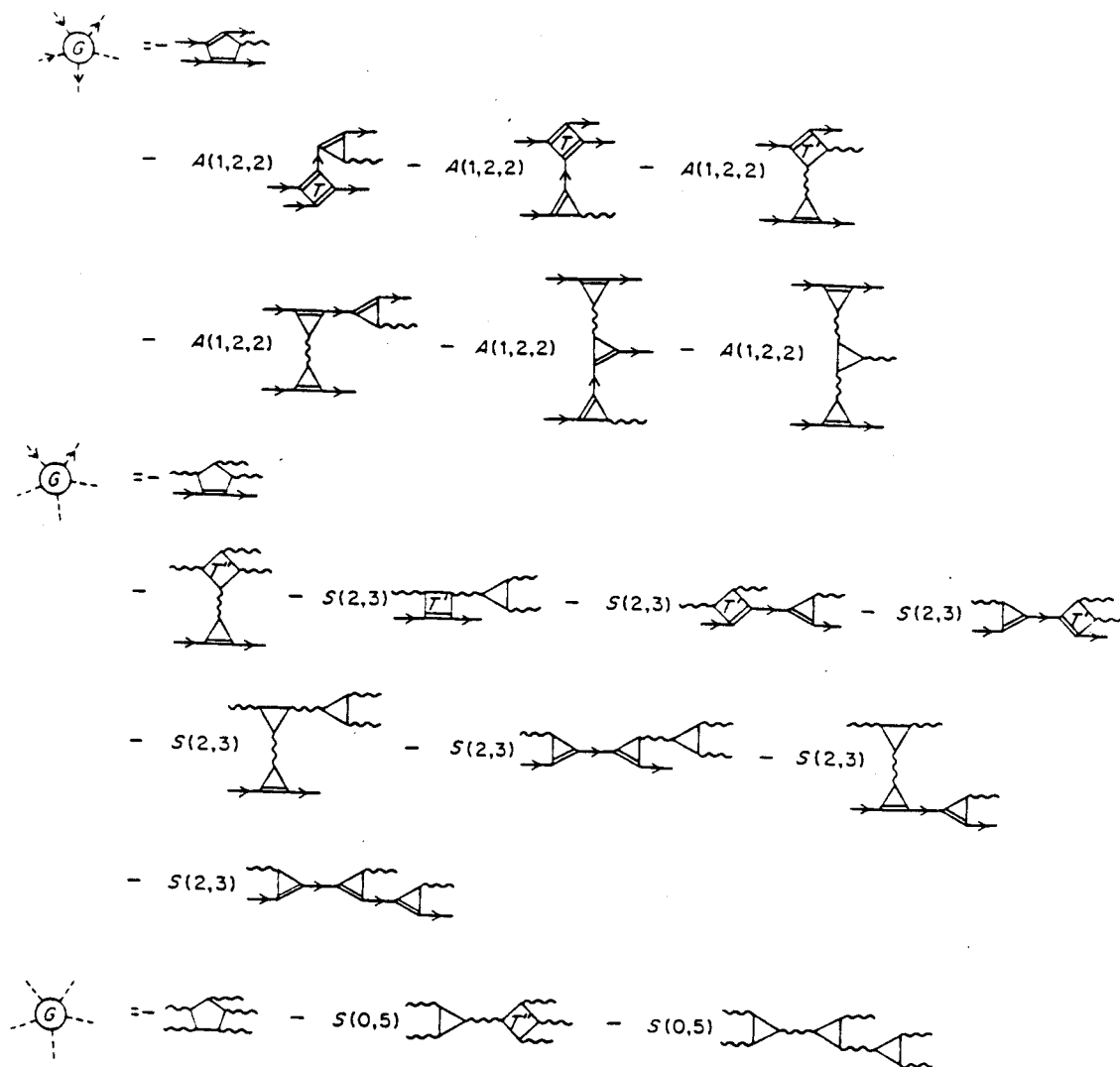


Fig. 3. Relation between the connected 5-point Green's functions and the 5-point vertex functions.

### 3. THE DYSON HIERARCHY

We are now ready to write down the Dyson hierarchy starting from a Lagrangian that contains bosonic and fermionic degrees of freedom interacting via 3- and 4-point interactions. We then truncate this hierarchy at the level of the connected 4-point Green's function using the  $T$  matrix ( $O(4)$ ).

#### 3.1 THE LAGRANGIAN AND THE EQUATIONS OF MOTION

The most general Lagrangian containing interacting boson fields  $\phi_a$  and fermion spinors  $\psi_a$ , sufficient for the discussion of fundamental as well as phenomenological field theories, is:

$$\begin{aligned}
 \mathcal{L}(x) = & \frac{1}{2} \sum_{\alpha,\beta} [\partial_\mu \phi_\alpha(x) B_{\alpha\nu}^{\mu\beta} \partial^\nu \phi_\beta(x) - \phi_\alpha(x) m_{\alpha\beta}^2 \phi_\beta(x)] \\
 & + \sum_a \bar{\psi}_a(x) (i \gamma^\mu \partial_\mu - M_a) \psi_a(x) \\
 & - \sum_{\alpha,\beta,\gamma} \int dy dz \phi_\gamma(z) \Gamma_{(0)\alpha\beta\gamma}^{(3)}(x,y,z) \phi_\beta(y) \phi_\alpha(x) \\
 & - \sum_{\alpha,b,c} \int dy dz \bar{\psi}_c(z) \Gamma_{(0)abc}^{(3)}(x;y,z) \psi_b(y) \phi_\alpha(x) \\
 & - \sum_{\alpha,\beta,\gamma,\delta} \int dw dy dz \phi_\delta(w) \phi_\gamma(z) \Gamma_{(0)\alpha\beta\gamma\delta}^{(4)}(x,y,z,w) \phi_\beta(y) \phi_\alpha(x) \\
 & - \sum_{a,b,c,d} \int dw dy dz \bar{\psi}_d(w) \bar{\psi}_c(z) \Gamma_{(0)abcd}^{(4)}(x,y,z,w) \psi_b(y) \psi_a(x) \\
 & - \sum_{\alpha,\beta,c,d} \int dw dy dz \phi_\beta(w) \bar{\psi}_d(z) \Gamma_{(0)\alpha\beta cd}^{(4)}(x,y;z,w) \psi_c(y) \phi_\alpha(x). \tag{3.1}
 \end{aligned}$$

Here  $B_{\alpha\nu}^{\mu\beta}$  is a bilinear metric that can be found by comparison with the actual Lagrangian. This tensor has a block diagonal form with the rank of the submatrices equal to the rank of the representation in space-time or in flavor space of the particles described by this submatrix.

The 3- and 4-point interactions between the fields are necessary and sufficient to describe all fundamental interactions but they are only sufficient to describe a phenomenological field theory. For example non-relativistic QED contains 4-point interactions, but in general no higher order interactions (there is the possibility of higher-order non-linear terms but even the electron-phonon coupling is in general not taken up to higher orders than 4<sup>[10]</sup>). Another example is hadronic matter. Here the Walecka model<sup>[11]</sup> shows that 3-point interactions alone cannot produce stable matter therefore we have to go up at least to 4-point interactions to make the system bound. Thus, while the

structure of the 4 fundamental theories and the demand to regularize them limits us naturally to 3- and 4-point interactions for them, we have to cut off higher order interactions ( $O(5)$ ) in phenomenological theories using the argument that 3- and 4-point interactions seem to be sufficient to describe the system of interest.

The Lagrangian contains all the information about our system in a compact form. To make this information more easily accessible, we derive the equations of motion for all the  $n$ -point vertex functions from the Lagrangian. The set of all equations of motion forms then the Dyson hierarchy. The equations of motion are obtained by varying the action  $A$  (2.4) with the additional condition that the fields obey the usual equal time commutation relations. A more practical approach is to vary the generating functional for the Green's function  $Z$  (2.2 and 2.3) with respect to the degrees of freedom of the system. For the boson field  $\phi_\alpha$  we thus obtain:

$$0 = \int \mathcal{D}(\phi; \psi, \bar{\psi}) \left[ \frac{\delta I}{\delta \phi_\alpha(x)} + j_\alpha(x) \right] e^{iA} \quad (3.2)$$

We replace now the fields in (3.2) with the variation of  $W$  with respect to the appropriate source term:

$$0 = \left[ \frac{\delta I}{\delta \phi_\alpha(x)} \left( \frac{\delta}{i\delta j}; \frac{\delta}{i\delta \bar{\eta}}, -\frac{\delta}{i\delta \eta} \right) + j_\alpha(x) \right] Z(j; \eta, \bar{\eta}). \quad (3.3)$$

Expressing the classical action  $I$  (2.5) using the Lagrangian in (3.1) we obtain:

$$\begin{aligned} 0 = & \left\{ j_\alpha(x) - \frac{1}{2} \sum_{\beta} \left[ B_{\alpha\nu}^{\mu\beta} \partial^\nu \partial_\mu + B_{\beta\nu}^{\mu\alpha} \partial^\nu \partial_\mu + m_{\alpha\beta}^2 + m_{\beta\alpha}^2 \right] \frac{\delta}{i\delta j_\beta(x)} \right. \\ & - \sum_{\beta\gamma} \int dy dz \Gamma_{(S)\alpha\beta\gamma}^{(3)}(x,y,z) \frac{\delta}{i\delta j_\gamma(z)} \frac{\delta}{i\delta j_\beta(y)} \\ & - \sum_{bc} \int dy dz \Gamma_{(0)abc}^{(3)}(x;y,z) \frac{\delta}{-i\delta \eta_c(z)} \frac{\delta}{i\delta \bar{\eta}_b(y)} \\ & - \sum_{\beta\gamma\delta} \int dw dy dz \Gamma_{(S)\alpha\beta\gamma\delta}^{(4)}(x,y,z,w) \frac{\delta}{i\delta j_\delta(w)} \frac{\delta}{i\delta j_\gamma(z)} \frac{\delta}{i\delta j_\beta(y)} \\ & \left. - \sum_{\beta\alpha d} \int dw dy dz \Gamma_{(S)\alpha\beta cd}^{(4)}(x;w;y,z) \frac{\delta}{i\delta j_\beta(w)} \frac{\delta}{-i\delta \eta_d(z)} \frac{\delta}{i\delta \bar{\eta}_c(y)} \right\} e^W \quad (3.4) \end{aligned}$$

The definitions of the different symmetrized bare vertex functions (labeled with the

subscript (S)) are tabulated in table 4. If we carry out the differentiations with respect to the sources we obtain our field equation for the bosonic degree of freedom:

$$\begin{aligned}
0 = & j_\alpha(x) + \sum_{\alpha_1} \int dx_1 \Gamma_{(0)\alpha\alpha_1}^{(2)}(x, x_1) \frac{\delta W}{i\delta j_{\alpha_1}(x_1)} \\
& - \sum_{\beta\gamma} \int dydz \Gamma_{(S)\alpha\beta\gamma}^{(3)}(x, y, z) \left[ \frac{\delta^2 W}{i\delta j_\gamma(z)i\delta j_\beta(y)} + \frac{\delta W}{i\delta j_\gamma(z)} \frac{\delta W}{i\delta j_\beta(y)} \right] \\
& - \sum_{bc} \int dydz \Gamma_{(0)abc}^{(3)}(x; y, z) \left[ \frac{\delta^2 W}{-i\delta\eta_c(z)i\delta\bar{\eta}_b(y)} + \frac{\delta W}{-i\delta\eta_c(z)} \frac{\delta W}{i\delta\bar{\eta}_b(y)} \right] \\
& - \sum_{\beta\gamma\delta} \int dwdydz \Gamma_{(S)\alpha\beta\gamma\delta}^{(4)}(x, y, z, w) \left[ \frac{\delta^3 W}{i\delta j_\delta(w)i\delta j_\gamma(z)i\delta j_\beta(y)} + \frac{\delta^2 W}{i\delta j_\delta(w)i\delta j_\gamma(z)} \frac{\delta W}{i\delta j_\beta(y)} \right. \\
& \left. + \frac{\delta^2 W}{i\delta j_\delta(w)i\delta j_\beta(y)} \frac{\delta W}{i\delta j_\gamma(z)} + \frac{\delta^2 W}{i\delta j_\gamma(z)i\delta j_\beta(y)} \frac{\delta W}{i\delta j_\delta(w)} + \frac{\delta W}{i\delta j_\delta(w)} \frac{\delta W}{i\delta j_\gamma(z)} \frac{\delta W}{i\delta j_\beta(y)} \right] \\
& - \sum_{\beta\alpha d} \int dwdydz \Gamma_{(S)\alpha\beta cd}^{(4)}(x; w; y, z) \left[ \frac{\delta^3 W}{i\delta j_\beta(w)-i\delta\eta_d(z)i\delta\bar{\eta}_c(y)} \right. \\
& \left. + \frac{\delta^2 W}{i\delta j_\beta(w)-i\delta\eta_d(z)} \frac{\delta W}{i\delta\bar{\eta}_c(y)} + \frac{\delta^2 W}{-i\delta\eta_d(z)i\delta\bar{\eta}_c(y)} \frac{\delta W}{i\delta j_\beta(y)} \right. \\
& \left. + \frac{\delta W}{-i\delta\eta_d(z)} \frac{\delta^2 W}{i\delta j_\beta(w)i\delta\bar{\eta}_c(y)} + \frac{\delta W}{i\delta j_\beta(w)} \frac{\delta W}{-i\delta\eta_d(z)} \frac{\delta W}{i\delta\bar{\eta}_c(y)} \right] \quad (3.5)
\end{aligned}$$

Here we used the definition of the free-boson wave operator.

$$\Gamma_{(0)\alpha\alpha_1}^{(2)}(x, x_1) \equiv -\frac{1}{2} \left[ B_{\alpha\nu}^{\mu\alpha_1} \partial^\mu \partial_\nu + B_{\alpha_1\nu}^{\mu\alpha} \partial^\nu \partial_\mu + m_{\alpha\alpha_1}^2 + m_{\alpha_1\alpha}^2 \right] \delta(x - x_1) \quad (3.6)$$

We will use equation (3.5), the field equation for the bosonic degree of freedom, to derive all equations of motion for the all-boson  $n$ -point vertex functions by taking higher-order derivatives of (3.5) with respect to the source  $j$  and then taking all the sources to zero (see section 3.2).

We can use now the same procedure to derive the field equation for the fermionic degrees of freedom. First we vary the generating functional  $Z$  with respect to the fermion field  $\psi_a$ ,

$$0 = \left[ \frac{\delta I}{\delta \psi_a(x)} \left( \frac{\delta}{i\delta j}; \frac{\delta}{i\delta \eta}, -\frac{\delta}{i\delta \bar{\eta}} \right) + \eta_a(x) \right] W(j; \eta, \bar{\eta}), \quad (3.7)$$

then express again the classical action  $I$  (2.5) in terms of the Lagrangian  $\mathcal{L}$  in (3.1) and carry out the differentiations:

$$\begin{aligned}
0 = & \eta_a(x) + \Gamma_{(0)a'a}^{(2)}(x',x) \frac{\delta W}{i\delta\bar{\eta}_a(x)} \\
& - \sum_{\beta c} \int dy dz \Gamma_{(0)\beta ca}^{(3)}(y;z,x) \left[ \frac{\delta^2 W}{i\delta\bar{\eta}_c(z)i\delta j_\beta(y)} + \frac{\delta W}{i\delta\bar{\eta}_c(z)} \frac{\delta W}{i\delta j_\beta(y)} \right] \\
& - \sum_{bcd} \int dw dy dz \Gamma_{(A)b c d a}^{(4)}(w,y,z,x) \left[ \frac{\delta^3 W}{-i\delta\eta_d(z)i\delta\bar{\eta}_c(y)i\delta i\delta\eta_b(w)} \right. \\
& + \frac{\delta^2 W}{-i\delta\eta_d(z)i\delta\bar{\eta}_c(y)} \frac{\delta W}{i\delta\bar{\eta}_b(w)} + \frac{\delta^2 W}{i\delta\bar{\eta}_c(y)i\delta\bar{\eta}_b(w)} \frac{\delta W}{-i\delta\eta_d(z)} + \frac{\delta^2 W}{i\delta\bar{\eta}_b(w)-i\delta\eta_d(z)} \frac{\delta W}{i\delta\bar{\eta}_c(y)} \\
& \left. + \frac{\delta W}{i\delta\bar{\eta}_b(w)} \frac{\delta W}{i\delta\bar{\eta}_c(y)} \frac{\delta W}{-i\delta\eta_d(y)} \right] \\
& - \sum_{\beta\gamma d} \int dw dy dz \Gamma_{(0)\beta\gamma da}^{(4)}(y;w;z,x) \left[ \frac{\delta^3 W}{i\delta j_\beta(y)i\delta\bar{\eta}_d(z)i\delta j_\gamma(w)} \right. \\
& + \frac{\delta^2 W}{i\delta j_\beta(y)i\delta\bar{\eta}_d(z)} \frac{\delta W}{i\delta j_\gamma(w)} + \frac{\delta^2 W}{i\delta j_\beta(y)i\delta j_\gamma(w)} \frac{\delta W}{i\delta\bar{\eta}_d(z)} + \frac{\delta^2 W}{i\delta j_\gamma(w)i\delta\bar{\eta}_d(z)} \frac{\delta W}{i\delta j_\beta(y)} \\
& \left. + \frac{\delta W}{i\delta j_\gamma(w)} \frac{\delta W}{i\delta j_\beta(y)} \frac{\delta W}{i\delta\bar{\eta}_d(z)} \right] \tag{3.8}
\end{aligned}$$

The definitions of the antisymmetrized bare vertex function (labeled with the subscript (A)) is given in table 4 and the free-fermion wave operator is defined as:

$$\Gamma_{(0)a'a}^{(2)}(x',x) \equiv \delta_{a'a}(i\gamma^\mu \partial'_\mu + M_a) \delta(x' - x) \tag{3.9}$$

Equation (3.8) is the field equation for the fermionic degree of freedom and we will obtain all  $n$ -point vertex functions containing fermion legs by taking further derivatives with respect to the fields and then taking the sources to zero.

Finally let's inspect the expectation value of the field equations, taking the sources to zero:  $j\eta \rightarrow 0$ . We obtain from (3.8) identically zero which is the same as realizing that fermion fields have a zero expectation value to conserve fermion number. From (3.5) on the other hand we obtain the expectation value of the field  $\phi_\alpha$ .

$$\begin{aligned}
\sum_{\alpha_1} \int dx_1 \Gamma_{(0)\alpha\alpha_1}^{(2)}(x, x_1) \langle \phi_{\alpha_1}(x_1) \rangle = & \\
& + \sum_{\beta\gamma} \int dydz \Gamma_{(S)\alpha\beta\gamma}^{(3)}(x, y, z) [G_{\beta\gamma}^{(2)}(y, z) + \langle \phi_{\beta}(y) \rangle \langle \phi_{\gamma}(z) \rangle] \\
& - \sum_{bc} \int dydz \Gamma_{(0)abc}^{(3)}(x; y, z) G_{cb}^{(2)}(z, y) \\
& + \sum_{\beta\gamma\delta} \int dw dy dz \Gamma_{(S)\alpha\beta\gamma\delta}^{(4)}(x, y, z, w) [G_{\beta\gamma\delta}^{(3)}(y, z, w) + G_{\gamma\delta}^{(2)}(z, w) \langle \phi_{\beta}(y) \rangle \\
& + G_{\beta\delta}^{(2)}(y, w) \langle \phi_{\gamma}(z) \rangle + G_{\beta\gamma}^{(2)}(y, z) \langle \phi_{\delta}(w) \rangle + \langle \phi_{\delta}(w) \rangle \langle \phi_{\beta}(y) \rangle \langle \phi_{\gamma}(z) \rangle] \\
& - \sum_{\beta\alpha d} \int dw dy dz \Gamma_{(S)\alpha\beta cd}^{(4)}(x; w; y, z) [G_{\beta cd}^{(3)}(w; z, y) + G_{db}^{(2)}(z, y) \langle \phi_{\beta}(y) \rangle] \quad (3.10)
\end{aligned}$$

Here we used the definitions of table 1. To be able to do the integrations necessary in equation (3.10) we need to know the Green's functions at equal times and coordinates to accommodate the locality of the bare vertices. But the Green's functions are defined as the expectation value of the time-ordered product of fields, so that we obviously get different results for  $G_{cb}^{(2)}$  depending on from which side we approach the equal time condition. This problem can be resolved by realizing that the terms of the Lagrangian responsible for the ambiguity represent the fermion density  $n_{cb}(z, y)$ , *i.e.* they represent  $\bar{\psi}\psi$  for particles and  $\psi\bar{\psi}$  for antiparticles. We have therefore to substitute :

$$G_{cb}^{(2)}(z, y) \rightarrow -n_{bc}(y, z) \quad \text{where} \quad n_{bc}(y, z) \equiv -G_{bc}^+(y, z) + G_{cb}^-(z, y) \quad (3.11)$$

Here  $G_{cb}^{\pm}(z, y)$  represent the propagators for particles and antiparticles respectively. By multiplying now (3.10) with the free-boson propagator and using (2.9) we obtain the Dyson equation for the expectation value of the boson field  $\phi_{\alpha}$  corresponding to the equation of motion for the connected 1-point Green's function:

$$\begin{aligned}
\langle \phi_{\varepsilon}(u) \rangle = & -i \sum_{\varepsilon} \int du G_{(0)\varepsilon\alpha}^{(2)}(u, x) \{ \\
& + \sum_{\beta\gamma} \int dydz \Gamma_{(S)\alpha\beta\gamma}^{(3)}(x, y, z) [G_{\beta\gamma}^{(2)}(y, z) + \langle \phi_{\beta}(y) \rangle \langle \phi_{\gamma}(z) \rangle] \\
& - \sum_{bc} \int dydz \Gamma_{(0)abc}^{(3)}(x; y, z) n_{bc}(y, z) \\
& + \sum_{\beta\gamma\delta} \int dw dy dz \Gamma_{(S)\alpha\beta\gamma\delta}^{(4)}(x, y, z, w) [\langle \phi_{\delta}(w) \rangle \langle \phi_{\beta}(y) \rangle \langle \phi_{\gamma}(z) \rangle
\end{aligned}$$

$$\begin{aligned}
& + G_{\gamma\delta}^{(2)}(z,w) \langle \phi_\beta(y) \rangle + G_{\beta\delta}^{(2)}(y,w) \langle \phi_\gamma(z) \rangle + G_{\beta\gamma}^{(2)}(y,z) \langle \phi_\delta(w) \rangle \\
& -i \sum_{\kappa\zeta\xi} \int dx_1 dx_2 dx_3 G_{\beta\xi}^{(2)}(y,x_3) \Gamma_{\xi\zeta\kappa}(x_3,x_2,x_1) G_{\zeta\gamma}^{(2)}(x_2,z) G_{\kappa\delta}^{(2)}(x_1,w) ] \\
& \quad - \sum_{\beta\alpha} \int dw dy dz \Gamma_{(S)\alpha\beta cd}^{(4)}(x;w;y,z) [ n_{bd}(y,z) \langle \phi_\beta(y) \rangle \\
& +i \sum_{\kappa ef} \int dx_1 dx_2 dx_3 n_{ed}(x_2,z) \Gamma_{\kappa ef}(x_1;x_2,x_3) G_{\kappa\beta}^{(2)}(x_1,w) n_{cf}(y,x_3) ] \} \quad (3.12)
\end{aligned}$$

The diagrammatic representation of this integral equation is given in figure 4. It represents the Hartree equation for a mean field built up out of 3- and 4-point interactions. The equation looks more familiar if we only consider 3-point interactions. The diagrammatic representation of this relation is shown in figure 10.










bare vertex in equation of motion	diagrammatic representation	relation to the bare vertices of the Lagrangian
$\Gamma_{(S)\alpha\beta\gamma}^{(3)}(x,y,z)$		$\Gamma_{(0)\alpha\beta\gamma}^{(3)}(x,y,z) + \Gamma_{(0)\beta\gamma\alpha}^{(3)}(y,z,x)$ $+ \Gamma_{(0)\gamma\alpha\beta}^{(3)}(z,x,y)$
$\Gamma_{(S)\alpha\beta\gamma\delta}^{(4)}(x,y,z,w)$		$\Gamma_{(0)\alpha\beta\gamma\delta}^{(4)}(x,y,z,w) + \Gamma_{(0)\delta\alpha\beta\gamma}^{(4)}(w,x,y,z)$ $+ \Gamma_{(0)\gamma\delta\alpha\beta}^{(4)}(z,w,x,y) + \Gamma_{(0)\beta\gamma\delta\alpha}^{(4)}(y,z,w,x)$
$\Gamma_{(S)\alpha\beta cd}^{(4)}(x,w;y,z)$		$\Gamma_{(0)\alpha\beta cd}^{(4)}(x,w;y,z) + \Gamma_{(0)\beta\alpha cd}^{(4)}(w,x;y,z)$
$\Gamma_{(A)abcd}^{(4)}(z,y,w,x)$		$\Gamma_{(0)abcd}^{(4)}(z,y,w,x) - \Gamma_{(0)abdc}^{(4)}(z,y,w,x)$
$\Gamma_{(0)\alpha\beta\gamma}^{(3)}(x,y,z)$		
$\Gamma_{(0)\alpha bc}^{(3)}(x;y,z)$		
$\Gamma_{(0)\alpha\beta\gamma\delta}^{(4)}(x,y,z,w)$		
$\Gamma_{(0)\alpha\beta cd}^{(4)}(x,w;y,z)$		
$\Gamma_{(0)abcd}^{(4)}(z,y,w,x)$		

Table 4. Relations between the bare vertices in the equation of motion and the bare vertices in the Lagrangian.



$$\begin{aligned}
 X &= - \text{[Diagram 1]} + \text{[Diagram 2]} - \text{[Diagram 3]} \\
 &- \text{[Diagram 4]} + S(1,3) \text{[Diagram 5]} - \text{[Diagram 6]} \\
 &- \text{[Diagram 7]} + \text{[Diagram 8]}
 \end{aligned}$$

Fig. 4. Mean-field equation for the boson field.

### 3.2 DERIVATION AND TRUNCATION OF THE DYSON EQUATIONS

Based on the field equations for the bosonic and fermionic degrees of freedom we will now derive the Dyson hierarchy by using derivatives of the field equations (3.5) and (3.8) with respect to the sources and then take the sources to zero. The integral equations appearing in this derivation are rather lengthy and we therefore develop first a diagrammatic procedure to obtain these Dyson equations.

Let's derive first the Dyson equation for the boson propagator. We start from the field equation for the bosonic degree of freedom (3.5), differentiate it with respect to  $i\dot{\alpha}_2$ , take the sources to zero and use the definitions of the connected Green's function in table 1 to obtain:

$$\begin{aligned}
i\delta_{\alpha_2\alpha}\delta(x_2-x) &= \sum_{\alpha_1} \int dx_1 \Gamma_{(0)\alpha\alpha_1}^{(2)}(x,x_1) G_{\alpha_1\alpha_2}^{(2)}(x_1,x_2) \\
&\quad + \left\{ - \sum_{bc} \int dydz \Gamma_{(0)\alpha bc}^{(3)}(x;y,z) G_{\alpha_2 cb}^{(3)}(x_2; z,y) \right. \\
&\quad - \sum_{\beta\gamma} \int dydz \Gamma_{(S)\alpha\beta\gamma}^{(3)}(x,y,z) \left[ G_{\beta\gamma\alpha_2}^{(3)}(y,z,x_2) + G_{\gamma\alpha_2}^{(2)}(z,x_2) \langle\phi_\beta(y)\rangle + G_{\beta\alpha_2}^{(2)}(y,x_2) \langle\phi_\gamma(z)\rangle \right] \\
&\quad - \sum_{\beta\gamma\delta} \int dwdydz \Gamma_{(S)\alpha\beta\gamma\delta}^{(4)}(x,y,z,w) \left[ G_{\beta\gamma\delta\alpha_2}^{(4)}(y,z,w,x_2) + G_{\beta\gamma\alpha_2}^{(3)}(z,w,x_2) \langle\phi_\beta(y)\rangle \right. \\
&\quad + G_{\beta\delta\alpha_2}^{(3)}(y,w,x_2) \langle\phi_\gamma(z)\rangle + G_{\beta\gamma\alpha_2}^{(3)}(y,z,x_2) \langle\phi_\delta(w)\rangle + G_{\gamma\delta}^{(2)}(z,w) G_{\beta\alpha_2}^{(2)}(y,x_2) \\
&\quad + G_{\beta\delta}^{(2)}(y,w) G_{\gamma\alpha_2}^{(2)}(z,x_2) + G_{\beta\gamma}^{(2)}(y,z) G_{\delta\alpha_2}^{(2)}(w,x_2) + G_{\delta\alpha_2}^{(2)}(w,x_2) \langle\phi_\gamma(z)\rangle \langle\phi_\beta(y)\rangle \\
&\quad \left. + G_{\gamma\alpha_2}^{(2)}(z,x_2) \langle\phi_\delta(w)\rangle \langle\phi_\beta(y)\rangle + G_{\beta\alpha_2}^{(2)}(y,x_2) \langle\phi_\delta(w)\rangle \langle\phi_\gamma(z)\rangle \right] \\
&\quad - \sum_{\beta\alpha d} \int dwdydz \Gamma_{(S)\alpha\beta cd}^{(4)}(x;w;y,z) \left[ - G_{\beta\alpha_2 dc}^{(4)}(w,x_2; z,y) \right. \\
&\quad \left. - G_{\alpha_2 cb}^{(3)}(x_2; z,y) \langle\phi_\beta(w)\rangle - G_{cb}^{(2)}(z,y) G_{\beta\alpha_2}^{(2)}(w,x_2) \right] \left. \right\} \quad (3.13)
\end{aligned}$$

If we multiply equation (3.13) by  $\sum_{\alpha} \int dx G_{(0)\alpha'\alpha}^{(2)}(x',x)$  we obtain an equation of the form

$$G_{\alpha'\alpha_2}^{(2)}(x',x_2) = G_{(0)\alpha'\alpha_2}^{(2)}(x',x_2) + i \sum_{\alpha} \int dx G_{(0)\alpha'\alpha}^{(2)}(x',x) \Sigma_{\alpha'\alpha}^{(2)}(x,x_2), \quad (3.14)$$

where the polarization function  $\Sigma$  contains all the corrections due to the interactions in matter.  $\Sigma$  is given by the curly bracket in (3.13). The diagrammatic representation of equation (3.14) is given in figure 5 in terms of connected Green's functions. The dressed propagators which hook up this connected Green's function to the rest of the diagram are drawn as dashed lines. Arrows indicate fermion lines. Phase factors for dashed loops and tadpoles are not taken into account. The symmetrization operators have to be applied to the bare vertices. Now we have to replace these connected Green's functions in terms of the vertex functions using table 2 or figure 2. The result is given in figure (7a).

We apply now the same procedure to obtain the fermion propagator. Starting from the field equation for the fermionic degree of freedom (3.8), we take a derivative with respect to  $-i\eta_{a_1}$ , take the sources to zero and use the definitions for the connected Green's functions from table 1:

$$\begin{aligned}
-i\delta_{aa_1}\delta(x-x_1) = & -\sum_{a_2} \int dx_2 \Gamma_{(0)a_2a}^{(2)+}(x_2,x) G_{a_1a_2}^{(2)}(x_1,x) \\
& + \left\{ \sum_{\beta c} \int dydz \Gamma_{(0)\beta ca}^{(3)}(y;z,x) \left[ G_{\beta a_1 c}^{(3)}(y;x_1,z) + G_{a_1 c}^{(2)}(x_1,z) \langle \phi_\beta(y) \rangle \right] \right. \\
& + \sum_{\beta \gamma d} \int dw dy dz \Gamma_{(0)\beta \gamma da}^{(4)}(y;w;z,x) \left[ G_{\gamma \beta a_1 d}^{(4)}(w,y;x_1,z) + G_{\beta a_1 d}^{(3)}(y;x_1,z) \langle \phi_\gamma(w) \rangle \right. \\
& + G_{\gamma a_1 d}^{(3)}(w;x_1,z) \langle \phi_\beta(y) \rangle + G_{a_1 d}^{(2)}(x_1,z) \langle \phi_\beta(y) \rangle \langle \phi_\gamma(w) \rangle + G_{a_1 d}^{(2)}(x_1,z) G_{\gamma \beta}^{(2)}(w,y) \left. \right] \\
& + \sum_{bcd} \int dw dy dz \Gamma_{(A)bcda}^{(4)}(y;w,z,x) \left[ G_{dba_1 c}^{(4)}(z,w,x_1,y) \right. \\
& \left. - G_{dx}^{(2)}(z,y) G_{a_1 b}^{(2)}(x_1,w) + G_{db}^{(2)}(z,w) G_{a_1 c}^{(2)}(x_1,y) \right] \left. \right\} \quad (3.15)
\end{aligned}$$

Multiplying (3.14) by  $\sum_a \int dx G_{(0)a_3}^{(2)}(x,x_3)$ , we obtain an equation of the form:

$$G_{a_1 a_3}^{(2)}(x_1, x_3) = G_{(0)a_1 a_3}^{(2)}(x_1, x_3) + i \sum_a \int dx G_{(0)a_3}^{(2)}(x, x_3) \Pi_{a_1 a}(x_1, x) \quad (3.16)$$

Again the polarization function  $\Pi$  contains all the information about the corrections due to the interactions in matter and is given by the curly bracket in (3.15). The diagrammatic representation of (3.16) is given in figure 5. After replacing the connected Green's functions with their corresponding vertex functions from table 2 we obtain the Dyson equation for the fermion propagator (shown in figure 6b).

The Dyson equations for the 3-point vertex functions are obtained from the field equations by taking second derivatives. For the 3-boson vertex function we take first the derivative of (3.5) with respect to  $i\hat{b}_2$  and secondly with respect to  $i\hat{b}_3$ , take the sources to zero and use again the definitions of the connected Green's functions from table 1:

$$\begin{aligned}
0 = & \sum_{\alpha_1} \int dx_1 \Gamma_{(0)\alpha\alpha_1}^{(2)}(x,x_1) G_{\alpha_1\alpha_2\alpha_3}^{(3)}(x_1,x_2,x_3) \\
& + \sum_{bc} \int dydz \Gamma_{(0)abc}^{(3)}(x;y,z) G_{\alpha_2\alpha_3cb}^{(4)}(x_2,x_3;z,y) \\
& - \sum_{\beta\gamma} \int dydz \Gamma_{(S)\alpha\beta\gamma}^{(3)}(x,y,z) \left[ G_{\beta\gamma\alpha_2\alpha_3}^{(4)}(y,z,x_2,x_3) + G_{\gamma\alpha_2\alpha_3}^{(3)}(z,x_2,x_3) \langle \phi_\beta(y) \rangle \right. \\
& + G_{\beta\alpha_2\alpha_3}^{(3)}(y,x_2,x_3) \langle \phi_\gamma(z) \rangle + G_{\gamma\alpha_2}^{(2)}(z,x_2) G_{\beta\alpha_3}^{(2)}(y,x_3) + G_{\beta\alpha_2}^{(2)}(y,x_2) G_{\gamma\alpha_3}^{(2)}(z,x_3) \\
& - \sum_{\beta\gamma\delta} \int dwdydz \Gamma_{(S)\alpha\beta\gamma\delta}^{(4)}(x,y,z,w) \left[ G_{\beta\gamma\delta\alpha_2\alpha_3}^{(5)}(y,z,w,x_2,x_3) \right. \\
& + G_{\gamma\delta\alpha_2\alpha_3}^{(4)}(z,w,x_2,x_3) \langle \phi_\beta(y) \rangle + G_{\beta\delta\alpha_2\alpha_3}^{(4)}(y,w,x_2,x_3) \langle \phi_\gamma(z) \rangle \\
& + G_{\beta\gamma\alpha_2\alpha_3}^{(4)}(y,z,x_2,x_3) \langle \phi_\delta(w) \rangle + G_{\gamma\delta\alpha_2}^{(3)}(z,w,x_2) G_{\beta\alpha_3}^{(2)}(y,x_3) \\
& + G_{\gamma\delta\alpha_3}^{(3)}(z,w,x_3) G_{\beta\alpha_2}^{(2)}(y,x_2) + G_{\beta\alpha_2\alpha_3}^{(3)}(y,x_2,x_3) G_{\gamma\delta}^{(2)}(z,w) \\
& + G_{\beta\delta\alpha_2}^{(3)}(y,w,x_2) G_{\gamma\alpha_3}^{(2)}(z,x_3) + G_{\beta\delta\alpha_3}^{(3)}(y,w,x_3) G_{\gamma\alpha_2}^{(2)}(z,x_2) \\
& + G_{\gamma\alpha_2\alpha_3}^{(3)}(z,x_2,x_3) G_{\beta\delta}^{(2)}(y,w) + G_{\beta\gamma\alpha_2}^{(3)}(y,z,x_2) G_{\delta\alpha_3}^{(2)}(w,x_3) \\
& + G_{\beta\gamma\alpha_3}^{(3)}(y,z,x_3) G_{\delta\alpha_2}^{(2)}(w,x_2) + G_{\delta\alpha_2\alpha_3}^{(3)}(w,x_2,x_3) G_{\beta\gamma}^{(2)}(y,z) \\
& + G_{\delta\alpha_2\alpha_3}^{(3)}(w,x_2,x_3) \langle \phi_\gamma(z) \rangle \langle \phi_\beta(y) \rangle + G_{\gamma\alpha_2\alpha_3}^{(3)}(z,x_2,x_3) \langle \phi_\delta(w) \rangle \langle \phi_\beta(y) \rangle \\
& \quad + G_{\beta\alpha_2\alpha_3}^{(3)}(y,x_2,x_3) \langle \phi_\delta(w) \rangle \langle \phi_\gamma(z) \rangle \\
& + G_{\delta\alpha_2}^{(2)}(w,x_2) G_{\gamma\alpha_3}^{(2)}(z,x_3) \langle \phi_\beta(y) \rangle + G_{\delta\alpha_2}^{(2)}(w,x_2) G_{\beta\alpha_3}^{(2)}(y,x_3) \langle \phi_\gamma(z) \rangle \\
& + G_{\gamma\alpha_2}^{(2)}(z,x_2) G_{\delta\alpha_3}^{(2)}(w,x_3) \langle \phi_\beta(y) \rangle + G_{\gamma\alpha_2}^{(2)}(z,x_2) G_{\beta\alpha_3}^{(2)}(y,x_3) \langle \phi_\delta(w) \rangle \\
& \left. + G_{\beta\alpha_2}^{(2)}(y,x_2) G_{\delta\alpha_3}^{(2)}(w,x_3) \langle \phi_\gamma(z) \rangle + G_{\beta\alpha_2}^{(2)}(y,x_2) G_{\gamma\alpha_3}^{(2)}(z,x_3) \langle \phi_\delta(w) \rangle \right] \\
& + \sum_{\beta\alpha d} \int dwdydz \Gamma_{(S)\alpha\beta cd}^{(4)}(x;w;y,z) \left[ G_{\beta\alpha_2\alpha_3 dc}^{(5)}(w,x_2,x_3;z,y) + G_{\alpha_2\alpha_3 cb}^{(4)}(x_2,x_3;z,y) \langle \phi_\beta(w) \rangle \right]
\end{aligned}$$

$$\begin{aligned}
& + G_{\alpha_2 cb}^{(3)}(x_2; z, y) G_{\beta \alpha_3}^{(2)}(w, x_3) + G_{\alpha_3 cb}^{(3)}(x_3; z, y) G_{\beta \alpha_2}^{(2)}(w, x_2) \\
& \quad + G_{\beta \alpha_2 \alpha_3}^{(3)}(w, x_2, x_3) G_{cb}^{(2)}(z, y) ] \tag{3.17}
\end{aligned}$$

We see that we need to calculate  $\Gamma_{(0)\alpha\alpha_1}^{(2)}(x, x_1)$  to be able to solve for the 3-boson vertex. We obtain  $\Gamma_{(0)}^{(2)}$  from equation (3.13) by multiplying by  $\sum_{\alpha_2} \int dx_2 \Gamma_{(0)\alpha_2\alpha'}^{(2)}(x_2, x')$ .

$$\Gamma_{(0)\alpha\alpha'}^{(2)}(x, x') = \Gamma_{\alpha\alpha'}^{(2)}(x, x') + i \sum_{\alpha_2} \int dx_2 \Gamma_{\alpha_2\alpha'}^{(2)}(x_2, x') \Pi_{\alpha\alpha_2}(x, x_2) \tag{3.18}$$

The diagrammatic representation of equation (3.18) is given in figure 8. The dots in the circles representing the connected Green's functions indicate the joint where we hook up the external boson legs. With the help of the graphical representation of (3.18) (figure 8) we can obtain the diagrammatic representation of (3.17) where we then replace the connected Green's functions with vertex functions using table 2 and thus obtain the Dyson equation for the 3-boson vertex (figure 9a). There are diagrams in figure 9 which are multiplied with the product of two symmetrization operators. Of these symmetrization operators, one operates on the legs of the bare vertex function contained in the diagram while the other one permutes the external legs of the diagram representing the three corners of the 3-point vertex function. The identification of which operator does which operation is straightforward.

The result in figure 9 already made use of the definitions of the 4- and 5-point Green's function in terms of the full or completely reducible  $T$  matrix and the full or completely reducible 5-point vertex function  $P$  defined in figure 11 and figure 12 respectively. These quantities are directly accessible to experiment and can therefore easily be parametrized. The exact relationship between this truncation of the hierarchy and the various relations between Green's and vertex function will be intensively studied in chapter 4, where we perform crossing symmetric reductions of the 2-particle intermediate states. In a numerical solution we would have to parametrize the 2-particle irreducible kernels of the  $T$  matrix and the pentagon. For massive particles all the singularities of the kernels would lie at high momenta, so that for a theory describing low excitations, we could parametrize the kernels smoothly. We would obtain so on- and off-shell values for the  $T$  matrix and the pentagon and could fix our parameters by comparison with the experimental on-shell data.

Now we are finally ready to derive the Dyson equation for the 2-fermion-1-boson

vertex. We start from the field equation for the fermionic degree of freedom (3.8), take first the derivative with respect to  $-i\bar{\eta}_1$  and secondly with respect to  $-i\bar{\eta}_{c_1}$ , take the sources to zero and use again the definitions of the connected Green's functions from table 1:

$$\begin{aligned}
0 = & \sum_{\alpha_1} \int dx_1 \Gamma_{(0)\alpha\alpha_1}^{(2)}(x, x_1) G_{\alpha_1 b_1 c_1}^{(3)}(x_1; u, v) \\
& - \sum_{\beta\gamma} \int dydz \Gamma_{(S)\alpha\beta\gamma}^{(3)}(x, y, z) \left[ G_{\beta\gamma b_1 c_1}^{(4)}(y, z; u, v) \right. \\
& \left. + G_{\gamma b_1 c_1}^{(3)}(z; u, v) \langle \phi_\beta(y) \rangle + G_{\beta b_1 c_1}^{(3)}(y; u, v) \langle \phi_\gamma(z) \rangle \right] \\
& + \sum_{bc} \int dydz \Gamma_{(0)abc}^{(3)}(x; y, z) \left[ G_{bcb_1 c_1}^{(4)}(z, y, u, v) - G_{b_1 b}^{(2)}(u, y) G_{cc_1}^{(2)}(z, v) \right] \\
& - \sum_{\beta\gamma\delta} \int dw dydz \Gamma_{(S)\alpha\beta\gamma\delta}^{(4)}(x, y, z, w) \left[ G_{\beta\gamma\delta b_1 c_1}^{(5)}(y, z; w; u, v) \right. \\
& + G_{\gamma\delta b_1 c_1}^{(4)}(z, w; u, v) \langle \phi_\beta(y) \rangle + G_{\beta\delta b_1 c_1}^{(4)}(y, w; u, v) \langle \phi_\gamma(z) \rangle + G_{\beta\gamma b_1 c_1}^{(4)}(y, z; u, v) \langle \phi_\delta(w) \rangle \\
& + G_{\beta b_1 c_1}^{(3)}(y; u, v) G_{\gamma\delta}^{(2)}(z, w) + G_{\gamma b_1 c_1}^{(3)}(z; u, v) G_{\beta\delta}^{(2)}(y, w) + G_{\delta b_1 c_1}^{(3)}(w; u, v) G_{\beta\gamma}^{(2)}(y, z) \\
& + G_{\delta b_1 c_1}^{(3)}(w; u, v) \langle \phi_\gamma(z) \rangle \langle \phi_\beta(y) \rangle + G_{\gamma b_1 c_1}^{(3)}(z; u, v) \langle \phi_\delta(w) \rangle \langle \phi_\beta(y) \rangle \\
& \left. + G_{\beta b_1 c_1}^{(3)}(y; u, v) \langle \phi_\gamma(z) \rangle \langle \phi_\delta(w) \rangle \right] \\
& - \sum_{\beta\alpha d} \int dw dydz \Gamma_{(S)\alpha\beta cd}^{(4)}(x; w; y, z) \left[ -G_{\beta dcb_1 c_1}^{(5)}(w; z, y, u, v) \right. \\
& + G_{\beta dc_1}^{(3)}(w; z, v) G_{b_1 c}^{(2)}(u, y) + G_{\beta b_1 c}^{(3)}(w; u, y) G_{dc_1}^{(2)}(z, v) - G_{\beta b_1 c_1}^{(3)}(w; u, v) G_{cb}^{(2)}(z, y) \\
& \left. - G_{dcb_1 c_1}^{(4)}(z, y, u, v) \langle \phi_\beta(w) \rangle + G_{dc_1}^{(2)}(z, v) G_{b_1 c}^{(2)}(u, y) \langle \phi_\beta(w) \rangle \right] \quad (3.19)
\end{aligned}$$

We use then the diagrammatic representation of (3.18) (figure 8) to display (3.19) graphically and replace the connected Green's function with the corresponding vertex functions from table 2.

Again we truncate the hierarchy using the  $T$  matrix and the pentagon  $P$ . The resulting Dyson equation is represented in figure (9b).

Higher-order Dyson equations can be derived analogously by taking higher order derivatives, but we stop here since our truncation procedure, *i.e.* our parametrized 2-particle irreducible 4- and 5-point vertex functions include all the higher-order information

via their parametrization and thus via their experimental input. For completeness we show the Dyson equations to  $O(4)$  with only 3-point interactions in the Lagrangian in figure (10). Figure 13 finally shows the Dyson equations for the fields and the propagators after substitution of the  $T$  matrix.

The diagrammatic representation of equation (3.13) is shown as a series of terms:

- Term 1: A wavy line with a dot, followed by an equals sign, then a wavy line, a minus sign, a dashed loop with a vertex labeled  $G$ , a dashed line, a minus sign,  $S(1,2)$ , a wavy line with a dot, and a cross.
- Term 2: A plus sign, a wavy line with a dot, a dashed loop with arrows and a vertex labeled  $G$ , a dashed line, a minus sign, a wavy line with a dot, a dashed loop with a vertex labeled  $G$ , and a dashed line.
- Term 3: A minus sign,  $i S(1,3)$ , a wavy line with a dot, a dashed loop with a vertex labeled  $G$ , a dashed line, a minus sign,  $S(1,3)$ , a wavy line with a dot, and a loop.
- Term 4: A minus sign,  $S(1,3)$ , a wavy line with a dot, a plus sign, a wavy line with a dot, a dashed loop with arrows and a vertex labeled  $G$ , and a dashed line.
- Term 5: A plus sign, a wavy line with a dot, a dashed loop with arrows and a vertex labeled  $G$ , a dashed line, a plus sign, a wavy line with a dot, and a loop.

Fig. 5. Diagrammatic representation of equation (3.13).



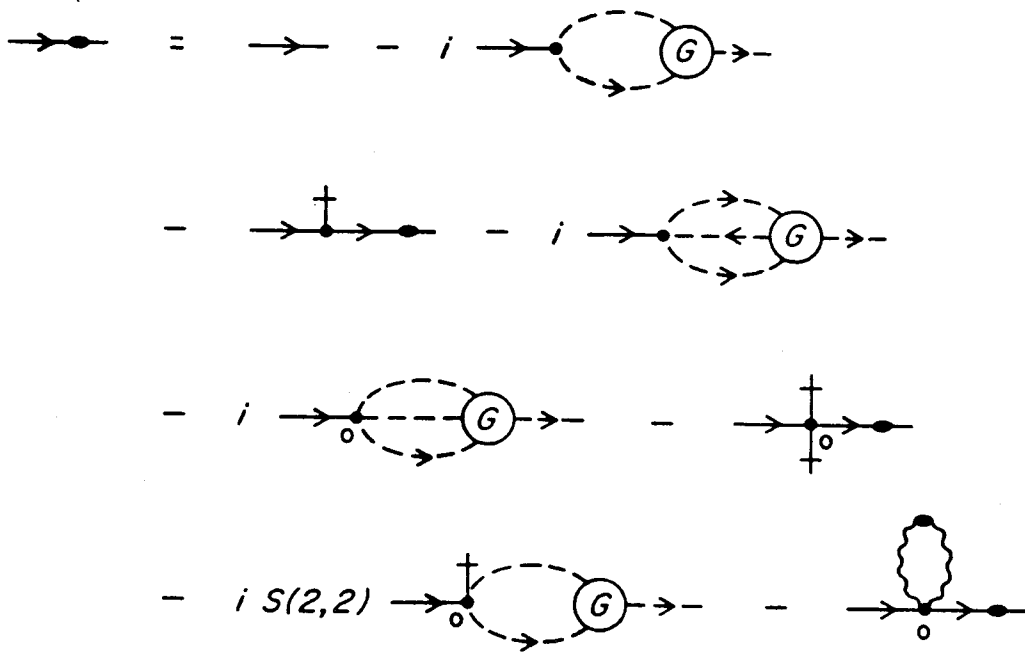



Fig. 6. Diagrammatic representation of equation (3.14).



$$\begin{aligned}
\Gamma_{(0)\alpha\alpha_1}^{(2)}(x, x_1) &= \Gamma_{\alpha\alpha_1}^{(2)}(x, x_1) + \text{diagram 1} + S(1,2) \text{diagram 2} \\
&- \text{diagram 3} + \text{diagram 4} + S(1,3) \text{diagram 5} \\
&- S(1,3) \text{diagram 6} + S(1,3) \text{diagram 7} - \text{diagram 8} \\
&- \text{diagram 9} + \text{diagram 10}
\end{aligned}$$



Fig. 8. Diagrammatic representation of the equation for the bare 2-boson vertex function (equation 3.18).

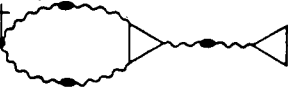
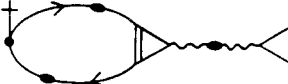
a.)  $\triangleleft = S(1,2) \bullet -$    $+ \img alt="Diagram: an oval loop with a square box labeled T on the right side." data-bbox="548 211 656 251"/>$

$+ \img alt="Diagram: a scalloped loop connected to a triangle via a wavy line." data-bbox="254 278 441 321"/>  $- \img alt="Diagram: an oval loop connected to a triangle via a wavy line." data-bbox="498 281 685 321"/>$$

$- \img alt="Diagram: a scalloped loop with a square box labeled P on the right side." data-bbox="254 348 361 391"/>  $+ \img alt="Diagram: an oval loop with a square box labeled P on the right side." data-bbox="408 351 515 391"/>$$

$+ \img alt="Diagram: a scalloped loop with a square box labeled T on the right side, connected to a triangle via a wavy line." data-bbox="254 418 428 461"/>  $- \img alt="Diagram: an oval loop with a square box labeled T on the right side, connected to a triangle via a wavy line." data-bbox="485 421 665 461"/>$$

$+ S(1,2)S(1,3) \dagger - S(1,3) \dagger$    $+ \dagger$  

$+ S(1,3) \dagger$    $- \dagger$  



$+ S(1,2)S(1,3)$    $- S(1,2)$  

Fig. 9. Diagrammatic representation of the Dyson equations for the 3-point vertex functions.  
 a.) 3-boson vertex function, b.) 2-fermion-1-boson vertex function.

b.)  $\triangleleft = \bullet - \text{[Diagram 1]} + \text{[Diagram 2]}$

$+ \text{[Diagram 3]} - \text{[Diagram 4]}$

$- \text{[Diagram 5]} + \text{[Diagram 6]}$



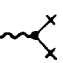
$+ \text{[Diagram 7]} - \text{[Diagram 8]}$



$+ \dagger - S(1,3) \text{[Diagram 9]} + \text{[Diagram 10]}$


$+ S(1,3) \text{[Diagram 11]} - \text{[Diagram 12]}$



$+ S(1,2) \text{[Diagram 13]}$



Fig. 9. continued



a.)  $X = -$    $+$    $-$  

b.)  $\text{wavy line} = \text{wavy line} - S(1,2) \text{wavy line with cross}$   
 $+$    $-$  

$\text{arrow} = \text{arrow} - \text{arrow with cross}$   
 $+$  

c.)  $\triangleleft = S(1,2) \bullet -$    $+$  

$- S(1,2)$    $+ S(1,2)$  

$\triangleleft = \bullet -$    $+$  



$- S(1,2)$    $-$  

Fig. 10. Dyson equations for the a.) fields, b.) propagators and c.) 3-point vertex functions for a Lagrangian containing only 3-point interactions.

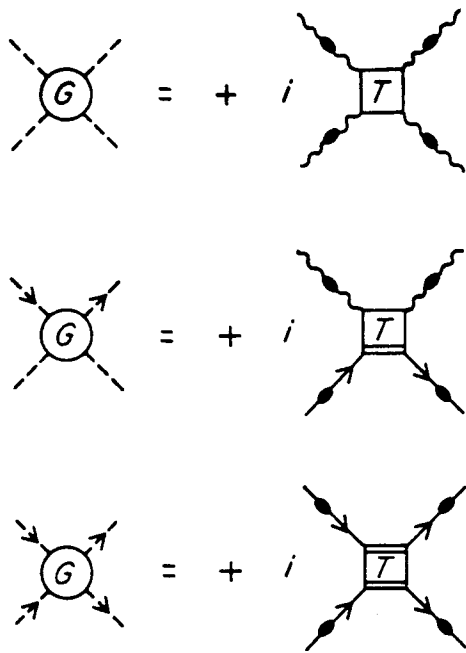


Fig. 11. Definition of the  $T$  matrix.

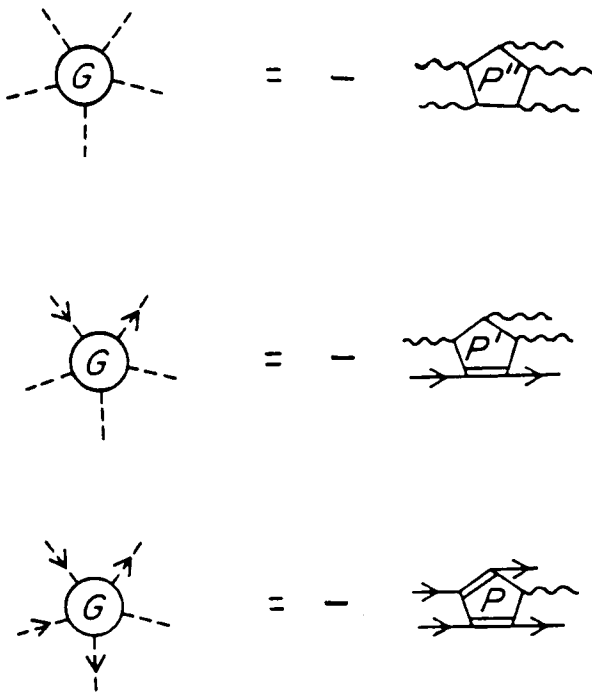


Fig. 12. Definition of the completely reducible 5-point vertex function  $P$ .



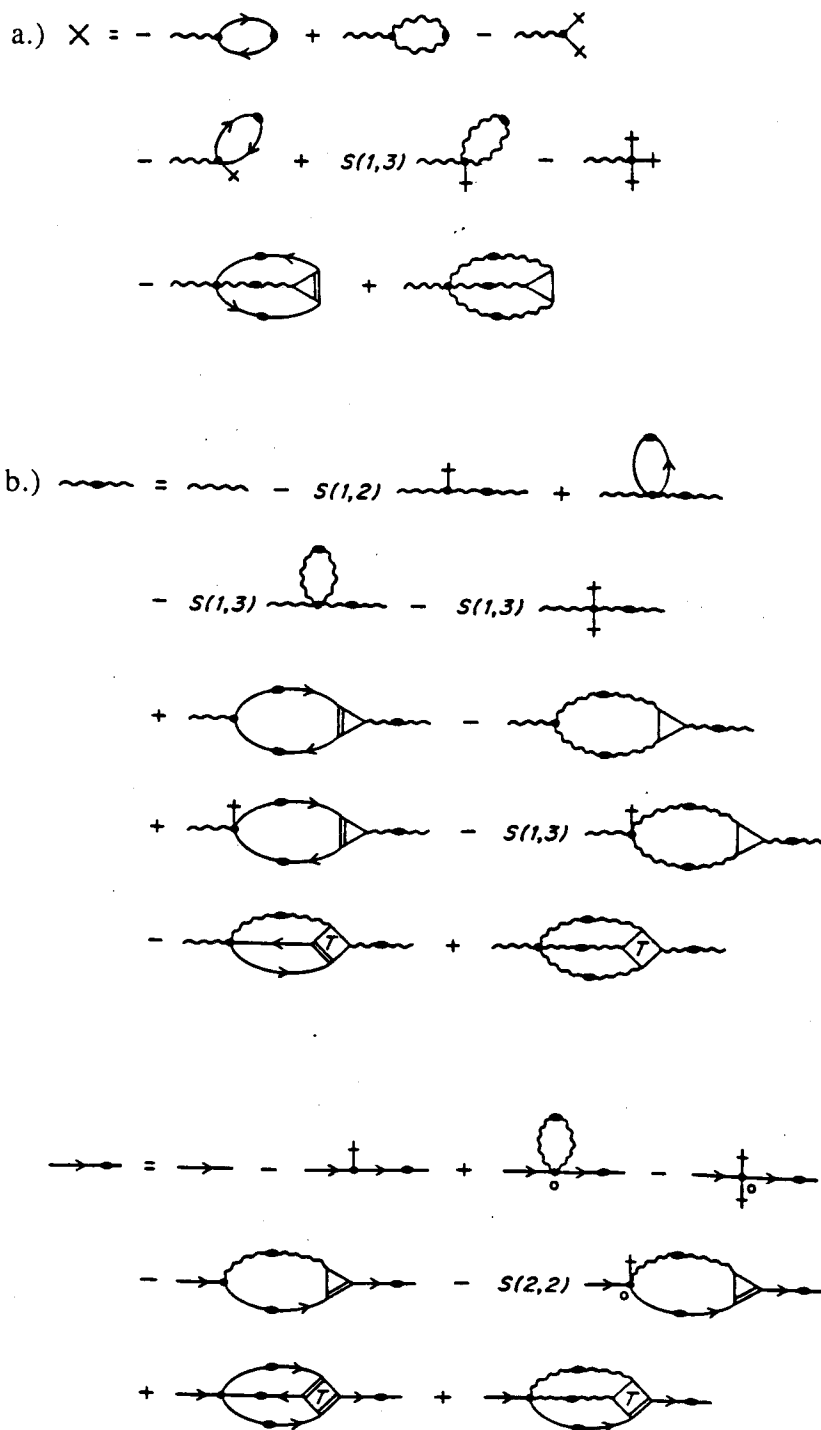


Fig. 13. Diagrammatic representation of the Dyson equations up to  $O(3)$  after introduction of the  $T$  matrix. a.) fields, b.) propagators.

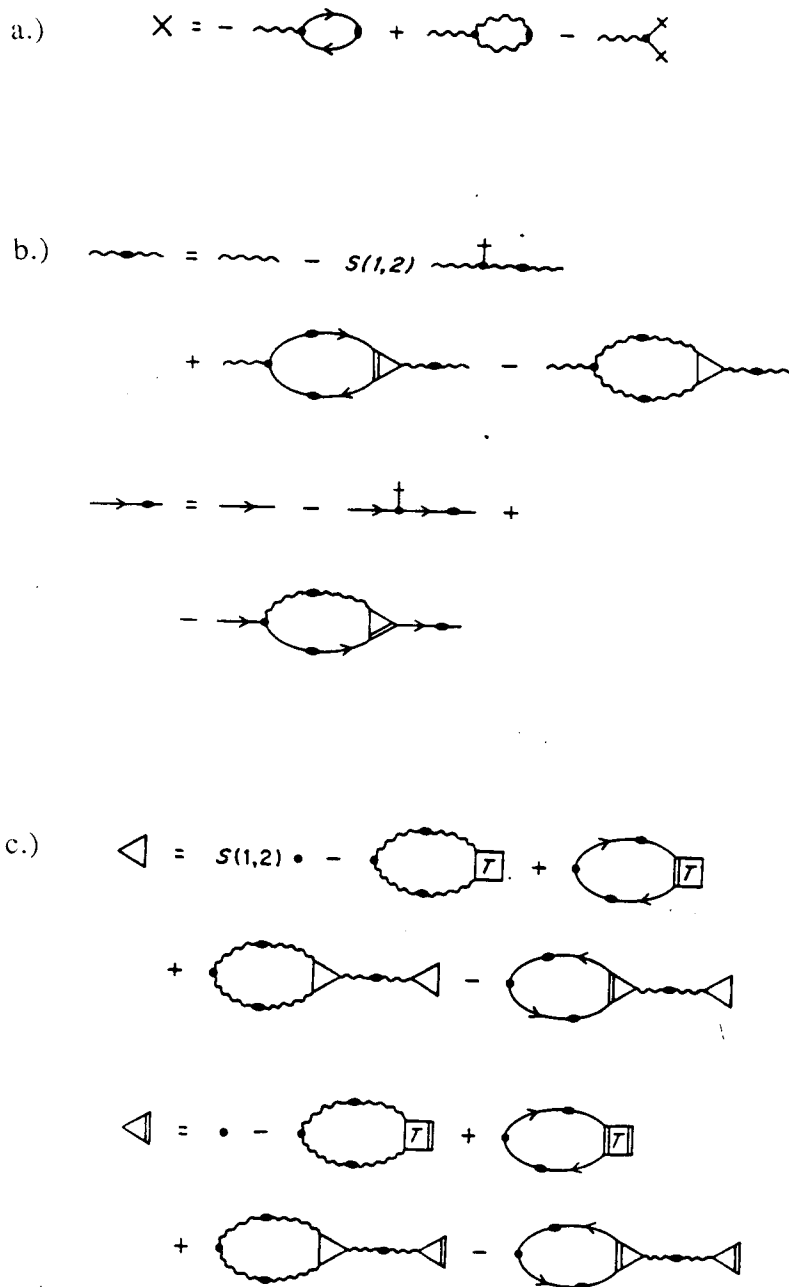


Fig. 14. Diagrammatic representation of the Dyson equations up to  $O(4)$  after introduction of the  $T$ -matrix with only 3-point interactions in the Lagrangian. a.) fields, b.) propagators, c.) 3-point vertex function.

## 4. CROSSING-SYMMETRIC REDUCTION

In this chapter we perform the complete crossing-symmetric reduction for the 2-particle intermediate states of the  $T$  matrix and the pentagon. We show that we obtain a reduction hierarchy which we truncate on the level of the 6-point vertex function ( $\alpha(6)$ ) to be consistent with the truncation of the Dyson hierarchy ( $\alpha(4)$ ). The reduction hierarchy can furthermore be used to test the quality of the approximation, *i.e.* the truncation. This chapter is a generalization and extension of work done by Korpa and Siemens<sup>[9]</sup> who performed the crossing-symmetric 2-particle reduction of the  $T$  matrix.

### 4.1 TOPOLOGICAL CLASSIFICATION AND THE REDUCTION HIERARCHY

In chapter 3 we truncated the Dyson hierarchy on the level of the 4-point vertex function through introduction of the  $T$  matrix. If we now compare the Dyson equations for the fields, propagators, and the 3-point vertex functions first for only 3-point interactions in the Lagrangian (Fig. 14) and then for 3- and 4-point interactions in the Lagrangian (Fig. 13,9) we realize that 3- and 4-point interactions in the Lagrangian introduce 2 and 3-particle intermediate states respectively. The topological classification of diagrams containing these intermediate states is depicted in Figure 15. The second column represents diagrams containing 1-particle intermediate states. These diagrams are generated by the sources which also represent interactions in the Lagrangian. We removed the sources through the Legendre transformation from the Lagrangian and thus made the vertex functions 1-particle irreducible but we still obtain 1-particle reducible diagrams in the Dyson hierarchy. They reappear after we replace the connected  $n$ -leg Green's function with the appropriate vertex functions (compare the first column of Fig. 15 with Table 2 and Fig. 3). Diagrams (h) and (i) do not appear explicitly in these equations since we have no 5-point interactions in the Lagrangian and the Dyson equations connect only Green's functions of order  $n$  to Green's functions of order  $(n + 1)$  and  $(n + 2)$ .

In general an  $n$ -point interaction in the Lagrangian will generate  $(n - 1)$ -particle intermediate states in the Dyson hierarchy. All higher order intermediate states will then be generated if we solve the Dyson hierarchy iteratively. Since we truncate the Dyson hierarchy on the level of the 4-point vertex function ( $O(4)$ ) we lose all the information about 2- and 3-particle intermediate states of the 4- and 5-point vertex functions which are explicitly contained in the Dyson equations for the fields, propagators and 3-point vertex functions. For consistency we have therefore to perform a reduction of the 2 and 3-particle

intermediate states for the  $T$  matrix and the pentagon. This reduction has to be crossing-symmetric since crossing-symmetry is a generic property of a system of interacting particles.

In this chapter we develop a crossing-symmetric reduction of the  $T$  matrix and the pentagon with respect to the 2-particle intermediate states. The crossing-symmetric reduction for the 3-particle intermediate states is rather difficult and therefore outside the scope of this text. We must note that a 2-particle reduction is necessary and sufficient for all Lagrangians containing only 3-point interactions while it is necessary but not sufficient for Lagrangians containing also 4-point interactions. Still, in a lot of applications the 2-particle reduction will be satisfactory since either the masses of the particles involved suppress the 3-particle intermediate states (e.g. QHD) or conservation laws forbid most of them (e.g. non-relativistic QED).

Next to diagram (a) of Fig. 15 which represents the 2-particle reducible diagrams of the 3-point vertex function, we have two topologically distinct diagrams representing the 4-point vertex function and containing 2-particle intermediate states. Diagram (b) of Fig. 15 represents a scattering process and we call this topological class of diagrams a 2-particle reducible scattering diagram or in short, a scattering reducible diagram. Diagram (c) of Fig. 15 on the other hand represents a decay process and we therefore call this class a 2-particle reducible decay diagram, or decay reducible diagram. Diagrams (d) and (e) along with all higher order topological classes of diagrams containing 2-particle intermediate states should be contained in this reduction explicitly. However, we will truncate this reduction hierarchy by setting the 6-point vertex function (hexagon) to zero and thus have only to take care of diagram (d) when discussing the reduction of the pentagon. This truncation ( $\alpha(6)$ ) is consistent with the truncation of the Dyson hierarchy ( $\alpha(4)$ ).

Inspecting the procedure previously developed (particularly Fig. 15) it seems reasonable to ask about the general structure of the reduction hierarchy. Until this point we have talked only about a hierarchy in terms of the order of the vertex functions characterizing a specific topological class. Obviously the complete reduction hierarchy is also a hierarchy in terms of the different topological classes, representing the  $n$ -particle intermediate states. We are using then the Dyson hierarchy to truncate the complete reduction hierarchy on the level of the topological class representing a 4-particle intermediate state ( $\alpha(4)$ ). The complete reduction hierarchy by itself represents a necessary and sufficient infinite set of equations to solve the field theory. The crucial difference between both approaches, the complete reduction hierarchy and the Dyson hierarchy combined with the reduction hierarchy truncated in one direction, is that they divide the set of all diagrams up into an infinite number of different subsets. Each subset contains an

infinite number of diagrams characterized by distinct topological features. The topological features are, in the case of the Dyson hierarchy, the number of legs of the connected Green's function, while for the complete reduction hierarchy we classify the subsets according to the number of intermediate states. Each subset is represented by an integral equation which sums up the infinite number of diagrams contained in each subset. We use these two independent ways to solve the field theory as a test for the convergence of the Dyson hierarchy by comparing the results of both schemes order by order. For the truncation of the complete reduction hierarchy in its topological classes representing  $n$ -particle intermediate states, special care has to be taken for the types of particles in the intermediate states, since this series does not have to converge if the particle is massless. The Dyson hierarchy combined with the truncated reduction hierarchy seems therefore to be the more generic and more easily accessible way to solve the field theory.

To start the development of the reduction procedures necessary for both types of hierarchies to order 3 in the intermediate states we will finish this section by discussing the 2-particle reducible diagrams of the 3-point vertex function (diagram (a) of Fig. 15). In section 4.2 we will perform the crossing-symmetric 1-particle reduction of the  $T$  matrix and the pentagon and will then develop the crossing-symmetric 2-particle reduction of the scattering diagrams, as well as the 2-particle reduction of the pentagon-like class of diagrams (diagrams (d) of Fig. 15). Finally in section 4.3 we conclude the reduction schemes of the 2-particle reducible diagrams by discussing the decay reducible diagrams.

Let's finish this section by discussing the 2-particle reduction of the 3-point vertex function as an example of the reduction procedure (Fig. 16). The 3-point vertex function is automatically 1-particle irreducible. To find now the 2-particle reduction of this 1-particle-irreducible 3-point vertex function  $V_{1PI}$  we have to find first the different topological classes of diagrams containing 2-particle intermediate states. There is only one, given by diagram (a) of Fig. 15. The next step is to find all reducibility classes of this diagram. The reducibility classes represent the different channels in which the diagram is 2-particle reducible. In the case of for example the 2-fermion-1-boson vertex function they correspond to the 3 sides of the triangle representing the vertex function and we label them  $\alpha|bc$ ,  $b|\alpha c$ ,  $c|\alpha b$  with the greek letters representing boson lines, the latin letters representing incoming fermion lines and the bold latin letters representing outgoing fermion lines (compare also Fig. 16). The 4-point vertex function contained in this 2-particle reducible diagram still contains 1-particle reducible pieces. These 1-particle reducible pieces allow us to construct in every reducibility class a diagram which is reducible in two other channels. We label this diagram  $\alpha|bc$  and have to subtract out 2 of these to avoid overcounting. The general rule here is that a diagram reducible in  $n$  different channels has

to be subtracted  $(n - 1)$  times to avoid over counting in the reduction scheme. The integral equation representing the 2-particle reduction of the 3-point vertex function is therefore given by:

$$V'_{1PI,\alpha bc} = V'_{2PI,\alpha bc} + V'_{\alpha|bc} + V'_{b|ac} + V'_{c|ab} - 2V'_{\alpha|b|c} \quad (4.1)$$

$$V''_{1PI,\alpha\beta\gamma} = V''_{2PI,\alpha\beta\gamma} + S(0,3)V''_{\alpha|\beta\gamma} - V''_{\alpha|\beta|\gamma} \quad (4.2)$$

The primed and double primed variables represent the boson-fermion and the all-boson case respectively. The symmetrization operator  $S(0,3)$  in the all-boson case takes account of the indistinguishability of the 3 boson legs and therefore also of the reducibility classes. These equations are shown diagrammatically in Fig. 16. The 2-particle reducible diagrams are shown in their topological form according to diagram (a) in Fig. 15. The factors of  $\frac{1}{2}$  correct for the indistinguishability of the intermediate boson lines.

We have to construct the 2-particle reducible pieces out of the 2-particle irreducible piece of the 3-point vertex function and the 1-particle irreducible piece of  $T$  matrix both in the appropriate channel. This allows us then to generate all rescattering or ladder diagrams in the  $T$  matrices.

To make sure that the 2-particle reducible pieces are still 1-particle irreducible we have to extract the appropriate 1-particle reducible piece  $R$  out of the  $T$  matrix. Conventionally the different reducibility classes of the  $T$  matrix are labelled  $S$ ,  $T$  and  $U$ . To allow for generalization to the 3- and 5-point vertex functions we introduce our labelling scheme. For 1- particle reducibility we have to partition the four external legs of the  $T$  matrix into two incoming and two outgoing legs corresponding to  $\frac{4!}{2!2!} = 3$  reducibility classes. Now we label again the external legs of, for example, the 2-fermion-2-boson vertex function with  $\alpha, \beta, c, d$ . The direct or  $S$ -channel can then be labelled as  $\alpha\beta|cd$ , the exchange or  $U$ -channel as  $\alpha c|\beta d$  and the  $T$ -channel as  $\alpha d|\beta c$ . Analogously we get for the decay reducible diagrams  $\frac{4!}{3!} = 4$  different reducibility classes labelled for example in the case of the all-boson  $T$  matrix with  $\alpha|\beta\gamma\delta$ ,  $\beta|\alpha\gamma\delta$ ,  $\gamma|\alpha\beta\delta$  and  $\delta|\alpha\beta\gamma$ . In the all-boson case the 4 reducibility classes would be summed up using the symmetrization operator  $S(0,4)$ . With the help of this labelling scheme we can reproduce the ladder summation shown in figure 16:

$$V'_{\alpha|bc} = (V'_{1PI,\alpha de} - V'_{\alpha|de}) G_{(de)} (T'_{debc} - R'_{de|bc})$$

$$+ \frac{1}{2} (V''_{1PI, \alpha \delta \varepsilon} - V''_{\alpha | \delta \varepsilon}) G_{(\delta \varepsilon)} (T'_{\delta \varepsilon bc} - R'_{\delta \varepsilon | bc}) \quad (4.3)$$

$$V'_{b| \alpha c} = (V'_{1PI, b \delta e} - V'_{b | \delta e}) G_{(\delta e)} (T'_{\delta e \alpha c} - R'_{\delta e | \alpha c}) \quad (4.4)$$

$$V''_{\alpha | \beta \gamma} = \frac{1}{2} (V''_{1PI, \alpha | \delta \varepsilon} - V''_{\alpha | \delta \varepsilon}) G_{(\delta \varepsilon)} (T''_{\delta \varepsilon \beta \gamma} - R''_{\delta \varepsilon | \beta \gamma}) \\ + (V'_{1PI, \alpha | d e} - V'_{\alpha | d e}) G_{(d e)} (T'_{d e \beta \gamma} - R'_{d e | \beta \gamma}) \quad (4.5)$$

The  $G$  stands for the two intermediate propagators with the subscripts indicating if the intermediate lines represent fermions or bosons. Equation (4.4) allows us to also determine the time-reversed case of this relation, corresponding to  $V'_{c| \alpha b}$  by replacing all incoming with outgoing fermion lines and vice versa. We have thus completed the 2-particle reduction of the 3-point vertex function. The 2-particle reduction equations corresponding to (4.3)-(4.5) but with the ladder summations in the 3-point vertex functions instead of the 4-point vertex function are given in equations (4.36)-(4.38).

The general procedure for the 2-particle reduction is thus first a topological classification of the diagrams to be reduced, second the 1-particle reduction, third determine and label the 2-particle reducibility classes of the topological classes, fourth find the overcounted diagrams, i.e. the diagrams reducible in more than one channel, fifth write down formally the integral equation representing the reduction of the topological class and sixth put in the ladder summations into the different reducibility channels. We apply this recipe in section 4.2 to the  $T$  matrix and the pentagon.

To study the relationship between the Dyson hierarchy and the reduction hierarchy we expand the 2-particle irreducible kernel of the 3-point vertex function perturbatively. The two lowest order terms for the all-boson case are shown in Fig. 17. The  $T$  matrices used in this expansion have to be 1-particle irreducible and 2-particle decay irreducible for the kernel to be 2-particle irreducible. If we compare this expansion with the corresponding Dyson equation (Fig. 13.c) we see that they are identical in the lowest order. All 2-particle irreducible higher-order terms in the Dyson equation have to come from diagrams containing pentagons. Actually the parts of the pentagon which are scattering reducible in two channels are the only pieces of the pentagon which account for this next lowest order. This will be straightforward to see from the results of section 4.2. The remarkable point here is that both hierarchies, although summing up different topological subsets of diagrams, give identical answers and therefore allow for an examination of the quality of the truncation scheme we introduced by comparing the results of both hierarchies order by order.



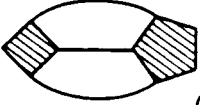

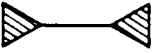


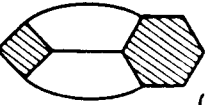
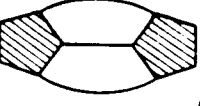

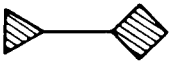

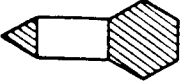
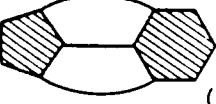
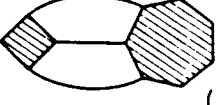
Vertex function	1-particle reducible diagrams	2-particle reducible diagrams	3-particle reducible diagrams
	—	 (a)	 (f)
		 (b)  (c)	 (g)  (h)
		 (d)  (e)	 (i)  (j)

Fig. 15. Topological classification of diagrams containing 1-, 2- and 3-particle intermediate states appearing in the Dyson hierarchy up to  $O(6)$ .



$$\begin{aligned}
 \alpha \triangle_{1PI \gamma}^{\beta} &= \alpha \triangle_{2PI \gamma}^{\beta} + \frac{1}{2} \alpha \text{ (wavy line) }_{\gamma}^{\beta} \\
 &\quad + \alpha \text{ (two vertical lines) }_{\gamma}^{\beta} \\
 &\quad + \frac{1}{2} \alpha \text{ (wavy line) }_{\gamma}^{\beta} + \frac{1}{2} \alpha \text{ (wavy line) }_{\gamma}^{\beta} - 2 \alpha \triangle_{1PI}^{\beta} \\
 &\quad + \alpha \text{ (two vertical lines) }_{\gamma}^{\beta} + \alpha \text{ (two vertical lines) }_{\gamma}^{\beta} - 2 \alpha \triangle_{1PI}^{\beta}
 \end{aligned}$$
  

$$\begin{aligned}
 \alpha \triangle_{1PI c}^b &= \alpha \triangle_{2PI c}^b + \alpha \text{ (two vertical lines) }_c^b + \frac{1}{2} \alpha \text{ (wavy line) }_c^b \\
 &\quad + \alpha \text{ (wavy line) }_c^b + \alpha \text{ (wavy line) }_c^b - 2 \alpha \triangle_{1PI}^b \\
 &\quad - 2 \alpha \triangle_{1PI}^b
 \end{aligned}$$

Fig. 16. 2-particle reduction of the 1-particle irreducible 3-point vertex function.

$$\begin{aligned}
 \triangle^{2PI} &= S(1,2) \bullet + S(1,2) \text{ [Diagram 1]} \\
 &+ S(1,2) \text{ [Diagram 2]} + S(1,2) \text{ [Diagram 3]} \\
 &+ S(1,2) \text{ [Diagram 4]} + \dots
 \end{aligned}$$

Fig. 17. Perturbative expansion of the 2-particle irreducible kernel of the 3-boson vertex function. We keep one leg fixed to allow for comparison to the corresponding Dyson equation (Fig. 9a and 13c).

## 4.2 CROSSING-SYMMETRIC REDUCTION OF THE SCATTERING TYPE OF 2-PARTICLE INTERMEDIATE STATES

The first step in our development is the crossing-symmetric reduction of the 1-particle intermediate states of the  $T$  matrix and the pentagon. For the  $T$  matrix this was done by Korpa and Siemens and we give their results using our labeling schemes. The diagrammatic representation of these equations is given in Fig. 18.

$$T_{abcd} = T_{1PI,abcd} + A(2,2)R_{abcd} \quad (4.6)$$

$$T'_{\alpha\beta cd} = T'_{1PI,\alpha\beta cd} + R'_{\alpha\beta|cd} + S(2,2)R'_{\alpha c|\beta d} \quad (4.7)$$

$$T''_{\alpha\beta\gamma\delta} = T''_{1PI,\alpha\beta\gamma\delta} + S(1,3)R''_{\alpha\beta|\gamma\delta} \quad (4.8)$$

In these equations the  $R$ 's describe the 1-particle reducible parts of the  $T$  matrix and the unprimed, primed and double-primed quantities represent the all-fermion, fermion-boson and all-boson cases of the  $T$  matrix respectively.

For the 1-particle reduction of the pentagon we encounter the same over counting problem we dealt with at the 2-particle reduction of the 3-point vertex function. There are diagrams which are 1-particle reducible in two channels and which therefore have to be subtracted once. These over counting terms can be determined by comparing the 1-particle reduction in terms of the full  $T$  matrix given in Fig. 19 with the one where we replace the full  $T$  matrix with its 1-particle-reducible and -irreducible pieces. The reduction equations in terms of the full  $T$  matrix (represented in Fig. 19) are:

$$P_{abcde} = P_{1PI,\alpha bcde} + A(1,2,2)\{Q'_{\alpha c|bed} + Q'_{\alpha b|cde} + Q'_{bc|ade} - Q'_{\alpha|bcde} - Q'_{b|ac|de} - Q'_{c|\alpha b|de}\} \quad (4.9)$$

$$P'_{\alpha\beta\gamma de} = P'_{1PI,\alpha\beta\gamma de} + Q'_{de|\alpha\beta\gamma} + S(2,3)\{Q'_{\alpha\beta|\gamma de} + Q'_{\alpha e|\beta\gamma d} + Q'_{\alpha d|\beta\gamma e} - Q'_{d|\alpha e|\beta\gamma} - Q'_{e|\alpha\beta|\gamma d} - Q'_{\alpha|\beta\gamma|de} - Q'_{\alpha|\beta e|\gamma d}\} \quad (4.10)$$

$$P''_{\alpha\beta\gamma\delta\epsilon} = P''_{1PI,\alpha\beta\gamma\delta\epsilon} + S(0,5)Q''_{\alpha\beta|\gamma\delta\epsilon} - S(0,5)Q''_{\alpha|\beta\gamma|\delta\epsilon} \quad (4.11)$$

The  $Q$ 's represent the 1-particle reducible parts of the pentagon and the unprimed, primed and double-primed quantities represent the 4-fermion-1-boson, 2-fermion-3-boson and all-boson 5-point vertex functions respectively. To better understand these equations look for example at legs  $d$  and  $e$  and at the partition. They appear in every possible ordering in the reducible parts  $Q$ . The symmetrization and antisymmetrization operators assure then that the remaining legs are permuted if they are indistinguishable ( $A(1,2,2)$  stands here for antisymmetrization of the pair of incoming and the pair of outgoing fermion lines). The last terms in every equation contain two partitions in their labeling and represent the over counting terms.

We are now ready for the 2-particle reduction of the scattering diagrams of the  $T$  matrix. As for the 1-particle reduction of the pentagon, we start with a classification of the diagrams which are 2-particle reducible in more than one channel. These diagrams are shown in Fig. 20 and we obtain:

$$T_{ab||ad} + T_{ab||ac} + T_{ac||ad} \quad (4.12)$$

$$T'_{\alpha\beta||\alpha d} + T''_{\alpha\beta||\alpha c} + T''_{\alpha c||\alpha d} \quad (4.13)$$

$$T''_{\alpha\beta||\alpha\delta} + T''_{\alpha\beta||\alpha\gamma} + T''_{\alpha\gamma||\alpha\delta} \quad (4.14)$$

Here we are using only the first two letter indices characterizing every reducibility channel and then separate them with a double partition to indicate that these diagrams are reducible in two channels. Special care has to be taken in determining the signs for the all-fermion case. Every exchange of 2 fermion indices generates a minus sign. Most of the reducibility classes contain two topological diagrams (in figure  $\phi$  depicted above each other) which we generate by exchanging all the fermion intermediate states with boson intermediate states and vice versa. For the all-boson case the lower diagram of every class can be drawn with two possible directions of the arrow of the fermion intermediate states. Both directions are generated by the symmetrization operator  $S(2,2)$ . This completes the over counting problem for the  $T$ -matrix and allows us to formally determine the integral equations for the 2-particle reduction of the scattering diagrams:

$$T_{1PI,abcd} = T_{2PI,abcd} + S(2,2)T_{ab|cd} + T_{ac|bd} - \{T_{ab||ad} + T_{ab||ac} + T_{ac||ad}\} \quad (4.15)$$

$$T'_{1PI,\alpha\beta cd} = T'_{2PI,\alpha\beta cd} + T'_{\alpha\beta|cd} + S(2,2)T'_{\alpha c|\beta d} - \{T'_{\alpha\beta||\alpha d} + T''_{\alpha\beta||\alpha c} + T''_{\alpha c||\alpha d}\} \quad (4.16)$$

$$T''_{1PI,\alpha\beta\gamma\delta} = T''_{2PI,\alpha\beta\gamma\delta} + S(1,3)T''_{\alpha\beta|\gamma\delta} - \{T''_{\alpha\beta||\alpha\delta} + T''_{\alpha\beta||\alpha\gamma} + T''_{\alpha\gamma||\alpha\delta}\} \quad (4.17)$$

The symmetrization operators used here sum up the  $S$ - and  $T$ -channel. The next step is to put the ladder summations into the 2-particle-reducible classes. Let's discuss first the all-boson case. The 2-particle-reducible  $T$  matrix  $T''_{ijkl}$  can be expressed as:

$$T''_{\alpha\beta|\gamma\delta} = \frac{1}{2} (T''_{\alpha\beta\varepsilon\phi} - R''_{\alpha\beta|\varepsilon\phi}) G_{(\varepsilon\phi)} (T''_{\varepsilon\phi\gamma\delta} - T''_{\varepsilon\phi|\gamma\delta} - R''_{\alpha\beta|\gamma\delta}) \\ + (T'_{\alpha\beta\varepsilon\phi} - R'_{\alpha\beta|\varepsilon\phi}) G_{(\varepsilon\phi)} (T'_{\varepsilon\phi\gamma\delta} - T'_{\varepsilon\phi|\gamma\delta} - R'_{\alpha\beta|\gamma\delta}) \quad (4.18)$$

We generate the ladders in the first factor where we assume only 1-particle irreducibility in the appropriate channel. In the last factor we also extract the 2-particle-reducible pieces of the  $T$  matrix.

We apply the same procedure to the fermion-boson case. Here we have to write out two relations corresponding to the cases where the reducibility channels cut only boson or only fermion lines and the case where the channels cut mixed boson-fermion 2-particle intermediate states.

$$T'_{\alpha\beta|cd} = (T'_{\alpha\beta ef} - R'_{\alpha\beta|ef}) G_{(ef)} (T'_{efcd} - T'_{ef|cd} - R'_{ef|cd}) \\ + \frac{1}{2} (T''_{\alpha\beta\varepsilon\phi} - R''_{\alpha\beta|\varepsilon\phi}) G_{(\varepsilon\phi)} (T'_{\varepsilon\phi cd} - T'_{\varepsilon\phi|cd} - R'_{\varepsilon\phi|cd}) \quad (4.19)$$

$$T'_{\alpha c|bd} = (T'_{\alpha c ef} - R'_{\alpha c|ef}) G_{(ef)} (T'_{efbd} - T'_{ef|bd} - R'_{ef|bd}) \quad (4.20)$$

The second equation (4.20) has only one term on the right hand side to assure fermion number conservation.

We obtain the all-fermion case analogously:

$$T_{ac|bd} = (T_{acef} - R_{ac|ef}) G_{(ef)} (T_{efbd} - T_{ef|bd} - R_{ef|bd}) \quad (4.21)$$

$$T_{abcd} = - (T_{abef} - R_{ab|ef}) G_{(ef)} (T_{efcd} - T_{ef|cd} - R_{ef|cd}) \\ + \frac{1}{2} (T'_{ab\varepsilon\phi} - R'_{ab|\varepsilon\phi}) G_{(\varepsilon\phi)} (T'_{\varepsilon\phi cd} - T'_{\varepsilon\phi|cd} - R'_{\varepsilon\phi|cd}) \quad (4.22)$$

The only new rule we have to take into account to understand these equations is the minus sign generated for every antisymmetrization. If we compare in equations (4.21) and (4.22) the diagrams containing 2-fermion intermediate states, we can fix the relative minus sign by recognizing the necessary exchange of two-fermion indices between the diagrams.

We have now collected all the rules needed to develop the 2-particle reduction of the pentagon  $P$ . The topological class to which these type of diagrams belong is depicted in diagram (d) of Fig. 15. It corresponds to diagram (b) of Fig. 15 and is therefore also a scattering-reducible type of diagram. Again we start with the over counting problem. For the all-boson case we obtain for possible overcountings (compare to Fig. 21.a):

$$S(0,5)\{P''_{\alpha\epsilon\parallel\beta\gamma} + 2P''_{\alpha\epsilon\parallel\gamma} + 4P''_{(5)}\} \quad (4.23)$$

The three terms in equation (4.23) represent the overcounted diagrams reducible in 2, 3 and 5 channels respectively. In our labeling scheme we represent the diagrams reducible in two channels with a double partition and by numbering the legs of the 1-particle irreducible  $T$  matrices. Diagrams reducible in three channels are labeled with a triple partition and by numbering the legs of the 1-particle-irreducible  $T$  matrix and the 3-point vertex function which is singled out by not being a neighbor of this 1-particle-irreducible  $T$  matrix. Diagrams reducible in five channels are labeled by the subscript (5).

The over counting problem is solved by comparing the diagrams containing the full  $T$ -matrix with the one where we replaced the full  $T$  matrix with its 1-particle-reducible and -irreducible pieces. We find that in general diagrams reducible in  $n$  channels are over counted  $(n - 1)$  times which explains the factors of 2 and 4 in front of the 2-particle reducible pieces in 3 and 5 channels respectively. In Fig. 21 we show the over counted diagrams in terms of the 1-particle-irreducible  $T$  matrix since we need precisely this collection of diagrams in the reduction equations. Note that in the diagrammatic representation of Fig. 21.a we have again two types of diagrams in every reducibility class corresponding to the exchange of boson intermediate states with fermion intermediate states and vice versa. The classes representing diagrams reducible in 2 and 3 channels contain 60 diagrams while the class representing diagrams reducible in 5 channels contains 120 diagrams. This enormous collection of diagrams is summed up using the symmetrization operator. For example in the case of the diagrams reducible in 2 channels the  $S(0,5)$  in front of the case with bosons in the intermediate state sums up 30 diagrams while the  $S(0,5)$  in front of the case with fermions in the intermediate state sums up 15 diagrams for each direction a fermion can run.

The direction in which the intermediate fermion lines are running is, in the case of the 2-fermion-3-boson vertex function, related to the arrows of the external legs. Therefore we cannot sum up these different diagrams into one reducibility class (in Fig. 21.b the diagrams obtainable from each other by exchanging the arrows of the fermion lines corresponding to the time reversal operation are the first 5 neighbouring pairs). We sum up different diagrams of a reducibility class by permuting the three boson legs using the symmetrization operator  $S(2,3)$ .

$$\begin{aligned}
& S(2,3) \{ P'_{\alpha b \parallel \gamma \delta} + P'_{\alpha b \parallel \gamma \delta} + P'_{\alpha b \parallel \gamma d} + P'_{\alpha \beta \parallel c d} \\
& + 2(P'_{\alpha b \parallel \gamma} + P'_{\alpha b \parallel \gamma} + P'_{\alpha \beta \parallel c} + P'_{\alpha \beta \parallel c} + P'_{\alpha b \parallel c} + P'_{\alpha b \parallel c} + P'_{\alpha \beta \parallel \gamma} + P'_{a b \parallel \gamma}) \\
& + 4P_{(5)} \} \tag{4.24}
\end{aligned}$$

The rules we learned from the all-boson vertex function and the 2-fermion-3-boson vertex function allow us finally to solve the over counting problem for the 4-fermion-1-boson vertex function (Fig. 21.c). Again we generate diagrams from each other exchanging the direction of the fermion line (the first two diagrams as well as line 2 and 3 and line 4 and 5 are time reversed to each other), obtain the different diagrams of one reducibility class from each other by exchanging fermion and boson intermediate lines and determine all reducibility classes reducible in a certain number of channels by permuting the fermion legs (leg  $c$  and  $d$  are therefore our legs of reference). The antisymmetrization can be described with the antisymmetrization operator  $A(3,2)$ :

$$\begin{aligned}
& A(3,2) \{ P_{a b \parallel c \delta} + P_{a b \parallel c \delta} + P_{a b \parallel c d} + P_{a b \parallel c \delta} + P_{a b \parallel c \delta} \\
& + 2(P_{a b \parallel \gamma} + P_{a b \parallel \gamma} + P_{a b \parallel c} + P_{a b \parallel c} + P_{a \beta \parallel c} + P_{a \beta \parallel c}) \\
& + 4P_{(5)} \} \tag{4.25}
\end{aligned}$$

In most reducibility classes we get only one diagram since we have to hook up the internal to the external fermion lines. But in the classes  $P_{a b \parallel c \delta}$  and  $P_{a b \parallel c \delta}$  this same requirement generates 3 possible diagrams.

We proceed now by formally writing down the 2-particle reduction of the pentagon :

$$P''_{1PI,\alpha\beta\gamma\delta\epsilon} = P''_{2PI,\alpha\beta\gamma\delta\epsilon} + S(0,5)P''_{\alpha\beta|\gamma\delta\epsilon} - S(0,5)\{P''_{\alpha\epsilon||\beta\gamma} + 2P''_{\alpha\epsilon||\gamma} + 4P''_{(5)}\} \quad (4.26)$$

$$\begin{aligned} P'_{1PI,\alpha\beta\gamma\delta\epsilon} = & P'_{2PI,\alpha\beta\gamma\delta\epsilon} + P'_{\alpha\beta|\gamma\delta\epsilon} + P'_{de|\alpha\beta\gamma} + P'_{e\alpha|\beta\gamma\delta} + P'_{d\alpha|\beta\gamma\epsilon} \\ & - S(2,3)\{P'_{\alpha b||\gamma\delta} + P'_{\alpha b||\gamma\delta} + P'_{\alpha b||\gamma d} + P'_{\alpha b||c d} \\ & + 2(P'_{\alpha b||\gamma} + P'_{\alpha b||\gamma} + P'_{\alpha\beta||\gamma c} + P'_{\alpha\beta||\gamma c} + P'_{\alpha b||\gamma c} + P'_{\alpha b||\gamma c} + P'_{\alpha\beta||\gamma} + P'_{ab||\gamma}) \\ & + 4P'_{(5)}\} \end{aligned} \quad (4.27)$$

$$\begin{aligned} P_{1PI,abcde} = & P_{2PI,abcde} + P_{bc|\alpha de} + P_{ce|\alpha bd} + P_{bd|\alpha ce} + P_{\alpha b|cde} + P_{\alpha c|bde} \\ & - A(3,2)\{P_{ab||c\delta} + P_{ab||c\delta} + P_{ab||cd} + P_{ab||c\delta} + P_{ab||c\delta} \\ & + 2(P_{ab||\gamma} + P_{ab||\gamma} + P_{ab||\gamma c} + P_{ab||\gamma c} + P_{a\beta||\gamma c} + P_{a\beta||\gamma c}) \\ & + 4P_{(5)}\} \end{aligned} \quad (4.28)$$

It is now straightforward to put the ladder summations into the 2-particle-reducible classes of the pentagon since we just have to add a boson leg to the corresponding integral equations for the  $T$  matrix (4.18-4.22). For the all-boson 5-point vertex function we obtain:

$$\begin{aligned} P''_{\alpha\beta|\gamma\delta\epsilon} = & \frac{1}{2}(T''_{\alpha\beta\rho\pi} - R''_{\alpha\beta|\rho\pi}) G_{(\rho\pi)} (P''_{\rho\pi\gamma\delta\epsilon} - P''_{\rho\pi|\gamma\delta\epsilon} - S(2,3)Q''_{\gamma\delta|\rho\pi\epsilon} + S(2,3)Q''_{\gamma|\rho\pi|\delta\epsilon}) \\ & + (T'_{\alpha\beta\rho\pi} - R'_{\alpha\beta|\rho\pi}) G_{(r\rho)} (P'_{r\rho\gamma\delta\epsilon} - P'_{r\rho|\gamma\delta\epsilon} - S(2,3)Q'_{\gamma\delta|\rho\pi\epsilon} + S(2,3)Q'_{\gamma|\rho\pi|\delta\epsilon}) \end{aligned} \quad (4.29)$$

In the pentagon part of the 2-particle-reducible diagrams we have to assure 2-particle irreducibility in the appropriate channel. We achieve this again by subtracting out the pieces which are 1- and 2- particle reducible in the channel under consideration. The 1-particle reducible pieces of the pentagon are given in terms of the full  $T$  matrix. This creates again an over counting problem and we have to add back in all the 1-particle-reducible pieces we subtracted out too often. We avoided an over counting problem in the 2-particle reducibility channel by determining here the diagrams reducible in more than one channel in terms of the 1-particle-irreducible  $T$  matrices (4.23-4.25).

For the 2-fermion-3-boson vertex function we obtain:

$$P'_{de|\alpha\beta\gamma} = \frac{1}{2}(T'_{de\rho\pi} - R'_{de|\rho\pi}) G_{(\rho\pi)} (P''_{\rho\pi\gamma\delta\epsilon} - P''_{\rho\pi|\gamma\delta\epsilon} - S(2,3)Q''_{\gamma\delta|\rho\pi\epsilon} + S(2,3)Q''_{\gamma|\rho\pi|\delta\epsilon})$$



$$+(T_{derp} - R_{delrp}) G_{(rp)} (P'_{rpy\delta\epsilon} - P'_{rpl\gamma\delta\epsilon} - S(2,3)Q'_{\gamma\delta lrp\epsilon} + S(2,3)Q'_{\gamma lrp l\delta\epsilon}) \quad (4.30)$$

$$\begin{aligned} P'_{\alpha\beta lde\gamma} = & \frac{1}{2} (T''_{\alpha\beta r\pi} - R''_{\alpha\beta lrp\pi}) G_{(r\pi)} (P'_{r\pi de\gamma} - P'_{r\pi lde\gamma} \\ & - Q'_{delrp\gamma} - Q'_{d\gamma lrp\epsilon} - Q'_{e\gamma lrp d} + Q'_{\gamma lrp lde} + Q'_{e lrp l d\gamma} + Q'_{d lrp l e\gamma}) \\ & + (T'_{\alpha\beta rp} - R'_{\alpha\beta lrp}) G_{(rp)} (P_{rp de\gamma} - P_{rp lde\gamma} \\ & - Q_{delrp\gamma} - Q_{d\gamma lrp\epsilon} - Q_{e\gamma lrp d} + Q_{\gamma lrp lde} + Q_{e lrp l d\gamma} + Q_{d lrp l e\gamma}) \end{aligned} \quad (4.31)$$

$$\begin{aligned} P'_{\alpha d l\beta e\gamma} = & \frac{1}{2} (T'_{\alpha d r\pi} - R'_{\alpha d lrp\pi}) G_{(r\pi)} (P'_{r\pi\beta e\gamma} - P'_{r\pi l\beta e\gamma} \\ & - S(3,2)Q'_{\beta e lrp\gamma} - Q'_{\beta\gamma lrp\epsilon} + S(3,2)Q'_{\beta lrp l\gamma e} + Q'_{e lrp l\beta\gamma}) \end{aligned} \quad (4.32)$$

Again we use time reversal upon (4.32) to generate the leftover reducibility class.

Finally we are also ready to write down the ladder summation for the 4-fermion-1-boson vertex function:

$$\begin{aligned} P_{ab lde\gamma} = & \frac{1}{2} (T'_{abr\pi} - R'_{ab lrp\pi}) G_{(r\pi)} (P'_{r\pi de\gamma} - P'_{r\pi lde\gamma} \\ & - Q'_{delrp\gamma} - Q'_{d\gamma lrp\epsilon} - Q'_{e\gamma lrp d} + Q'_{\gamma lrp lde} + Q'_{e lrp l d\gamma} + Q'_{d lrp l e\gamma}) \\ & + (T_{abr p} - R_{ab lrp}) G_{(rp)} (P_{rp de\gamma} - P_{rp lde\gamma} \\ & - Q_{delrp\gamma} - Q_{d\gamma lrp\epsilon} - Q_{e\gamma lrp d} + Q_{\gamma lrp lde} + Q_{e lrp l d\gamma} + Q_{d lrp l e\gamma}) \end{aligned} \quad (4.33)$$

$$\begin{aligned} P_{\alpha d l\beta e\gamma} = & - (T''_{\alpha d r\pi} - R''_{\alpha d lrp\pi}) G_{(r\pi)} (P_{r\pi\beta e\gamma} - P_{r\pi l\beta e\gamma} \\ & - S(3,2)Q_{\beta e lrp\gamma} - Q_{e\gamma lrp\beta} + S(3,2)Q_{e lrp l\beta\gamma} + Q_{e lrp l\beta\gamma}) \end{aligned} \quad (4.34)$$

$$\begin{aligned} P_{ab lde\gamma} = & - (T_{abr p} - R_{ab lrp}) G_{(rp)} (P_{rp de\gamma} - P_{rp lde\gamma} - Q_{delrp\gamma} \\ & - S(3,2)Q_{d\gamma lrp\epsilon} + Q_{\gamma lrp lde} + S(3,2)Q_{e lrp l d\gamma}) \end{aligned} \quad (4.35)$$

We are again using time reversal to generate two more reducibility classes from (4.34) and (4.35). The relative minus signs of the equations can be determined by counting the necessary permutations of the anticommuting fermion indices.

In this reduction procedure we generated the ladder summations for the 3-point vertex function and the pentagon in the  $T$ -matrix part of the 2-particle reducible diagram. We could also do this in the other part contained in the diagram, i.e. in the 3-point and 5-

point vertex functions for the 3-point vertex functions and the pentagon respectively. Since the  $T$  matrix is symmetric in in- and outgoing legs we would obtain identical equations by applying this procedure. We conclude now this section by giving the equations for the scattering reduction of the 3-point vertex functions and the pentagon with the ladder summations in the 3-point and 5-point vertex functions respectively.

$$V'_{\alpha|bc} = V'_{1PI,\alpha de} G_{(de)} (T'_{debc} - T'_{delbc} - R'_{delbc}) + \frac{1}{2} V''_{1PI,\alpha\delta\epsilon} G_{(\delta\epsilon)} (T'_{\delta ebc} - T'_{\delta\epsilon|bc} - R'_{\delta\epsilon|bc}) \quad (4.36)$$

$$V'_{b|\alpha c} = V'_{1PI,b\delta e} G_{(\delta e)} (T'_{\delta e\alpha c} - T'_{\delta\epsilon|\alpha c} - R'_{\delta\epsilon|\alpha c}) \quad (4.37)$$

$$V''_{\alpha|\beta\gamma} = \frac{1}{2} V''_{1PI,\alpha l\delta\epsilon} G_{(\delta\epsilon)} (T''_{\delta\epsilon\beta\gamma} - T''_{\delta\epsilon|\beta\gamma} - R''_{\delta\epsilon|\beta\gamma}) + V'_{1PI,\alpha lde} G_{(de)} (T'_{de\beta\gamma} - T'_{de|\beta\gamma} - R'_{de|\beta\gamma}) \quad (4.38)$$

$$P''_{\alpha\beta|\gamma\delta\epsilon} = \frac{1}{2} (T''_{\alpha\beta\rho\pi} - T''_{\alpha\beta|\rho\pi} - R''_{\alpha\beta|\rho\pi}) G_{(\rho\pi)} (P''_{\rho\pi\gamma\delta\epsilon} - S(2,3)Q''_{\gamma\delta|\rho\pi\epsilon} + S(2,3)Q''_{\gamma|\rho\pi|\delta\epsilon}) + (T'_{\alpha\beta rp} - T'_{\alpha\beta|rp} - R'_{\alpha\beta|rp}) G_{(rp)} (P'_{rp\gamma\delta\epsilon} - S(2,3)Q'_{\gamma\delta|rp\epsilon} + S(2,3)Q'_{\gamma|rp|\delta\epsilon}) \quad (4.39)$$

$$P'_{de|\alpha\beta\gamma} = \frac{1}{2} (T'_{de\rho\pi} - T'_{de|\rho\pi} - R'_{de|\rho\pi}) G_{(\rho\pi)} (P'_{\rho\pi\gamma\delta\epsilon} - S(2,3)Q'_{\gamma\delta|\rho\pi\epsilon} + S(2,3)Q'_{\gamma|\rho\pi|\delta\epsilon}) + (T'_{derp} - T'_{de|rp} - R'_{de|rp}) G_{(rp)} (P'_{rp\gamma\delta\epsilon} - S(2,3)Q'_{\gamma\delta|rp\epsilon} + S(2,3)Q'_{\gamma|rp|\delta\epsilon}) \quad (4.40)$$

$$P'_{\alpha\beta|de\gamma} = \frac{1}{2} (T''_{\alpha\beta\rho\pi} - T''_{\alpha\beta|\rho\pi} - R''_{\alpha\beta|\rho\pi}) G_{(\rho\pi)} (P'_{\rho\pi de\gamma} - Q'_{de|\rho\pi\gamma} - Q'_{d\gamma|\rho\pi\epsilon} - Q'_{e\gamma|\rho\pi d} + Q'_{\gamma|\rho\pi|de} + Q'_{e|\rho\pi|d\gamma} + Q'_{d|\rho\pi|e\gamma}) + (T'_{\alpha\beta rp} - T'_{\alpha\beta|rp} - R'_{\alpha\beta|rp}) G_{(rp)} (P'_{rp de\gamma} - Q'_{de|rp\gamma} - Q'_{d\gamma|rp\epsilon} - Q'_{e\gamma|rp d} + Q'_{\gamma|rp|de} + Q'_{e|rp|d\gamma} + Q'_{d|rp|e\gamma}) \quad (4.41)$$

$$P'_{\alpha d|\beta e\gamma} = \frac{1}{2} (T'_{\alpha d\rho\pi} - T'_{\alpha d|\rho\pi} - R'_{\alpha d|\rho\pi}) G_{(\rho\pi)} (P'_{\rho\pi\beta e\gamma} - S(3,2)Q'_{\beta e|\rho\pi\gamma} - Q'_{\beta\gamma|\rho\pi e} + S(3,2)Q'_{\beta|\rho\pi|\gamma e} + Q'_{e|\rho\pi|\beta\gamma}) \quad (4.42)$$

$$P'_{ab|de\gamma} = \frac{1}{2} (T'_{ab\rho\pi} - T'_{ab|\rho\pi} - R'_{ab|\rho\pi}) G_{(\rho\pi)} (P'_{\rho\pi de\gamma} - Q'_{de|\rho\pi\gamma} - Q'_{d\gamma|\rho\pi e} - Q'_{e\gamma|\rho\pi d} + Q'_{\gamma|\rho\pi|de} + Q'_{e|\rho\pi|d\gamma} + Q'_{d|\rho\pi|e\gamma})$$

$$\begin{aligned}
& + (T_{abr\rho} - T_{ab\rho r} - R_{ab|\rho r}) G_{(r\rho)} (P_{r\rho d e \gamma} \\
& \quad - Q_{d e l r \rho \gamma} - Q_{d \gamma l r \rho e} - Q_{e \gamma l r \rho d} + Q_{\gamma l r \rho l d e} + Q_{e l r \rho l d \gamma} + Q_{d l r \rho l e \gamma})
\end{aligned} \tag{4.43}$$

$$\begin{aligned}
P_{\alpha d | b e c} = & - (T''_{\alpha d \rho \rho} - T''_{\alpha d \rho \rho} - R''_{\alpha d | \rho \rho}) G_{(\rho \rho)} (P_{\rho \rho b e c} \\
& \quad - S(3,2) Q_{b e | \rho \rho c} - Q_{e c | \rho \rho b} + S(3,2) Q_{c | \rho \rho | b e} + Q_{e | \rho \rho | b c})
\end{aligned} \tag{4.44}$$

$$\begin{aligned}
P_{ab | d e \gamma} = & - (T_{abr\rho} - T_{ab\rho r} - R_{ab|\rho r}) G_{(r\rho)} (P_{r\rho d e \gamma} \\
& \quad - Q_{d e l r \rho \gamma} - S(3,2) Q_{d \gamma l r \rho e} + Q_{\gamma l r \rho l d e} + S(3,2) Q_{e l r \rho l d \gamma})
\end{aligned} \tag{4.45}$$

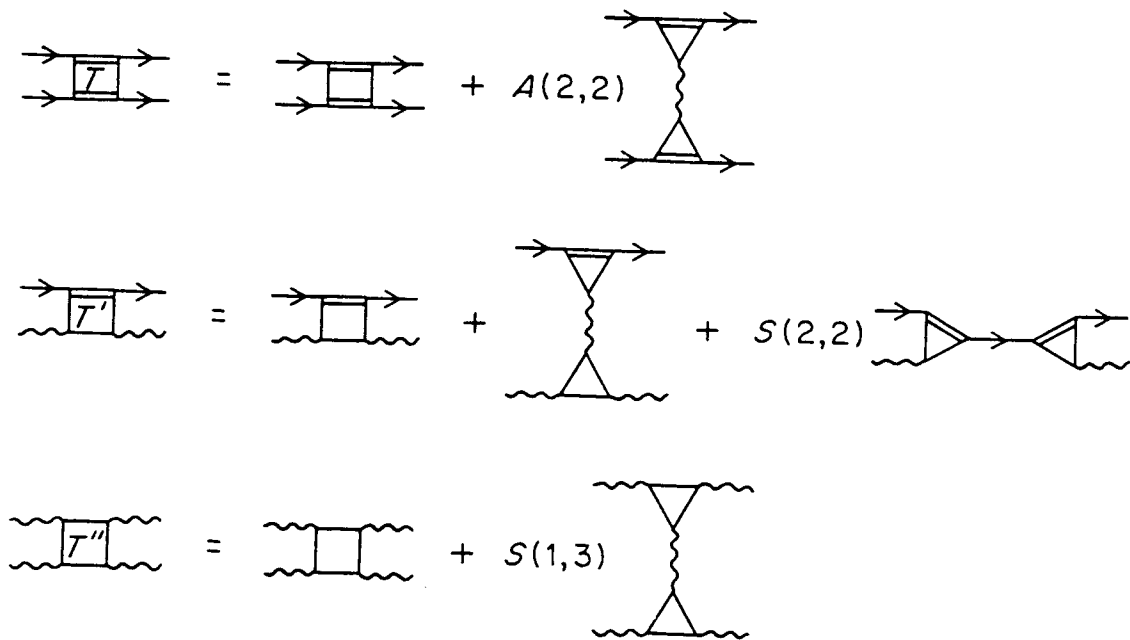


Fig. 18. Diagrammatic representation of the crossing-symmetric reduction of the 1-particle intermediate states of the  $T$  matrix.

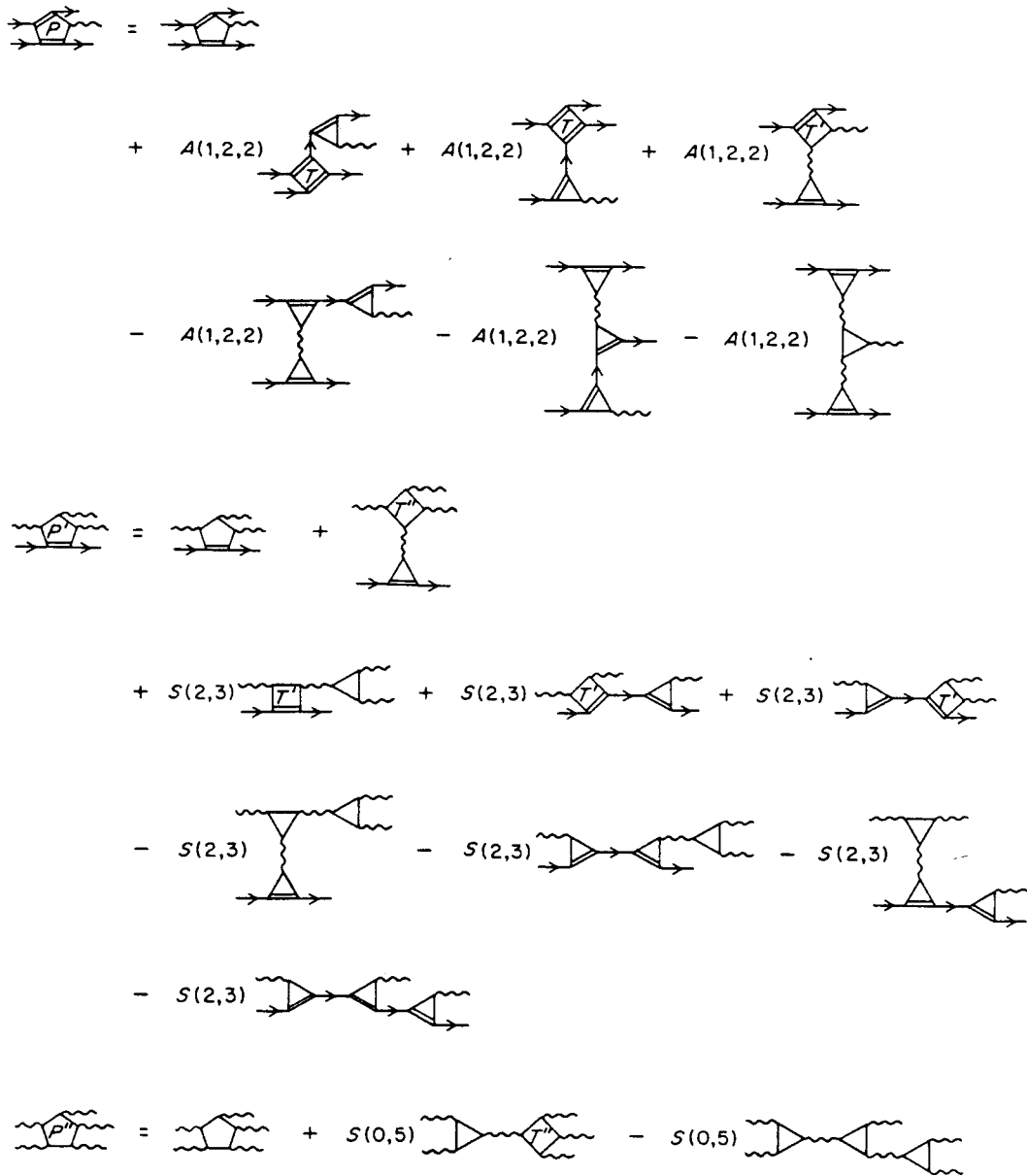


Fig. 19. Diagrammatic representation of the crossing-symmetric reduction of the 1-particle intermediate states of the pentagon.

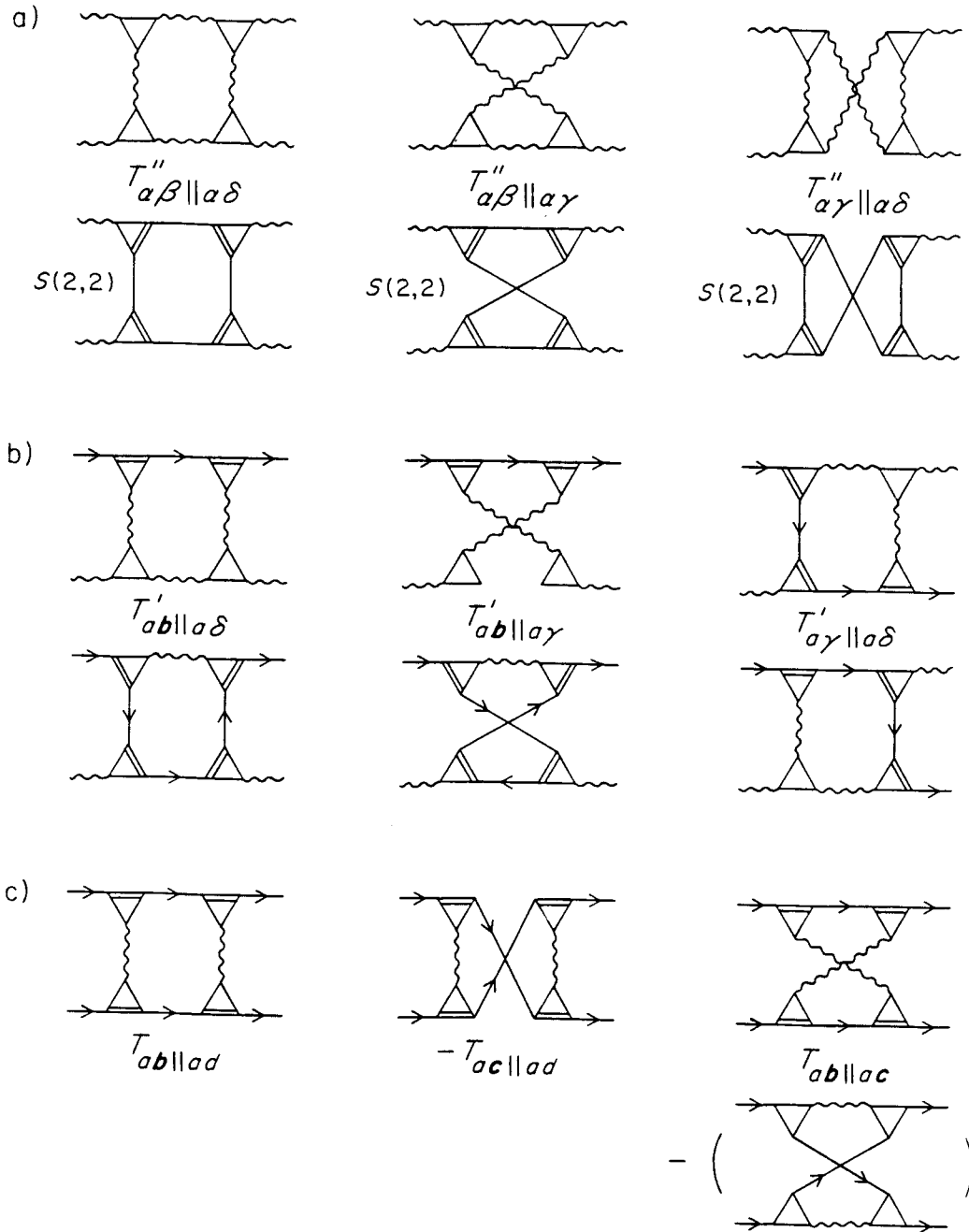


Fig. 20. Scattering reducible diagrams of the  $T$  matrix in two channels. a.) All-boson vertex function, b.) fermion-boson vertex function, c.) all-fermion vertex function.

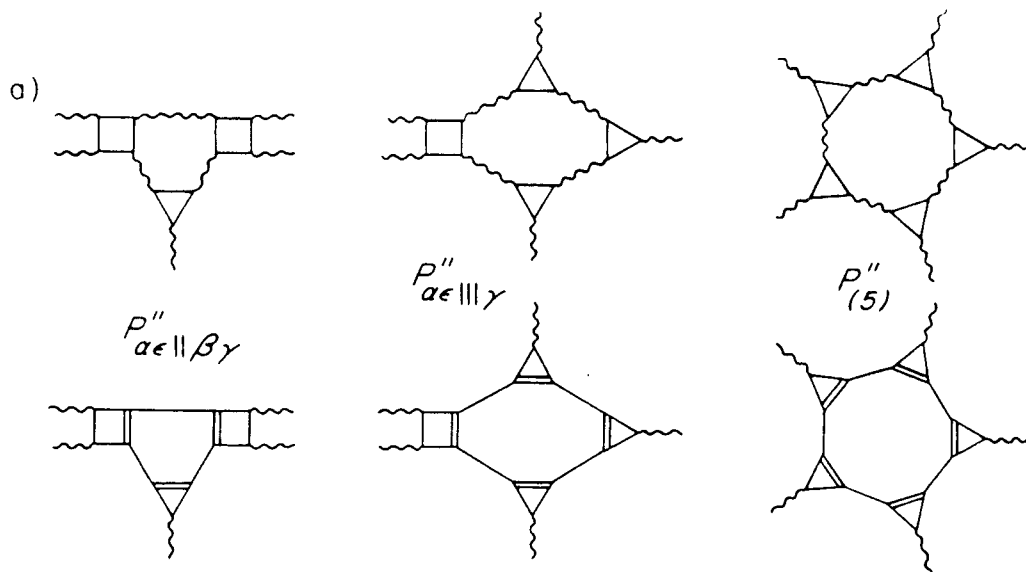


Fig. 21. Scattering reducible diagrams of the pentagon in more than one channel. a.) All-boson vertex function, b.) 2-fermion-3-boson vertex function, c.) 4-fermion-1-boson vertex function.

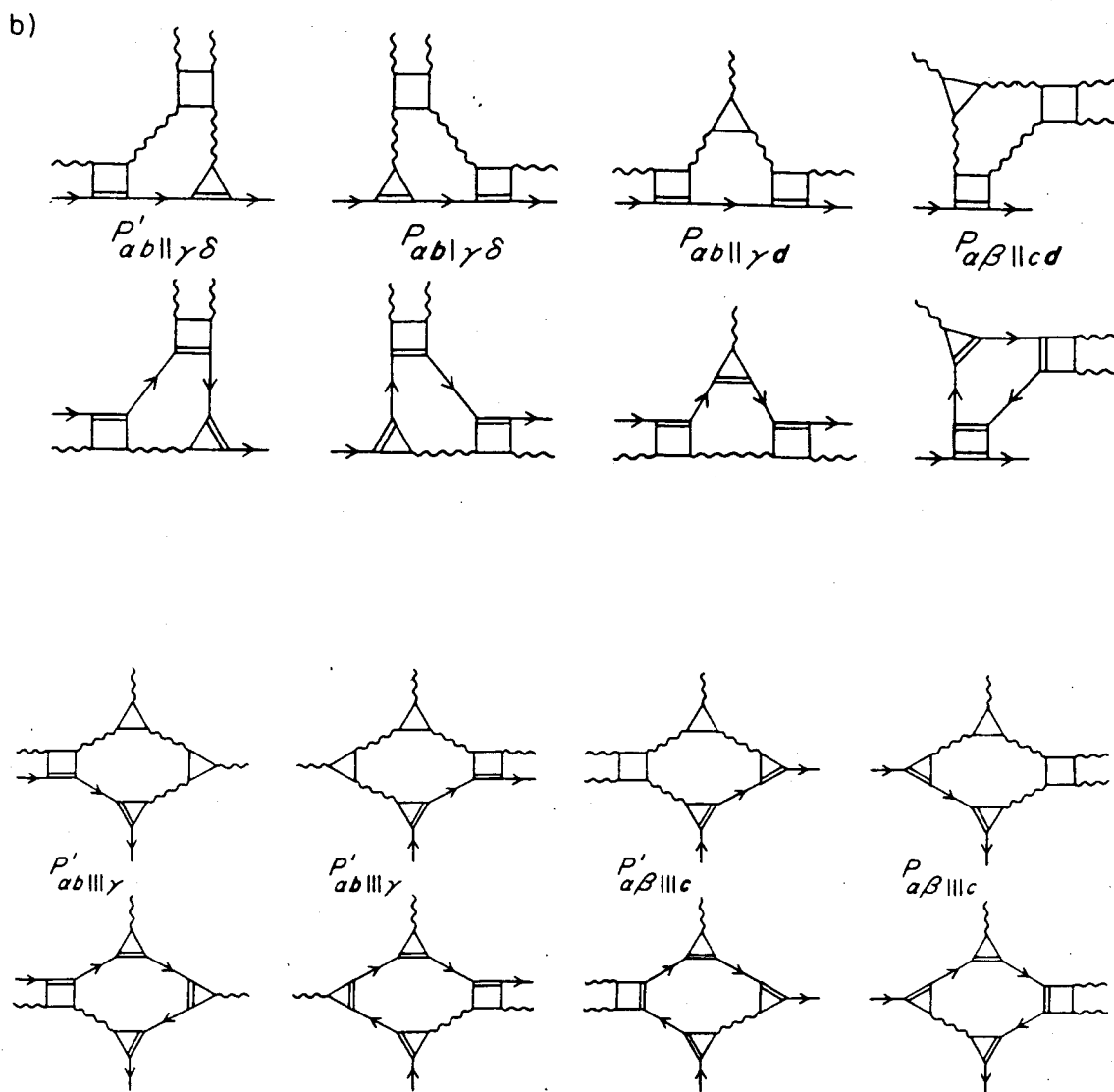


Fig. 21. continued



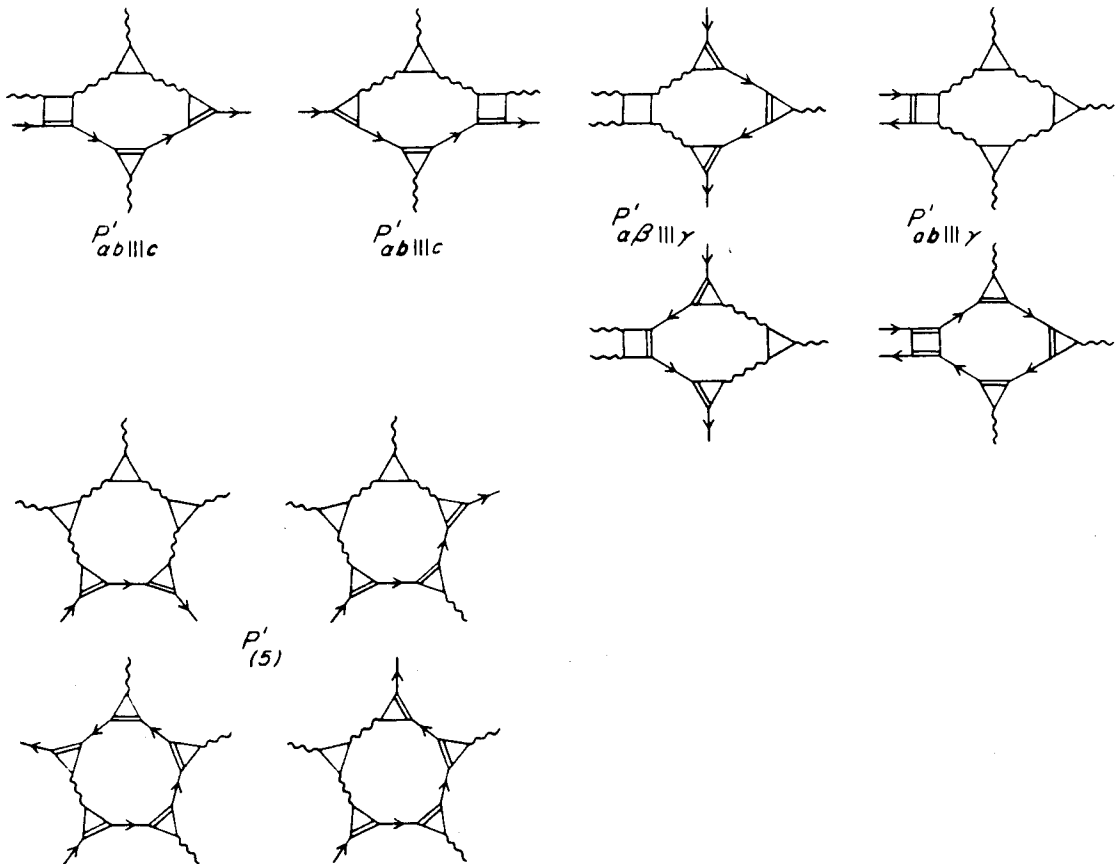


Fig. 21. continued

c)

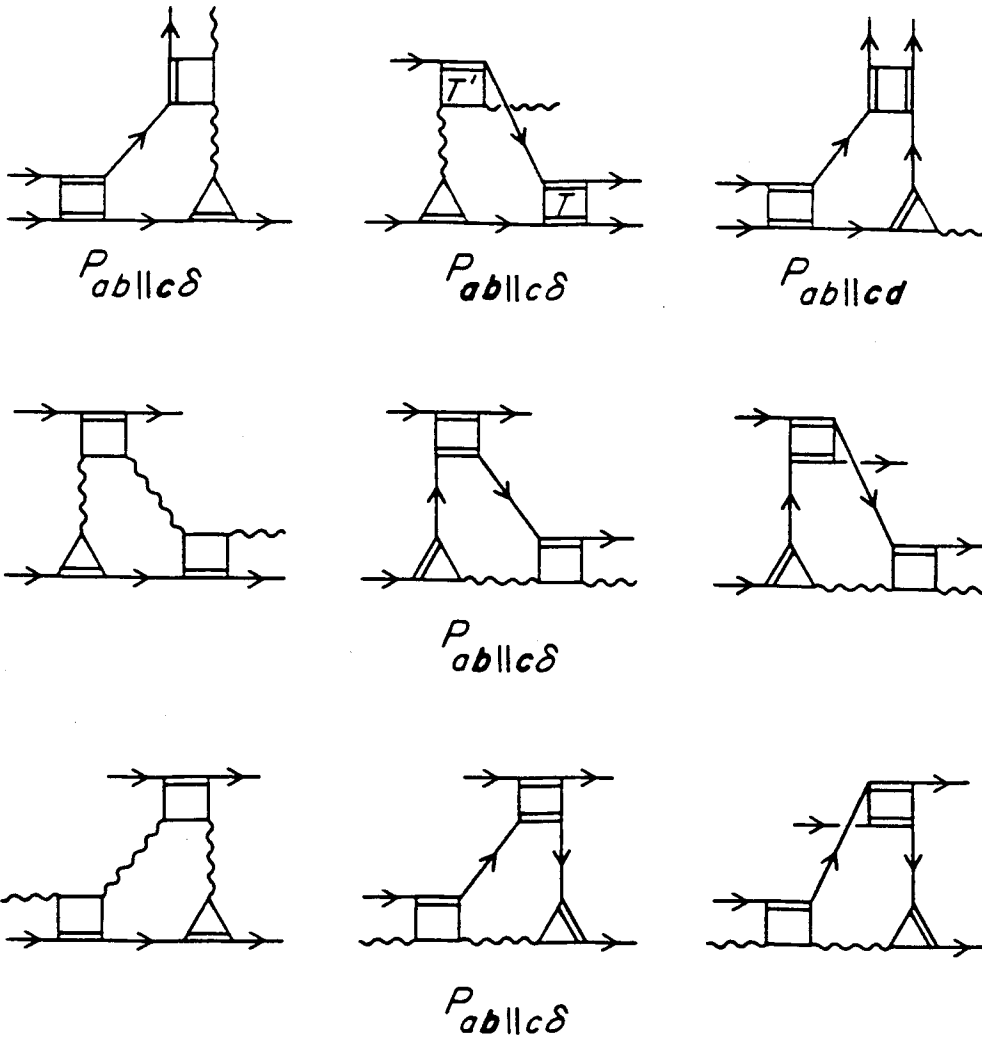


Fig. 21. continued

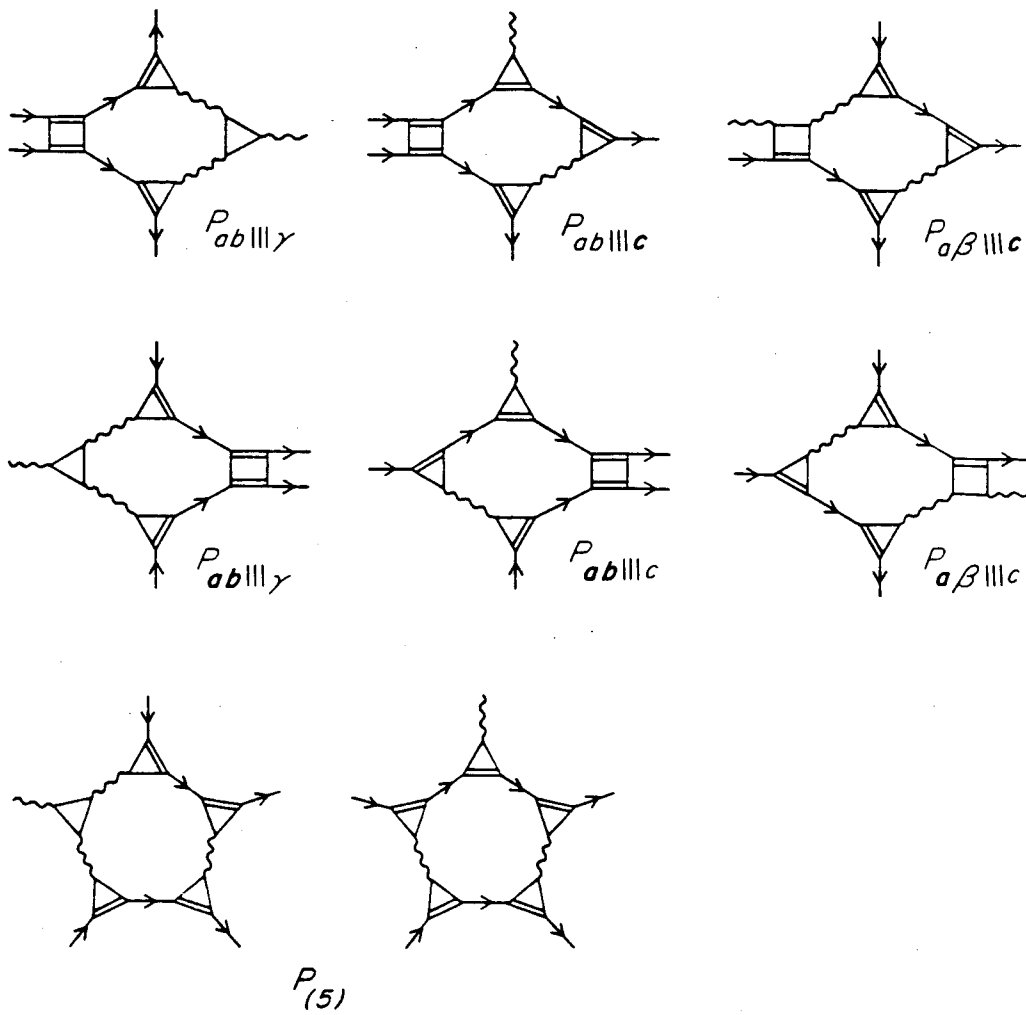


Fig. 21. continued

### 4.3 THE DECAY TYPE OF 2-PARTICLE INTERMEDIATE STATES

In section 4.2 we developed the crossing-symmetric-reduction scheme for the scattering type of 2-particle intermediate states. We could devise now an analogous procedure for the decay type of 2-particle intermediate states, but we would take into account diagrams already treated in the reduction of the scattering type of 2-particle intermediate states. If we would have solved the Dyson hierarchy completely then the equations would have taken care of this over counting automatically, now we have to do this explicitly.

Instead of devising a similar procedure to the one discussed in section 4.2 and then subtracting the multiply counted diagrams we split a generic decay-reducible (*DR*) diagram into its different generic pieces containing only 3-point vertex functions and 4-, 5-, 6, 7- and 8- point 2-particle-irreducible vertex functions (shown as squares, pentagons, hexagons, heptagons and octagons respectively in figure 22). The first two and last three generic pieces are also scattering reducible and we see that in general a diagram which is decay reducible in more than one channel is also scattering reducible and therefore is already taken care of. So we avoid an over counting problem and the only thing left to do is to extract out of the leftover diagrams all decay-reducible diagrams which are not scattering reducible. For these decay-reducible but scattering-irreducible pieces (*SI*) we develop again integral equations.

$$T''_{SI,\alpha\beta\gamma\delta} = T''_{I,\alpha\beta\gamma\delta} + S(0,4)T''_{SI,\alpha\beta\gamma\delta} + O(6) \quad (4.46)$$

$$T'_{SI,\alpha\beta cd} = T'_{I,\alpha\beta cd} + S(2,2)T'_{SI,\alpha\beta cd} + T'_{SI,c\alpha\beta d} + T'_{SI,d\alpha\beta c} + O(6) \quad (4.47)$$

$$T_{SI,abcd} = T_{I,abcd} + S(2,2)T_{SI,abcd} + S(2,2)T_{SI,blacd} + O(6) \quad (4.48)$$

The subscript I stands here for complete scattering and decay irreducibility. We neglected here all diagrams which contain vertex functions with more than 6 legs ( $O(6)$ ). This approximation does not correspond to the truncations we did until now. The truncations included the higher order terms via the parametrization of the  $T$  matrix and the pentagon. Here we really neglect these higher order processes since we have no way to actually calculate nor parametrize these objects without solving the reduction hierarchy to their corresponding orders which in turn introduces then even higher-order diagrams.

For the decay-reducible pieces of the diagram containing the pentagon we develop

integral equations analogous to the ones developed in section 4.2. Let's start again with the all-boson case. Our choices are to put the ladder summation either into the 3-point vertex function or into the pentagon. If we would put the ladder summation into the 3-point vertex function we would have to make the pentagon itself scattering irreducible in the appropriate channel, which means that the pentagon would have to be 1-particle irreducible for all channels and 2-particle irreducible in the channel under discussion.

$$T''_{SI,\alpha|\beta\gamma\delta} = \frac{1}{2} V''_{1PI,\alpha|\varepsilon\phi} G_{(\varepsilon\phi)} (P''_{1PI,\varepsilon\phi|\beta\gamma\delta} - P''_{\varepsilon\phi|\beta\gamma\delta}) + V'_{1PI,\alpha|ef} G_{(ef)} (P'_{1PI,ef|\beta\gamma\delta} - P'_{ef|\beta\gamma\delta}) \quad (4.49)$$

We could also use the peculiarity that scattering and decay reducibility in the case of the 3-point vertex function are identical since there is only one diagram in the topological class of the 3-point vertex function describing 2-particle intermediate states, and put the ladders into the pentagon. We would thus have only to assure scattering irreducibility in the appropriate channel for the 3-point vertex function and could use the 1-particle-irreducible pentagon.

$$T''_{SI,\alpha|\beta\gamma\delta} = \frac{1}{2} (V''_{1PI,\alpha|\varepsilon\phi} - V''_{\alpha|\varepsilon\phi}) G_{(\varepsilon\phi)} P''_{1PI,\varepsilon\phi|\beta\gamma\delta} + (V'_{1PI,\alpha|ef} - V'_{\alpha|ef}) G_{(ef)} P'_{1PI,ef|\beta\gamma\delta} \quad (4.50)$$

For the mixed fermion-boson case we have two cases:

$$T'_{SI,\alpha|\beta cd} = V'_{1PI,\alpha|ef} G_{(ef)} (P'_{1PI,ef|cd\beta} - P'_{ef|cd\beta}) + \frac{1}{2} V''_{1PI,\alpha|\varepsilon\phi} G_{(\varepsilon\phi)} (P'_{\varepsilon\phi|cd\beta} - P'_{\varepsilon\phi|cd\beta}) \quad (4.51)$$

$$T'_{SI,c|\alpha\beta d} = V'_{1PI,c|\varepsilon\phi} G_{(\varepsilon\phi)} (P'_{\varepsilon\phi|\alpha\beta d} - P'_{\varepsilon\phi|\alpha\beta d}) \quad (4.52)$$

$$T'_{SI,\alpha|\beta cd} = (V'_{1PI,\alpha|ef} - V'_{\alpha|ef}) G_{(ef)} P'_{1PI,ef|cd\beta} + \frac{1}{2} (V''_{1PI,\alpha|\varepsilon\phi} - V''_{\alpha|\varepsilon\phi}) G_{(\varepsilon\phi)} P'_{1PI,\varepsilon\phi|cd\beta} \quad (4.53)$$

$$T'_{SI,c|\alpha\beta d} = (V'_{1PI,c|\varepsilon\phi} - V'_{c|\varepsilon\phi}) G_{(\varepsilon\phi)} P'_{1PI,\varepsilon\phi|\alpha\beta d} \quad (4.54)$$

In the first two equations we put the ladders into the 3-point vertex function while we put it

in the pentagon for the last two equations. We use again time reversal to obtain the last decay reducibility class from (4.52) or (4.54).

Finally we determine the all-fermion case. Also here we can determine both reducibility classes from one equation using time reversal.

$$T_{SI,abcd} = V'_{1PI,a\epsilon f} G_{(\epsilon f)} (P_{1PI,\epsilon f bcd} - P_{\epsilon f bcd}) \quad (4.55)$$

$$T_{SI,abcd} = (V'_{1PI,a\epsilon f} - V'_{a|\epsilon f}) G_{(\epsilon f)} P_{\epsilon f bcd} \quad (4.56)$$

Again we put the ladder summation in (4.55) into the 3-point vertex function and in (4.56) into the pentagon. We have thus completed the crossing-symmetric reduction of the diagrams containing 2-particle intermediate states.

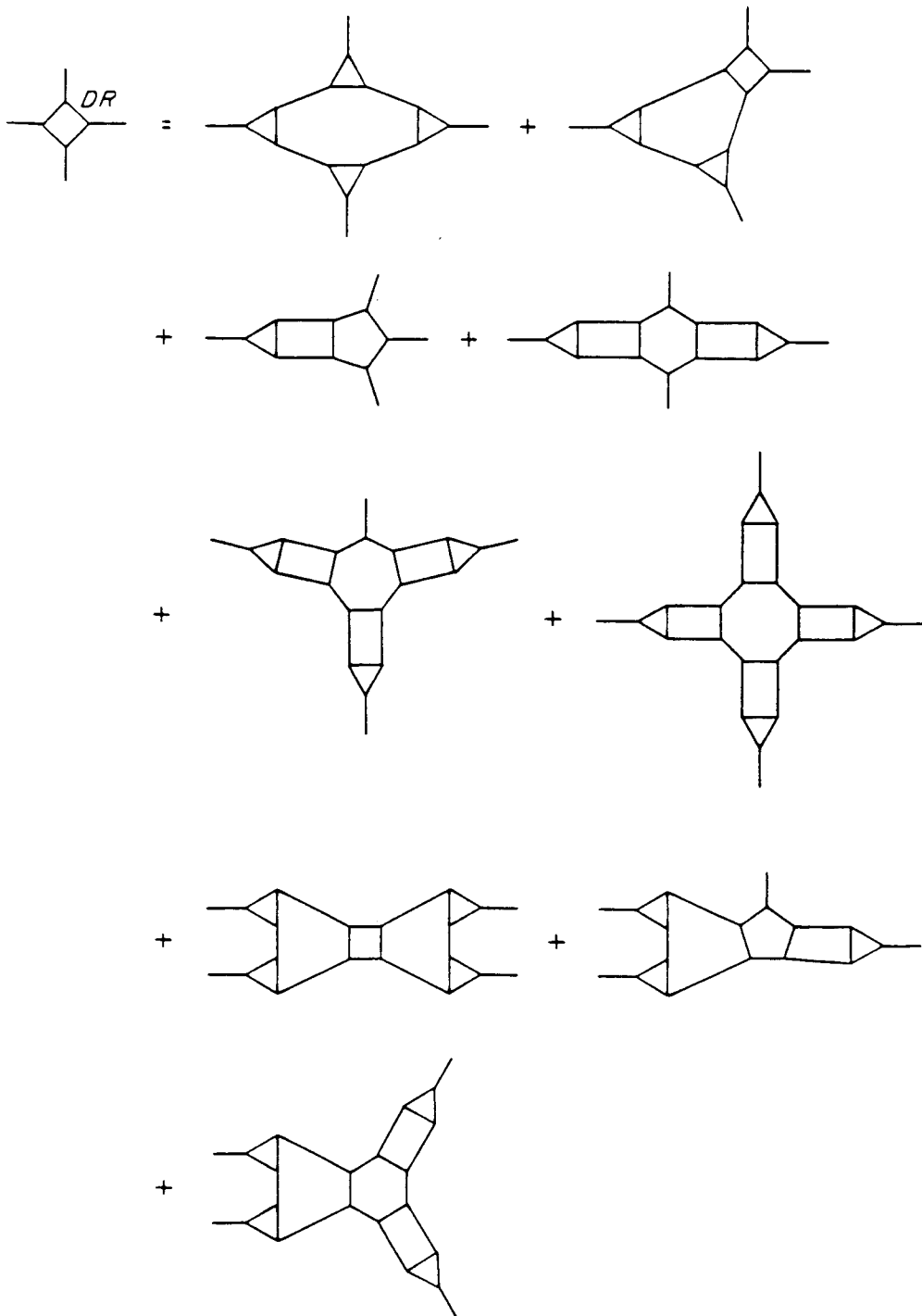


Fig. 22. Generic decay diagram and its different generic pieces in terms of 3-, 4-, 5-, 6-, 7-, and 8-point 2-particle scattering irreducible vertex functions.

## 5. REGULARIZATION

With the crossing-symmetric reduction done in chapter 4 we completed the discussion of the microscopic approach to the condensed state and so reached the goals we proposed in chapter 1. Still, although we have a satisfying theory, we cannot apply it unless we discuss the regularization of this procedure. In this chapter we want to discuss the main ideas involved in the regularization of hadronic matter without going into proofs or details. At the moment we have not completely evolved our ideas and feel, therefore, not confident to make explicit statements.

There are two main approaches to the understanding of the singularities appearing in any field theory. The one relates the singularity to the point-like interactions in the Lagrangian, which is of course a singular construct. This singularity can be expressed as the possibility of having a zero space-time separation  $\Delta x = 0$ . By imposing the condition  $\Delta x \neq 0$  on the field theory we could remove this singularity. The second approach in understanding the singular structure of a field theory is to look at the generic output of our theory, which are the Green's functions. These Green's functions are defined in terms of time-ordered products of fields which are ill-defined at equal times. This indefiniteness at equal times represents itself then as a singularity in momentum space, e.g. propagators have singular denominators and loop integrals develop ultraviolet singularities. We will use now both approaches to indicate possible ways out of this dilemma.

The condition of non-zero space-time separation is actually too weak since it allows an approach to the singularity via two independent degrees of freedom (i.e. the singularity lies at the origin of the space-time plane). One approach to remove this singularity is to assign form factors to every vertex, and then to maintain causality using dispersion relations<sup>[6,13]</sup>. A vertex function with one leg fixed contains eight more independent variables, three of which can be integrated out because of symmetries. The form factors then regularize three more variables corresponding to the invariants describing the sides of the triangle. The other two variables get fixed in more complicated diagrams due to their connection to other vertex functions of the diagram (e.g. consider the two-point loop). A tadpole, on the other hand, will still contain both singularities, since neither of the left-over degrees of freedom is fixed. The regularization of tadpoles for a Dyson hierarchy is discussed by Milana and Siemens<sup>[12]</sup>, who employ a Euclidean cutoff procedure. The



same counting of degrees of freedom works for the loop diagrams containing  $T$  matrices in the Dyson equations for the three-point vertex functions. Since Siemens *et al.*<sup>[6]</sup> regularize a Dyson hierarchy up to order four with three-point interactions in the Lagrangian, the method of form factors and dispersion relations works. In our case we don't have to redo the counting procedure since the 4-point interactions in the Lagrangian introduce only more highly connected diagrams (3-particle intermediate states).

Another approach to the regularization of a phenomenological theory like QHD would be to implement causal and covariant form factors directly into the action (the Lagrangian is an equal time operator). We would then achieve causality by using the 2-particle-irreducible kernels of the vertex functions, so that one event is not able to influence two disconnected events simultaneously. The singularities due to  $\Delta x^2 = 0$  lie on the light cone which is straightforward to realize by inspecting the Pauli-Jordan expansion of Green's functions<sup>[5]</sup>. This kind of singularity could be removed by a covariant form factor in the action of the type  $F(l^2 < x^2 < L^2)$  with  $L - l$  representing the size scale of the hadrons. If  $F$  is real we also obey unitarity, and by choosing a product of different  $F$ 's, corresponding to the different channels of the vertex function, we obey crossing symmetry and thus complete a sufficient approximation of the physical form factor without the trouble of the light-cone singularity. Again we have two leftover degrees of freedom, and we would have to find a possible way to remove the associated singularities if we are to obtain a regularized theory from the beginning.

The only covariant function which is not a function of  $x^2$  is the delta function  $\delta(x)$ . This choice of  $F$  brings us back to our first approach. This approach is intensively discussed in introductory field-theory textbooks<sup>[13]</sup> and its use in the case of hadronic matter is explicitly discussed by Siemens *et al.*<sup>[6]</sup> for a Lagrangian containing only 3-point interactions. Siemens *et al.* combine two steps in their discussion of regularization which we would like to separate here. They use dispersion relations to show how to introduce form factors in a causal way. These form factors are again real, to obtain unitarity, but they break crossing-symmetry because they include the Migdal approximation to make the Dyson equations numerically accessible. The Migdal approximation corresponds physically to the collapse of two neighboring points of a vertex function through introduction of a delta function in the coordinates of these two points. Their causal form factor then smears out this delta function so that, *e.g.* geometrically a 3-point vertex

function represented originally by a triangle changes to a  $\perp$  - shaped object. We see therefore that we lost one geometric degree of freedom: we replaced 3 sides of a triangle by its base and height, and lost an angle. The physical justification for this approximation is weak, and we see that the main advantage of this approximation is that it makes the theory numerically accessible.

Let us first generalize this approach by dropping the Migdal approximation. For our theory with also 4-point interactions in the Lagrangian we would have to develop all dispersion relations for loops up to the 5-point loop. The dispersion relations for more complicated singular diagrams (we are allowed to have 3-particle intermediate states) can then be easily constructed from the dispersion relations of the loops. A Dyson hierarchy with only 3-point interactions, on the other hand, would only need the dispersion relation for a 3-point loop in addition to the discussion for the 2-point loop and tadpole by Siemens *et al.* Since the development of dispersion relations for higher order loops is rather involved, we propose a different approach. Using the Migdal approximation on the Dyson hierarchy containing also 4-point interactions, it is easy to realize that we again only need dispersion relations for 2- and 3-point loops. Thus, with the additional discussion of the dispersion relation for 3-point loops, we could achieve a general regularization of a Dyson hierarchy with 3-point interactions in the Lagrangian, and also, using the Migdal approximation for vertex functions, a regularization of a Dyson hierarchy with 3- and 4-point interactions in the Lagrangian.

## 6. CONCLUSION

We developed a relativistic condensed matter theory based upon a microscopic, *i.e.* field theoretical picture. The Green's functions of the theory can be used to obtain the equations of state as well as the transport coefficients of this matter. The vertex functions were obtained by Legendre transforming the generating functional of the connected Green's functions and the relationship between the connected Green's functions and the vertex functions was derived. We developed the Dyson hierarchy as a tool to calculate the Green's functions of the field theory starting from a Lagrangian that contains bosonic and fermionic degrees of freedom interacting via 3- and 4-point interactions. We truncated this hierarchy at the level of the connected 4-point Green's function using the  $T$  matrix ( $O(4)$ ). Finally we performed a complete crossing symmetric reduction for the 2-particle intermediate states of the  $T$  matrix and the pentagon. We showed that in addition to the Dyson hierarchy we obtain a reduction hierarchy which we truncate on the level of the 6-point vertex function ( $O(6)$ ) to be consistent with the truncation of the Dyson hierarchy ( $O(4)$ ). The reduction hierarchy can furthermore be used to test the quality of the truncation procedure. The theory so far is completely general and can be used to describe fundamental as well as phenomenological theories. Then we proceeded with the discussion of regularization using hadronic matter as our system of interest. The conventional procedure of using form factors as cut-offs and dispersion relations to assure that these form factors satisfy causality was discussed and the Migdal reduction was introduced to make the theory numerically accessible. We furthermore explored the possibility of directly putting form factors into the action and showed how regularization is obtained so from the beginning.

We conclude this paper by discussing the possible future development necessary to introduce this theory into the framework of already existing theories.

- The first and most urgent step is to obtain numerical solutions from this theory which can then be compared to experiment. First results were obtained for the delta-nucleon-pion system<sup>[14]</sup>. Further application to other systems like the jellium model<sup>[10]</sup> are necessary.
- An investigation of the higher order diagrams ( $O(6)$ ) which appear in the discussion of the decay reducible diagrams is necessary.
- The applicability of putting the form factors into the action should be further explored.
- For consistency we should explore the possibility of a crossing symmetric reduction of the 3-particle intermediate states.
- The dispersion relations for higher order loops ( $O(3)$ ) should be developed.

## 7. REFERENCES

- [1] the following discussion is based on:  
Palash B. Pal, private communication; R. N. Mohapatra and Palash B. Pal, *Massive Neutrinos in Physics and Astrophysics* (World Scientific 1991), p.165 and p.262
- [2] the following discussion is based on:  
Kerson Huang, *Statistical Mechanics* (John Wiley & Sons 1987), p.65 and p.213
- [3] R. J. Rivers, *Path Integral Methods in Quantum Field Theory* (Cambridge Monographs on Mathematical Physics 1990)
- [4] L. H. Ryder, *Quantum Field Theory* (Cambridge University Press 1989)
- [5] N. N. Bogoliubov and D. V. Shirkov, *Quantum Fields* (Benjamin/Cummings Publishing Company, Inc. 1983)
- [6] P. J. Siemens, M. Soyeur, G. D. White, L. J. Lantto, K. T. R. Davies, *Phys. Rev. C* 40 (1989) 2641
- [7] the discussion of this section is based on references [3], [4] and [6], using the phaseconvention of [6] and the variable names of [3] and [4]
- [8] C. Itzykson and J. B. Zuber, *Quantum Field Theory* (Mac Graw Hill 1980)
- [9] C. L. Korpa and P. J. Siemens, to be published.
- [10] C. D. Mahan, *Many Particle Physics* (Plenum Press 1983)
- [11] B. D. Serot and J. D. Walecka, *Advances in Nuclear Physics*, 16 (Plenum Press 1986)
- [12] J. P. Milana and P. J. Siemens, *Phys. Rev. C* 43 (1991) 2377
- [13] J. D. Bjorken and S. D. Drell, *Relativistic Quantum Fields* (Mac Graw-Hill Publishing Company 1965), chapter 18
- [14] L. Xia, P. J. Siemens and M. Soyeur: "Coupling and Decoupling of Pions and Deltas in Nuclear Matter" in *Proceedings of the International Workshop XX on Gross Properties of Nuclei and Nuclear Excitations* (ed. by H. Feldmeier GSI-Darmstadt, Germany 1992)